MODULATION OF FOXO SIGNALLING BY GLUTATHIONE

Dissertation

zur Erlangung des akademischen Grades

„Doctor of Philosophy“ (PhD)

vorgelegt dem Rat der Biologisch-Pharmazeutischen Fakultät der Friedrich-Schiller-Universität Jena

von Dipl.-Biol. Dimitrios Tsitsipatis

geboren am 07.09.1989 in Thessaloniki/Griechenland

MODULATION OF FOXO SIGNALLING BY GLUTATHIONE

Dissertation

To Fulfill the

Requirements for the Degree of

„Doctor of Philosophy“ (PhD)

Submitted to the Council of the Faculty of Biology and Pharmacy

of the Friedrich Schiller University Jena

by Dipl.-Biol. Dimitrios Tsitsipatis

born on 07.09.1989 in Thessaloniki/Greece

Reviewers:

1. Prof. Lars-Oliver Klotz, Department of Nutrigenomics, Institute of Nutrition, Friedrich Schiller University, Jena, Germany

2. Prof. Frank Böhmer, Institute of Molecular Cell Biology, Friedrich Schiller University, Jena, Germany

3. Dr. Niki Chondrogianni, National Hellenic Research Foundation, Institute of Biology, Medicinal Chemistry and Biotechnology, Athens, Greece

Ph.D defence was held on: 28th September 2017

Table of contents

Zusammenfassung

Transkriptionsfaktoren der Forkhead Box O (FoxO)-Familie sind hochkonserviert und an der Regulation zahlreicher zellulärer und physiologischer Prozesse beteiligt, darunter Zellproliferation, Apoptose, die zelluläre Antwort auf oxidativen Stress, Langlebigkeit und Energiestoffwechsel. Im Kontext der Untersuchungen zur Redoxregulation von FoxO-Proteinen wird in der vorliegenden Arbeit die Bedeutung von (a) Glutathion und (b) FoxO1-Cysteinresten für die Modulation der FoxO-Aktivität analysiert. Dafür wurden sowohl kultivierte Zellen als auch ein *in vivo*-Modell, *Caenorhabditis elegans* (*C. elegans*) eingesetzt.

Zunächst wurde der Effekt untersucht, den Diethylmaleat (DEM), eine α,β-ungesättigte Carbonylverbindung und thiolmodulierende Substanz, auf die Lebensspanne von *C. elegans* hat. Niedrig dosiertes DEM bewirkte eine Verlängerung der Lebensspannne von *C. elegans*. Unter Einsatz *daf-16*- oder *skn-1*-defizienter Stämme sowie über Nachweis der Regulation von DAF-16- bzw. SKN-1-Zielgenen wurde sodann gezeigt, dass diese Verlängerung der Lebensspanne durch die Transkriptionsfaktoren DAF-16 und SKN-1, *C. elegans*-Homologe von FoxO bzw. Nrf2, vermittelt wird. Im Gegensatz hierzu hatte hochdosiertes DEM keine Änderung der Expression von DAF-16- oder SKN-1-Zielgenen zur Folge und verkürzte die Lebensspanne signifikant. Auf ähnliche Weise hatte auch Abschwächen der Glutathionbiosynthese durch RNA-Interferenz auf Ebene der *gcs-1*-Expression die gesteigerte Expression von Genen zur Folge, die für antioxidative Proteine codieren.

Zum Zweck der Analyse der Interaktion zwischen Glutathion und einem Säugerhomologen von DAF-16, FoxO1, untersuchten wir die Bedeutung von FoxO1-Cysteinresten für die Regulation der FoxO-Aktivität unter basalen und Stressbedingungen.

Transfektion von Zellen mit Wildtyp (WT)-FoxO1 oder cysteindefiziente FoxO1-Formen codierenden Plasmiden führte zur Stimulation FoxO-responsiver Promotoren, die im Falle der FoxO1-ΔCys1-7 überexprimierenden Zellen schwächer war als im Falle von WT-FoxO1. Eine einzelne Mutation in Cys612 vermittelte diese Abnahme der basalen Transaktivierungsaktivität von FoxO1, die wiederum zur Folge hatte, dass die Expression von FoxO-Zielgenen weniger stark stimuliert wurde als im Falle der Überexpression von WT-FoxO1.

Behandlung von Zellen mit Diamid, das S-Glutathionylierung in den Zellen steigerte, schwächte die Bindung von WT-FoxO1, nicht aber von FoxO1-ΔCys1-7, an DNA ab. Durch Diamid induzierte S-Glutathionylierung wurde durch Überexpression von Glutaredoxin (Grx)-1 erfolgreich rückgängig gemacht. Überexpression von Grx-1 beschleunigte die Wiederherstellung der DNA-Bindung durch FoxO1. Da lediglich Grx-1 mit intaktem Cys23 diese Wiederherstellung beschleunigte, während Cys26 hierfür unwichtig war, wurde

gefolgert, dass S-Glutathionylierung die diamidinduzierte Abnahme der DNA-Bindung durch FoxO1 vermittelt.

Zusammengefasst reguliert durch Thioldepletion hervorgerufener oxidativer Stress FoxO-Proteine, was zu einem nicht-linearen Effekt einer Thioldepletion auf die *C. elegans*-Lebensspanne führt. Darüber hinaus wurde S-Glutathionylierung als ein Weg identifiziert, über den Glutathion die FoxO1-Aktivität unter Stress beeinflusst.

Summary

The highly conserved transcription factors of the Forkhead box O (FoxO) family are involved in the regulation of several cellular and physiological processes, including cell proliferation, apoptosis, oxidative stress response, longevity, and fuel metabolism. Here, in the context of the analysis of a redox modulation of FoxO proteins, the role of (a.) glutathione and (b.) FoxO1 cysteine residues in modulating FoxO activity were assessed employing cultured cells and an *in vivo*-model, *Caenorhabditis elegans* (*C. elegans*).

Initially, the effects of diethyl maleate (DEM), an α,β-unsaturated carbonyl compound and thiol modulating agent, on *C. elegans* life span were explored. Low-dose-DEM elicited an extension of *C. elegans* life span. Using *daf-16* or *skn-1*-deficient strains and through the upregulation of DAF-16 or SKN-1 target genes this life span extension was then demonstrated to be mediated by transcription factors DAF-16 and SKN-1, *C. elegans* homologues of FoxO and Nrf-2, respectively. In contrast, exposure to high-dose-DEM did not alter the expression of DAF-16 or SKN-1 targets and significantly shortened lifespan. Similarly, downregulation of glutathione biosynthesis through RNA interference to lower *gcs-1* expression elicited the induced expression of genes encoding antioxidant proteins.

In order to analyze the interaction between glutathione and a mammalian DAF-16 homolog, FoxO1, we investigated the role of FoxO1 cysteine residues in regulating FoxO1 activity under basal and stressful conditions. In cells transfected with plasmids encoding wildtype (WT) FoxO1 or cysteine-deficient FoxO1 forms, stimulation of FoxO1-responsive promoters was less prominent in cells overexpressing FoxO1-ΔCys1-7 as compared to those transfected with WT FoxO1. A single mutation in Cys612 mediated this loss of basal transactivation of FoxO1 activity, which in turn caused less prominent stimulation in expression of FoxO1 target genes as compared to overexpression of WT FoxO1.

Exposure of cells to diamide, which promoted cellular S-glutathionylation, attenuated DNA binding of WT FoxO1, but not of FoxO1-ΔCys1-7. Diamide-induced S-glutathionylation was successfully reversed by overexpression of glutaredoxin (Grx)-1. In line with that, Grx-1 overexpression promoted an accelerated recovery of the impaired FoxO1 DNA binding. As only Grx-1 harboring an intact Cys23 was capable of accelerating recovery, whereas Cys26 was irrelevant, it was concluded that S-glutathionylation mediated diamide-induced attenuation of FoxO1 DNA binding.

In summary, oxidative stress induced by thiol depletion regulates FoxO proteins, resulting in a non-linear effect of thiol depletion on *C. elegans* life span. Moreover, S-glutathionylation was identified as one mode of action of glutathione affecting FoxO1 activity under stressful conditions.

1. Introduction

1.1 *C. elegans* as a model organism and its maintenance

Caenorhabditis elegans (*C. elegans*) was first introduced as model organism by Sydney Brenner in 1965, while the first publication was released in 1974 [1]. *C. elegans* is a small round transparent nematode (approx. 1 mm long) with a short life span, high number of progeny and relatively simple maintenance and manipulation. Although being evolutionarily far away from humans, *C. elegans* shares approx. 40% gene homology with *Homo sapiens* and therefore several signaling pathways are highly conserved. Thus, *C. elegans* has emerged as a model organism for studies mainly related to ageing and age-related diseases [2].

In nature, *C. elegans* lives in rotting vegetables from where it can be isolated [3]. In laboratories, it can be grown and maintained on agar plates spotted with *Escherichia coli* (*E. coli*). Upon bacteria depletion, an adult worm can utilize its fat supply, whereas in early developmental stages may arrest in a dauer stage [4]. Another important factor influencing *C. elegans* growth is temperature; temperatures higher than 25°C result in accelerated ageing of the worms [5]. Interestingly, exposure to high temperature for short periods of time is a frequently employed method to increase the amount of males [6]. Wild type *C. elegans* worms are usually grown and maintained at 20°C.

1.2 *C. elegans* anatomy

Wild type *C. elegans* has two sexual forms: a self-fertile hermaphrodite (XX) and a male (XO). Hermaphrodites are essentially females and are the dominant form; males occur at a frequency of 0.1-0.2 %. It should be noted that males are important for exchanging genetic material required for the generation of worms with diverse genetic composition. Both sexual forms share several similarities but also sex-related differences in their anatomy. An adult hermaphrodite has a constant amount of 959 somatic nuclei, of which 302 are neurons. In contrast, an adult male has 1033 somatic nuclei, of which 385 are neurons, mainly related to male mating behavior. Interestingly, males are thinner and slightly shorter (approx. 0.8 mm) than the hermaphrodites [7]. Independent of the gender, the cross section is cyclical with an inner and an outer tube separated by the pseudocoelomic space. Cuticle, hypodermis, excretory system, neurons and muscles are part of the outer tube and the inner tube consists of the pharynx, intestine and, in adult worms, gonad. Cuticle is the outer part of the worm, connecting the pharynx with the rectum. Various tissues, such as the excretory pore, vulva

and anus penetrate the cuticle. All the previously mentioned tissues are on the ventral side (Fig.1).

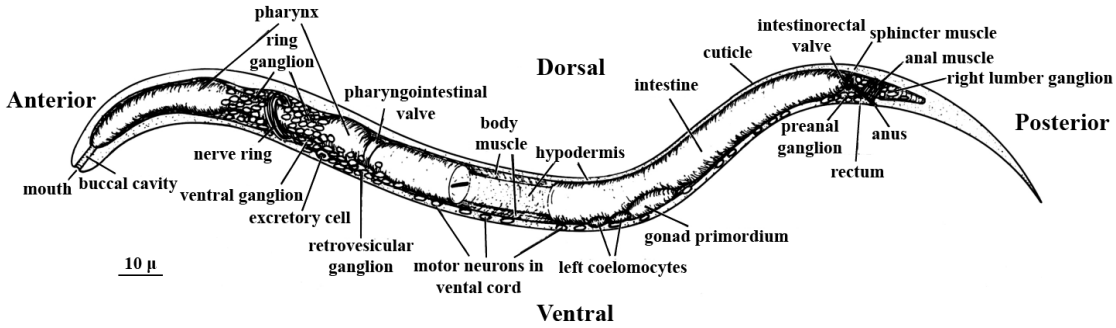

Figure 1:
General anatomy of a newly hatched L1 hermaphrodite larva. Despite being in such an early stage, the larva has already developed most of its tissues. The outer tube consists of the cuticle, hypodermis, excretory system, neurons and muscles In contrast to that, the pharynx, intestine and gonad belong to the inner part. Cuticle runs the entire body, connecting the pharynx with the rectum and is penetrated by various tissues. Modified figure from Sulton et al., 1980; permission obtained from Elsevier [8].

1.3 *C. elegans* life cycle and its genome

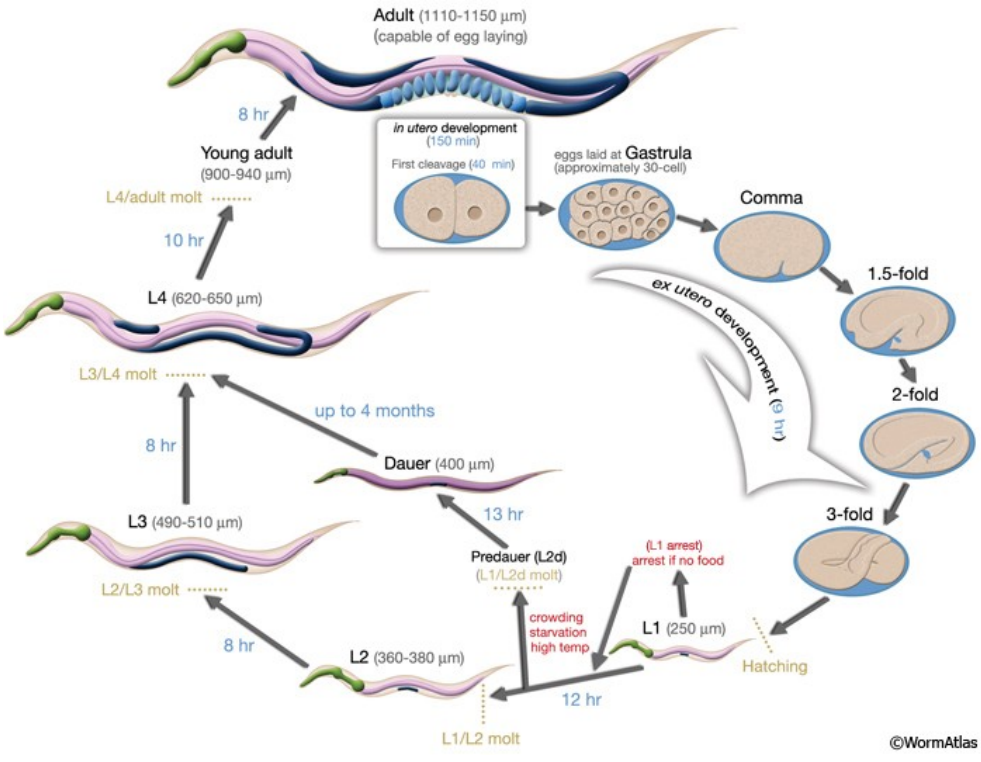

Figure 2:
C. elegans life cycle at 22°C. Shortly after fertilization, the first cleavage occurs. Following a 9-hour *ex utero* development, the egg hatches and the offspring enters the L1 stage. Under certain conditions, such as food shortage, *C. elegans* might arrest in L1 stage and survive for up to 10 days. Under physiological conditions, four post-hatching larval stages are required until adulthood. Under unfavorable conditions, the worm may enter the dauer stage where most of its activities are impaired, until the conditions become favorable again. An adult hermaphrodite is capable of laying approximately 300 eggs progeny (figure obtained from WormAtlas).

C. elegans life cycle is divided in to an embryonic stage and adulthood (Fig. 2). The end of each larval stage is characterized by a molting process, in which a new cuticle is synthesized that substitutes the old one. During molting, pharyngeal pumping ceases and the animal enters a brief lethargus.

1.3.1 Embryogenesis

Embryogenesis can be divided into two stages: proliferation and organogenesis/ morphogenesis [9]. Proliferation is then subdivided into two stages: the first phase (0-150 minutes) covers the time between zygote formation until the generation of founder cells and the second phase (150-350 min) covers the period from cell divisions and gastrulation until the beginning of organogenesis [10]. Each embryonic stage is characterized by specific cell migrations, alterations in number of cells, and synchronized stem-cell divisions. The first sign of sexual dimorphism becomes visible at 510 minutes. In late embryogenesis, the embryo has already established a main body plan and fully differentiated tissues and organs, which do not significantly alter during post-embryonic development [11].

1.3.2 Post-embryonic development

Three hours after hatching and under favorable conditions, a post-embryonic developmental program is initiated [12]. Normally, four larval stages are required until adulthood. Progenitor cells are divided in different constant patterns, giving rise to a certain number of cells, whose fates are pre-determined [13]. Under unfavorable conditions, such as in the absence of food, the young larvae may transition to an arrest stage and survive up to 10 days. As soon as a food source is again available, these arrested L1 larvae can normally progress [14].

Among all larval stages, L2 larval stage is unique due to the fact that under unfavorable environmental factors, such as absence of food and high temperature, a morphologically distinct L2-stage larva (L2d) may be formed [15]. An L2d larva may develop to a L3 larva or under unfavorable environmental conditions may form a dauer larva, with a thick cuticle and thin shape. On the dauer larval stage, activities, such as pumping and locomotion, are impaired. Upon favorable conditions, the worm exits the dauer state and molts to the L4 stage, after about 10 hours. [15, 16].

Approximately 45-50 hours post-hatching at 22°C-25°C, an adult, fertile hermaphrodite can lay eggs; fertile period lasts for about 4 days [17]. Following the fertile period, a mature adult may live for an additional 10-15 days, depending on environmental conditions. An adult hermaphrodite usually produces about 300 eggs of progeny, but upon mating the progeny

number can be increased to 1200-1400. Males can successfully mate with a hermaphrodite for 6 days and be responsible for the birth of approx. 3000 progeny [18].

1.3.3 *C. elegans* genome

C. elegans was the first multicellular eukaryotic organism to have its complete genome sequenced. Its genome is 100 Mb, containing 20.444 genes coding for proteins, packed in to five autosomal chromosomes and one sex chromosome [19]. *C. elegans* genes do not contain big introns and thus are smaller than the vertebrate genes, with an average gene size of 3 kb [20]. Most protein-coding mRNAs are trans-spliced and some genes are organized in operons [21]. Similar to mammals, *C. elegans* proteins may also be modified post-translationally through ubiquitination, phosphorylation, methylation, and glycosylation [22-24].

1.4 *C. elegans* signal transduction

As previously mentioned, several signaling pathways are highly conserved between humans and *C. elegans*. Thus, *C. elegans* has emerged as useful tool, frequently employed in studies related to signal transduction. For instance, Troemel et al. in 1995 described the members of the seven-transmembrane G-protein-coupled receptor class (7TM GPCRs) in *C. elegans* [25]. Han et al. in 1990 discovered that *let-60* encodes for ras protein [26]. Since then the receptor tyrosine kinase/Ras GTPase/mitogen-activated protein kinase (RTK/Ras/MAPK) pathway has been linked to several developmental processes in *C. elegans* (for a comprehensive overview, see [27]). The above-mentioned conserved pathways are just a few examples of active pathways in *C. elegans*. Herein, we will focus on DAF-2, the *C. elegans* homolog of insulin/insulin-like growth factor-1 (IGF-1) receptors, signaling pathway, which is responsible for DAF-16 modulation.

1.4.1 Insulin/IGF-1 signaling pathway

In mammals, the insulin/IGF-1 receptors are transmembrane receptors which belong to the class of receptor tyrosine kinases (RTK) and are activated by insulin and IGF-1, respectively [28]. The insulin/IGF-1 signaling pathway is widely conserved and phosphorylation-activation of the insulin/IGF-1 receptors by their ligands activates several other cascade, such as the phosphoinositide 3-kinase (PI3K)/Akt, Ras/MAPK, and mechanistic target of Rapamycin (mTOR) pathways [29, 30]. This insulin cascade is mainly responsible for the regulation of processes, like metabolism, growth, development, and

longevity. Initially, we will focus on the key components of the pathway in *C. elegans*, which to a great extent are similar to humans too.

1.4.2 Key components of DAF-2-dependent pathways in *C. elegans*

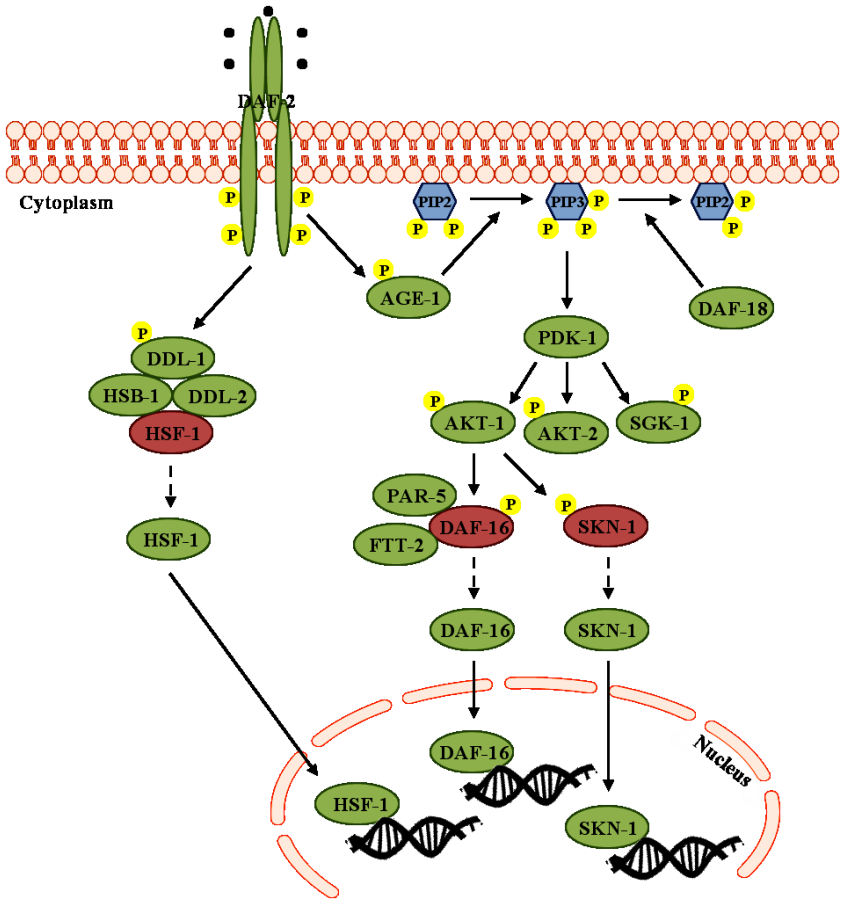

Figure 3:
DAF-2 (Insulin/IGF-1) signaling pathway in *C. elegans*. Upon stimulation of the DAF-2 receptor by its ligands (black dots), the DAF-2 receptor is activated and phosphorylates AGE-1. AGE-1 will then phosphorylate PIP2 to PIP3, which recruits PDK-1 that in turn phosphorylates AKT-1/AKT-2 and SGK-1. Phosphorylated AKT-1 induces phosphorylation of DAF-16 and SKN-1 and thus promotes their nuclear exclusion (colored red). When localized in the cytoplasm PAR-5 and FTT-2 block DAF-16 nuclear relocalization. Upon desphosphorylation of DAF-16 and SKN-1, both transcription factors become active and shuttle back to the nucleus, where they bind to DNA (colored green). Additionally, DAF-2 phosphorylates DDL-1, which in turn recruits DDL-2 and HSB-1. The recruited protein complex blocks nuclear localization of HSF-1 (colored red). As soon as HSF-1 is released from the protein complex, it then becomes active, translocates into the nucleus where it binds to DNA. DAF-2, insulin receptor homolog; AGE-1, PI3K homolog; DAF-18, PTEN homolog; AKT-1 and AKT-2, Akt homolog; PAR-5 and FFT-2, 14-3-3 proteins homologues; DAF-16, FoxO family homologues; SKN-1, Nrf-2 homolog.

DAF-2, *C. elegans* homolog of insulin receptor, and DAF-2 signaling was discovered during studies related to dauer regulation and genetic control of longevity [31]. It is now widely known that phosphorylated and activated DAF-2 receptor activates a phosphatidylinositol 3-kinase (AGE-1). Activated AGE-1 will then phosphorylate phosphatidylinositol bisphosphate (PIP2) to phosphatidylinositol trisphosphate (PIP3); DAF-

18 can dephosphorylate PIP3 and thus antagonizes AGE-1. Then PIP3 recruits 3-phosphoinositide-dependent protein kinase-1 (PDK-1), which in turn phosphorylates AKT-1/AKT-2 and serum/glucocorticoid-regulated kinase 1 (SGK-1). Activated AKT-1/AKT-2 phosphorylates DAF-16 and Skinhead-1 (SKN-1), leading to their nuclear exclusion. When DAF-16 is retained in the cytoplasm, PAR-5 and FTT-2 bind to the inactive DAF-16, and thus block DAF-16 nuclear translocation [32]. Additionally, activated DAF-2 can directly recruit and phosphorylate a DDL-1/DDL-2/HSB-1 complex, inducing the cytoplasmic retention of heat shock transcription Factor-1 (HSF-1) (Figure 3) [33]. Through the modulation of those transcription factors, the DAF-2 pathway plays a key role in regulating several processes, such as the L1 and dauer arrest, germline proliferation, stress resistance, fat metabolism, and ageing. Among the modulated transcription factors, herein we will mainly focus on DAF-16 and SKN-1.

1.4.2.1 DAF-16 transcription factor

DAF-16, the homolog of the mammalian forkhead box, class O (FoxO) family, is the main downstream target of the DAF-2 pathway (Fig. 3) [34]. In *C. elegans*, *daf-16* encodes for eight distinct transcripts of which *daf-16e* and *daf-16g* encode proteins lacking a DNA binding domain and thus their function is elusive. The other six mRNAs are controlled by three distinct promoters, which encode for proteins with different N-termini, and are comprised in three groups *daf-16a*, *daf-16b*, and *daf-16d/f/h* [35-37]. Each group shows a tissue-specific distribution; *daf-16a* and *daf-16d/f/h* are active in most tissues, but *daf-16b* is exclusively active in the pharynx, nervous system, and somatic gonad [36, 37]. In line with the *daf-16a* and *daf-16d/f/h* ubiquitous expression, overexpression of *daf-16a*-specific and *daf-16d/f/h*-specific transgenes efficiently rescued the dauer-constitutive and longevity phenotypes of *daf-16*-deficient; *daf-2* (e1370) double mutants [37]. Among the DAF-16 isoforms, DAF-16A and DAF-16D/F/H share a higher homology percentage with mammalian FoxO proteins as compared to the others. DAF-16A harbors all three RxRxxS/T motifs, which are directly phosphorylated by AKT-1/AKT-2; in contrast, DAF-16D/F/H harbors a QxRxxS/T motif in the N-terminus, leading to the hypothesis that distinct kinases may phosphorylate the two isoforms and thus separately regulate DAF-16A or DAF-16D/F/H [37]. A potentially unique regulator of DAF-16D/F/H might be the target of Rapamycin complex 1 (TORC1) [38]. In addition to the traditional AGE-1/AKT-driven DAF-16 regulation, other co-factors and regulators can modulate DAF-16 activity, which to a great extent, have homologues in humans (Table 2) [39].

Table 1: Regulators and co-factors modulating DAF-16 indepentently of AGE-1/AKT

Activators			Inhibitors		
Protein	**Reference**	**Background**	**Protein**	**Reference**	**Background**
AAK-2	[40]	Energy homeostasis	EAK	[41-44]	DAF-2 pathway
CST-1	[45]	Oxidative stress	RLE-1	[46, 47]	Ubiquitylation
JNK-1	[48]	Oxidative stres	HCF-1	[49]	Cell cycle
PRMT-1	[50]	Methylation			
BAR-1	[51]	Oxidative stres			
Sirtuin	[52, 53]	Deacylation			
CBP-1	[53, 54]	Acetylation			
SMK-1	[55]	DAF-2 pathway			
DPY-21	[56]	X-chromosome dosage compensation			
TRPA-1	[57]	Cation channel			
RHEB-1	[58]	Nutrient/energy/ redox sensor			

Activators and inhibitors acting on DAF-16 independently of AGE-1/AKT. AAK-2, AMPK gamma subunit homolog; CST-1, MST-1 homolog; JNK-1, Jnk homolog; PRMT-1, PRMT1 homolog; BAR-1, α, β-catenin homolog; CBP-1, p300 homolog; SMK-1, phosphatase 4 regulatory subunit 3A homolog; RHEB-1 Rheb homolog, TORC1 activator; RLE-1, Roquin homolog, E3 ubiquitin ligase homolog; HCF-1, host cell factor homolog.

As a transcription factor, DAF-16 binds to a DNA element, TTGTTTAC, known as DAF-16 binding element (DBE) and thus upregulates the expression of target genes involved in several cellular processes, such as in antioxidant defense, thermotolerance, maintenance of metabolic homeostasis, and resistance to heavy metals [59, 60]. These genes belong to the "Class 1 DAF-16 targets". In contrast, the "class 2 DAF-16 targets" contain an alternative DNA binding sequence in their promoters, CTTATCA, known as DAF-16 associated element (DAE) and thus these genes are downregulated [61]. For the regulation of the "class 2 DAF-16 targets", it was recently proposed that the zinc finger transcription factor PQM-1 acts as DAE-binding factor, antagonizing DAF-16 [62]. Most genes of the "class 2" are upregulated in response to pathogen exposure. In Table 1, five examples of highly regulated genes of each class and their potential role are presented, as suggested by Tepper et al., 2013 [62].

Table 2: Class 1 and Class 2 DAF-16 targets

Class 1 (upregulated)		Class 2 (downregulated)	
Gene	**Protein function**	**Gene**	**Protein function**
mtl-1	metallothionein-I	*dct-18*	Germline tumor
ftn-1	ferritin heavy chain	F54F11.2a	Zinc-binding metalloprotease
cdr-2	glutathione S-transferase	*nuc-1*	DNAse II homolog; apoptotic cell DNA degradation
sod-3	superoxide dismutase	*cpr-5*	cysteine thiol protease
gei-7	isocitrate lyase/malate synthase	*ins-7*	insulin-like peptide

Five examples of the top 50 most upregulated (Class 1) or downregulated (Class 2) transcriptional targets of DAF-16 as suggested by Tepper et al., 2013 [62].

1.4.2.2 SKN-1 transcription factor

In contrast to its mammalian homolog, nuclear factor-erythroid 2 p45-related factor 2 (Nrf-2), SKN-1 lacks the ZIP dimerization module, which is required for a stable DNA binding [63]. SKN-1 DNA binding domain harbors an additional peptide motif, and thus recognizes different bases in the DNA [63, 64]. In *C. elegans*, the *skn-1* gene encodes four distinct isoforms of which only three (*skn-1a*, *skn-1b* and *skn-1c*) are also expressed *in vivo*. Among these three isoforms, *skn-1a* and *skn-1c* are predominantly expressed in the intestine [65, 66]. In contrast, *skn-1b* is predominantly expressed and localized in the nucleus of the two ASI chemosensory neurons [65]. During larval development, minor *skn-1a* expression might be observed in some head neurons [66].

Regulation of SKN-1 activity can be achieved through different mechanisms in *C. elegans* (Table 3). Typically, SKN-1 regulation depends on PMK-1, *C. elegans* homolog of $p38^{MAPK}$, under oxidative stress. PMK-1 phosphorylates SKN-1 in two residues (Ser164 and Ser430), leading to SKN-1 nuclear accumulation and thus affects SKN-1 activity [67]. In addition, SKN-1 harbors an RxRxxS/T motif, which can directly be phosphorylated by AKT-1/AKT-2, inducing SKN-1 cytoplasmic retention (Fig. 3) [66]. Since *C. elegans* lacks a true Keap1 homolog, the interaction between Nrf-2 and Kelch-like ECH-associated protein 1 (Keap1), which is the major mechanism through which Nrf-2 is inactivated in mammals, ubiquitin-mediated proteolysis of SKN-1 in *C. elegans* occurs through WDR-23, an E3 ubiquitin ligase substrate adaptor [68-72].

Table 3: SKN-1 regulators

Activators			Inhibitors		
Protein	**Reference**	**Background**	**Protein**	**Reference**	**Background**
PMK-1	[67]	Oxidative stress	AKT-1/AKT-2	[66]	DAF-2 pathway
IRE1	[73]	ER-stress	WDR-23	[70-72]	Ubiquitylation
			GSK-3	[74, 75]	Ubiquitylation
			SGK-1	[38, 66]	DAF-2 pathway
			mTORC1	[38]	Nutrient/energy/ redox sensoring

Proteins which modulate SKN-1. PMK-1, p38 homolog; IRE1, Ire-1 homolog; AKT-1/AKT-2, Akt homolog; WDR-23, E3 ubiquitin ligase adaptor.

SKN-1 has a pivotal role in defense against oxidative and xenobiotic stress, protein homeostasis and metabolism, through the regulation of several genes, some of which are also downstream targets of DAF-16 [76-78]. Exposure to acute oxidative stress triggers SKN-1 accumulation in the nucleus, inducing the expression of various genes involved in all three detoxification phases, such as cytochrome P450, short-chain dehydrogenases, glutathione

(GSH) biosynthetic, glutathione-S-transferases (GSTs), UDP-glucuronosyl transferases and ATP-binding cassette transporters [76, 78-81]. In the absence of oxidative stress, SKN-1 also regulates the expression of several genes involved in several processes, such as proteostasis, transportation of metals and antimicrobial defense (Table 4) [76]. More specifically, SKN-1 upregulates the expression of proteasome subunit genes and thus influences proteasome activity [77, 82]. In a feedback loop, SKN-1 can both modulate and be modulated by several downstream targets of the unfolded protein response (UPR). Interestingly, UPR-driven regulation of SKN-1 does not significantly induce SKN-1 nuclear localization, but increases the SKN-1 protein levels. Upon UPR, nuclear SKN-1 might regulate its downstream targets in cooperation with UPR related factors, such as X-box binding protein-1 (XBP-1) [73].

Table 4: SKN-1 target genes regulated under non-stressed conditions

Upregulated		Downregulated	
Gene	**Protein function**	**Gene**	**Protein function**
gst-4	Glutathione S-transferase	*skr-5*	SCF ubiquitin ligase, Skp1 component
gst-10	Glutathione S-transferase	*spp-17*	Saposin-like Protein family
gst-13	Glutathione S-transferase	*lys-6*	N-acetylmuraminidase/lysozyme
F56A4.4	Glutathione S-transferase	*ins-7*	Insulin-like peptides
C35B1.5	Thioredoxin, nucleoredoxin and related proteins	*dhs-18*	Reductases with broad range of substrate specificities

Five examples of the most upregulated or downregulated transcriptional targets of SKN-1 under non-stressed conditions as suggested by Oliveira et al., 2009 [76].

1.5 Reactive oxygen species: a double-edged ax

Both DAF-16 and SKN-1 have a pivotal role in the antioxidant defense through regulation of the transcription of several target genes. An imbalance between antioxidants and oxidants may cause oxidative stress. Upon oxidative stress, reactive oxygen species (ROS) are accumulated, inducing several cellular processes. “ROS” is a term to describe chemical species which are formed upon incomplete reduction of oxygen and include superoxide, hydrogen peroxide, and hydroxyl radical. Although ROS were originally thought to strictly mediate oxygen toxicity, it is now widely accepted that they may also act as intracellular signaling molecules, activating pathways involved in cell proliferation, differentiation, and survival [83]. Herein we will mainly focus on antioxidant defense in *C. elegans* and humans.

1.5.1 Antioxidant defense in *C. elegans*

Enhanced oxidative stress resistance was long believed to be the cause of longevity in *C. elegans*. In line with that theory, increased oxidative stress resistance was detected under conditions that promote deceleration of ageing, such as in *daf-2*-deficient mutants or under dietary restriction [84, 85]. However, deletion of genes encoding superoxide dismutases (*sod* genes) did not significantly affect life span under the above-mentioned conditions, meaning that increased stress resistance is not necessarily required for longevity [86, 87]. Regardless of whether induction of stress resistance is the main reason for longevity, regulation of the redox state is quite important for survival of *C. elegans*.

To regulate its redox state, *C. elegans* has several antioxidant genes, such as *sod*, *catalases*, *peroxiredoxins* etc. For the purpose of this dissertation, we will mainly focus on few antioxidant genes, such as *sod-3*, *catalases* and genes that code for enzymes involved in either the thioredoxin or glutaredoxin system. *C. elegans* has six different *sod* genes that encode SOD enzymes localized in different compartments. Among these, *sod-3*, as well as *sod-2*, encodes MnSOD enzymes localized in the mitochondrial matrix [88]. Upregulation of *sod-3* was predominantly reported in dauers, *daf-2*-deficient mutants and under oxidative stress [86, 89, 90]. It should be noted that strains, in which both Mn- and CuZnSOD were knocked down, have similar life span as compared to wild type strains, despite being highly sensitive to multiple types of stress, which could potentially be explained through a counterbalance between superoxide toxicity and an adaptive response to reduced superoxide detoxification [91]. *C. elegans* contains three catalase enzymes with highly similar sequences [92]. CTL-2 seems to be responsible for the majority of the total catalase activity; *ctl-2* depletion leads to reduction of both mean life span and egg-laying capability [92, 93]. Surprisingly, overexpression of all catalases leads to life span reduction [86]. In addition, *C. elegans* contains four glutaredoxins (GLRXs), eight thioredoxins (TRXs), and two thioredoxin reductases (TRXRs). Knockout of *trx-1*, which is mainly expressed in specific pharyngeal neurons and intestine, induces paraquat resistance but accelerates ageing as compared to wild type [94]. On top of that, depletion of *trx-1* partially or completely reverses longevity driven by *daf-2* deletion or dietary restriction, respectively [95]. Genomic analysis of *C. elegans* revealed that 57 genes encode for GSTs. Upon oxidative stress, *gst-4* is upregulated which in turn increases oxidative stress resistance but does not alter life span [96]. Strains overexpressing *gst-10*, which encodes for a protein which catalyzes the detoxification of the lipid peroxidation end-product 4-hydroxynonenal (4-HNE), are more resistant to various stressful conditions, such as heat, ultraviolet radiation, and oxidative stress, and have an increased life span [97]. However, exclusive increase of HNE-induced damage can not sufficiently accelerate ageing in *C. elegans* [98].

1.5.2 Antioxidant defense in humans

All antioxidants can roughly be divided in enzymatic and non-enzymatic. In humans, enzymatic antioxidants comprise SODs, catalase, glutathione peroxidases (GPxs), heme oxygenase-1, thioredoxins (Trxs), thioredoxin reductases (Trxrs), peroxiredoxins (Prxs), and glutaredoxins (Grxs) to name a few [99]. Thiols are among the non-enzymatic scavengers, such as GSH, the most abundant non-protein thiol [100]. For the purpose of this dissertation, we will mainly focus on glutaredoxins and the non-enzymatic scavenger, GSH.

1.5.2.1 Glutaredoxins, the small redox enzymatic scavengers

Glutaredoxins (Grxs) are small redox enzymes that predominantly use glutathione as a co-substrate [101]. Members of this family can be categorized in two groups according to their active site motif; the general active site motif is Cys-X-X-Cys and it is present in the dithiol Grxs. However, there is another group, known as monothiol Grxs, in which the C-terminal active site thiol is replaced by a serine (Ser); yet members of this group maintain all structural and functional elements to use GSH as co-substrate [102]. In humans, at least four Grxs have been identified and they are located in different compartments. The dithiol Grx1 is located in the cytosol and is functionally homologues to *E. coli* and yeast Grx-1. Similarly, the predominantly mitochondrial Grx-2 (Grx-2a) is also a dithiol Grx [103, 104]. As a consequence of alternative transcription initiation and splicing, two additional Grx2 isoforms (Grx-2b and Grx-2c) may also be expressed in testicular cells and in some cancer cells. In addition to the dithiol Grxs, two monothiol Grxs (Grx3 and Grx5) are expressed in humans. Among all Grxs, only Grx3 contains a Trx-like domain [102]. Grxs may utilize both cysteine residues in their active site motif and thus catalyse the reversible reduction of protein disulfides [105]. Initially, the N-terminal thiol of the active site motif nucleophilically attacks the target disulfide. Afterwards, the mixed disulfide, formed between a Grx and a protein, is attacked by the C-terminal thiol of the active site motif. This disulfide in the active site can then be reduced by GSH, leading to a mixed disulfide between GSH and the N-terminal active site motif thiol. This intermediate mixed disulfide is thereafter reduced by another GSH molecule. It is worth to be mentioned that the reduction of disulfides formed between glutathione and proteins, which is known as S-glutathionylation, only requires the Cys residue located in the N-terminal part of the active site [102, 106]. S-glutathionylation is a post-translational modification and will be reviewed elsewhere.

1.5.2.2 Glutathione, the major cellular low-molecular-mass thiol

The non-enzymatic scavengers are mainly low-molecular-compounds, such as vitamins, β-carotene, uric acid, and GSH, the most abundant among the low-molecular-mass thiols [99]. GSH is a tripeptide and its biosynthesis occurs in two ATP-dependent steps. In the first step, γ-glutamylcysteine is formed from glutamate and cysteine, a reaction catalyzed by the enzyme γ-glutamylcysteine synthetase (glutamate-cysteine ligase, GCL). This reaction is the rate-limiting step in glutathione synthesis [107]. In the second step, the enzyme glutathione synthetase adds a glycine to the C-terminus of γ-glutamylcysteine. GSH may be oxidized to a disulfide form, glutathione disulfide (GSSG) (Fig. 4), and the GSH to GSSG ratio is often used to assess the cellular redox state [108, 109]. GSH is primarily localized in the cytosol; yet it can also be found in other compartments, such as in nucleus, mitochondria and ER [110, 111]. In addition to GSH contributing in to antioxidant defense and detoxification of xenobiotics, GSH is also involved in other cellular possesses, such as in regulation of cell cycle progression and apoptosis, storage of cysteine, maintenance of redox status, modulation of immune function and fibrogenesis [112-115].

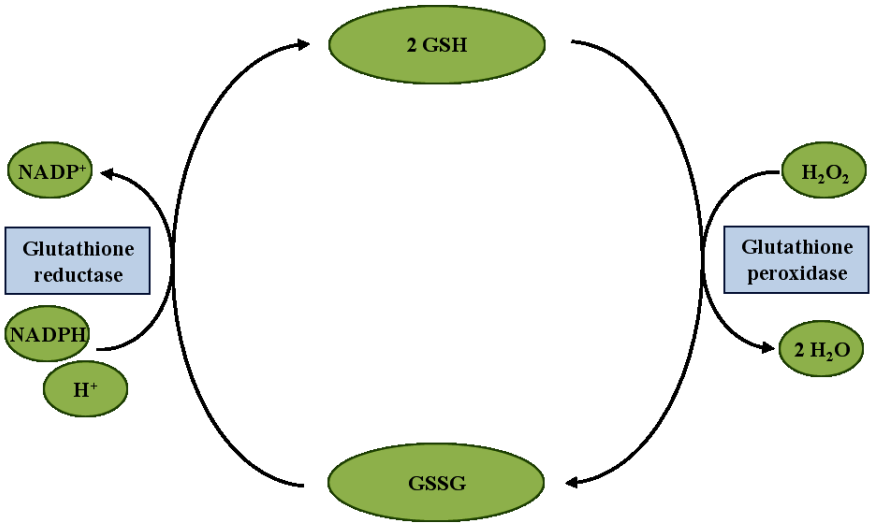

Figure 4:
Redox couple of glutathione. GSH may serve as an electron donor to reduce disulfide bonds. Upon oxidation, a GSH molecule can react with another GSH to form GSSG. Additionally, in a reaction catalyzed by GPx, GSH converts hydrogen peroxide to water molecules. In the final products, GSSG is also present [116]. GSSG is reduced back to two GSH molecules; this reaction is catalyzed by glutathione reductace [117]. In that reaction, NADPH serves as an electron donor.

The antioxidant function of GSH is tightly related to the GPx-catalyzed reaction, in which hydrogen peroxide or other hydroperoxides are reduced as GSH is oxidized to GSSG [116]. Glutathione reductase can reduce GSSG back to GSH in the presence of NADPH and thus a redox cycle is formed [117]. GSH has a pivotal role in defending the cell against

oxidative stress also in mitochondria [118]. Upon severe oxidative stress, GSSG is actively exported or reacts with a protein sulfhydryl group, to prevent a major shift in redox equilibrium [119].

GSH may also serve as a source of cysteine due to the γ-glutamyl cycle; an extremely important function, since cysteine is unstable and rapidly auto-oxidizes. GSH contributes new cysteines through the eventual cysteinylglycine hydrolysis by dipeptidase, leading to the regeneration of cysteine and glycine. As soon as cysteine is available, it is immediately incorporated, mainly into GSH and proteins, by the cells [100].

A growing body of evidence points to the association of enhanced GSH levels with a proliferative response and is essential for cell cycle progression [114, 119-122]. In hepatocytes, during the shift from G0 to G1 phase *in vitro*, GSH levels are increased; whereas blockage of elevated GSH levels significantly impair DNA synthesis [120, 121]. GSH-driven maintenance of Trxs and Grxs, which are essential for ribonucleotide reductase activity, the rate-limiting enzyme in DNA synthesis, seems to be the mechanism underlying the GSH-induced modulation of DNA synthesis [123]. Mitogenesis in liver cancer cells was reported to be regulated by the upregulation of GSH synthetic enzymes in a cell density-dependent manner [121]. Furthermore, reduced conditions mediated by GSH nuclear localization may affect the activity of several nuclear proteins, such as histones, and thus influence the cell cycle progression [114, 122].

GSH has a pivotal role in the regulation of cell death, both in apoptosis and necrosis [112, 124-126]. During apoptosis, ROS levels are elevated, leading to GSH oxidation, active GSSG secretion, and impaired GCL activity [124, 125]. Additionally, GSH regulates the expression/activity of important apoptotic signaling molecules, such as caspase 8 activation through tumor necrosis factor (TNF) or nuclear factor-kappa B (NF-κB)-dependent gene expression [112, 126]. Moreover, severe mitochondrial GSH depletion leads to elevated ROS levels, mitochondrial dysfunction and ATP depletion, which in turn leads to conversion of apoptotic to necrotic cells [126]. Lastly, GSH may interfere with various redox-dependent signaling pathways, through modifications on protein cysteine residues.

1.6 Protein S-glutathionylation, a post-translational modification

GSH can modify the oxidation state of cysteine residues of several proteins and thus can regulate redox-dependent cell signaling. More specifically, GSH can reversibly be bound to low-pKa cysteine residues and in turn generate glutathionylated proteins (protein-SSG) mainly under oxidative/nitrosative stress, but rarely also under physiological conditions [127]. Protein S-glutathionylation is induced mainly through four reactions: i) GSH can directly interact with partially oxidized protein sulfhydryls, such as thiyl radical, sulfenic acid, or S-

nitrosated proteins; ii) thiol/disulfide exchange reactions between protein thiols and GSSG or glutathionylated proteins; iii) intermediate S-nitrosothiols can react with protein thiols and thus modify protein sulfhydryl groups through either protein S-nitrosation or S-glutathionylation; iv) in the presence of several oxidants, GSH may directly interact and create a disulfide bond with a protein cysteine residue [127-129].

Protein S-glutathionylation has several roles, related to its reversibility [127]. Upon severe oxidative stress, S-glutathionylation protects protein cysteine residues from irreversible modifications, which may subsequently lead to proteasomal degradation of proteins. Upon oxidative stress alleviation, S-glutathionylated proteins may go back to their functional form [127, 130-132]. Additionally, S-glutathionylation may also induce a temporary loss of protein function; for instance in case that the modified cysteine residue is located on the active site of an enzyme [133, 134]. Moreover, transcription factors, such as c-Jun and NF-kB may also be inhibited by S-glutathionylation, which in turn may modulate gene expression [135-137]. In line with that, Fatelli et al. discovered that genes involved in various processes, such as in NF-kB activation, DNA methylation, and induction of cytokine production, were regulated in HL60 cells exposed to hydrogen peroxide [138]. Additionally, oxidative stress and consequently S-glutathionylation induction in human lung epithelial A549 and endothelial ECV304 cells regulates the mRNA levels of several chaperone genes, including heat shock proteins, DNA chaperones, and transcriptional regulators [139].

Under physiological conditions, S-glutathionylation serves as storage for the rapidly oxidized GSH, which may lead to GSSG secretion by the cells [140]. In addition to the proteins that undergo S-glutathionylation under oxidative/nitrosative stress, several proteins were found to be S-glutathionylated under physiological conditions. Hemoglobin in red blood cells, γ-crystallin from human lens, and actin in both human fibroblasts and epidermal A431 cells are a few examples of constitutively S-glutathionylated proteins [141-145]. Although the role of S-glutathionylation under physiological conditions is somewhat elusive, a potential role might be involvement in cellular signaling and redox regulation of protein functions. Several other proteins were identified as potentially S-glutathionylated; Ballatori et al. provide a comprehensive table [112].

As already mentioned, one very important aspect that makes S-glutathionylation a possible regulatory mechanism is its reversibility. As soon as the redox balance is restored, S-glutathionylation may be enzymatically reversed by Grxs and Trxs [127]. Grxs were the first to be identified as unique glutathione-mixed disulfide oxidoreductases [146]. Interestingly, in the presence of a GS-radical generating system, Grxs may also promote the formation of protein S-glutathionylation via distinct mechanisms [127, 147-149]. Deglutathionylation is catalyzed by the monothiol pathway, meaning that only the N-terminal cysteine of the Grx active site motif is required for this reaction [106].

1.7 FoxO proteins, the mammalian DAF-16 homologues

The "fork head" structure was first discovered in *Drosophila melanogaster* (*D. melanogaster*) [150, 151]. The same structure was thereafter recognized in several other proteins, such as in the hepatocyte-enriched nuclear factor (HNF)-3A, the first mammalian protein identified to harbor that structure, and thus proteins containing such a structure were categorized into different classes of forkhead box (Fox) transcription factors [152]. A subcategory of the Fox superfamily, FoxO, consists of four ubiquitously expressed members, FoxO1, FoxO3a, FoxO4, and FoxO6, which share two highly conserved cysteine residues, of which one is localized within the C-terminal transactivation domain (Fig. 5) [153, 154].

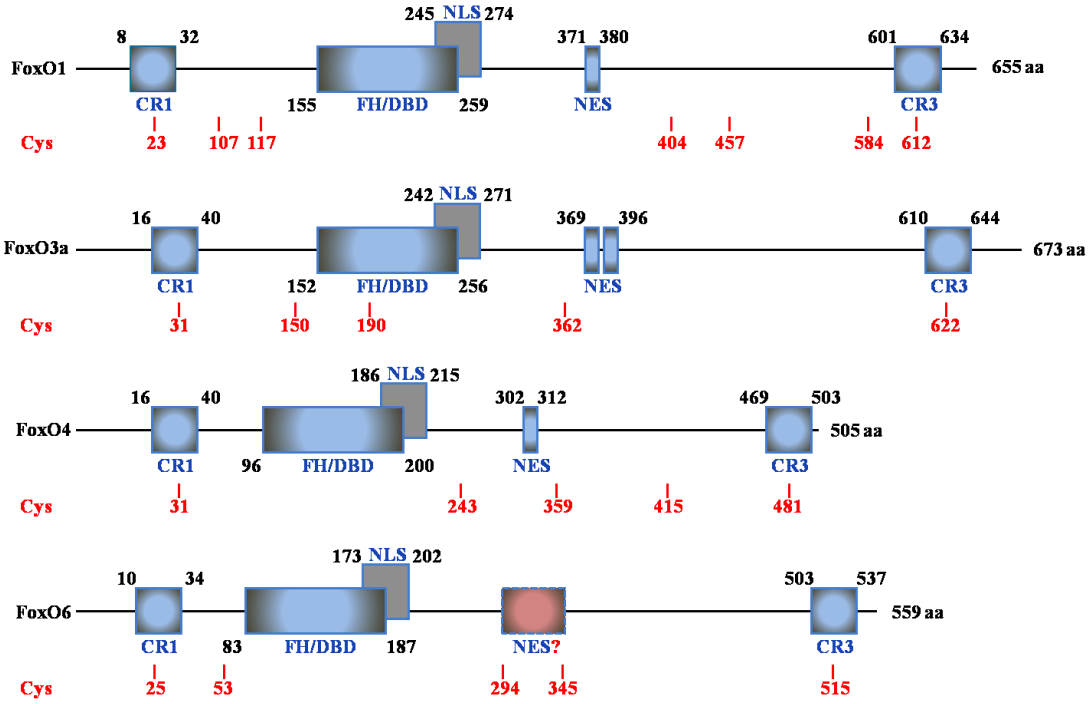

Figure 5:
Domain organization and localization of cysteine residues of FoxO isoforms. Conserved domains, their proposed functional role and the localization of cysteine residues are depicted. Total length of each FoxO protein is indicated in amino acids (aa) to the right. The numbers next to the domain indicate the beginning and end within the sequence. CR1 and CR3, conserved regions 1 and 3; CR3 represents a conserved C-terminal transactivation domain; FH/DBD, forkhead box/DNA-binding domain; NLS, nuclear localization signal; NES, nuclear export sequence. Numbers in red represent the precise position of cysteine residues. Figure modified from [155].

As already mentioned, a downstream target of the highly conserved insulin (the mammalian DAF-2 homolog) pathway is DAF-16, FoxO homolog. In a similar manner, stimulation of the insulin receptor leads to phosphorylation of PI3K, AGE-1 homolog, which leads to phosphorylation of Akt, AKT-1/AKT-2 homolog. Phosphorylated Akt will then phosphorylate members of the FoxO family, leading to their cytoplasmic retention (Fig. 3). On the one hand, FoxO transcription factors regulate the expression of several genes involved

in antioxidant defense, metabolism, cell death and proliferation. On the other hand, ROS-mediated post-translational modifications, such as phosphorylation and acetylation and interaction with coregulators, which eventually alter subcellular localization, protein synthesis and stability may modulate FoxO activity (For a general review about FoxO family see [155]).

1.7.1 ROS-driven regulation of FoxO activity

A complex system of several kinases may modulate FoxO activity in response to elevated ROS levels through several post-translational modifications or oxidative-stress-induced interactions with co-factors. Depending on the kinase-driven modification, FoxO phosphorylation may lead to either activation or inactivation of FoxO. Additionally, other post-translational modifications, like the lysine-related modifications acetylation and ubiquitination, may influence the consequences of FoxO phosphorylation upon exposure to different stressful stimuli.

Insulin-driven hydrogen peroxide generation, most likely through activation of NOX4, can reversibly oxidize a redox-sensitive cysteine residue of the protein-tyrosine phosphatase 1B (PTP1B), promoting its inhibition. Interestingly, when PTP1B is activated, it can then dephosphorylate the insulin receptor and thus inactivates the insulin signaling pathway, creating a feedback loop between insulin receptor and PTP1B, in which hydrogen peroxide plays a pivotal role [156-158]. Since FoxO proteins are downstream target of the insulin pathway, PTP1B may indirectly modulate FoxO activity.

In addition to the activation of the insulin receptor, other RTK-dependent signaling, such as the extracellular signal-regulated kinases (ERK)-1/2, $p38^{MAPK}$ and JNKs, may eventually affect FoxO transcription factors [159-161]. MAPK kinases phosphorylate serines or threonines followed by a proline residue and therefore are known as proline-directed kinases. Such motifs are frequently found in FoxO proteins, thus there was an assumption that MAPK may modulate FoxO activity. Indeed, Yang et al. 2008 showed that ERK-1/2 promotes tumorigenesis by phosphorylation/inhibition of FoxO3a, leading to FoxO3a poly-ubiquitination and subsequent degradation through murine double minute (MDM)-2 [159]. Additionally, Erk and $p38^{MAPK}$ phosphorylate/activate Foxo1, promoting a Foxo1/Ets-1 interaction, which in turns acts on the fetal liver kinase (Flk)-1 promoter in bovine carotid artery endothelial cells [160]. Induction of mild oxidative stress activates mediates a JNK-dependent phosphorylation of FOXO4, leading to its nuclear translocation and transcriptional activation [161]. In addition, other proline-directed kinases may modulate FoxO activity [162-164].

In a less explored field, ROS generation by mitochondria has also been associated with FoxO proteins. More specifically, mitochondrial dysfunction mediated by impaired glucose metabolism can lead to NOX activation and uncoupling of eNOS and thus to elevated ROS levels [165]. In line with that, in human aortic endothelial cells, elevated iNOS levels and LDL oxidation was mediated by upregulated FoxO1, under hyperglycemic conditions [166].

Additionally, redox-active compounds, such as copper ions (Cu^{2+}), doxorubicin, and arsenite, may induce ROS elevation and thus potentially affect FoxO activity. In human hepatoma cells, exposure to Cu^{2+} phosphorylates/inactivates FoxO1 through activation of the insulin signaling cascade and independently of the elevated ROS levels [167]. In line with that, other metal ions, such as zinc and cadmium (Zn^{2+} and Cd^{2+}, respectively), were also reported to stimulate the insulin signaling cascade, but less prominently as compared to Cu^{2+}-induced stimulation [167, 168]. In case of Zn^{2+} exposure, direct interaction with PTEN might be a potential mechanism underlying the signaling initiation [169]. Furthermore, doxorubicin, a DNA intercalating agent and topoisomerase inhibitor which is also known as a ROS-generator, was shown to induce FoxO3a phosphorylation, leading to nuclear accumulation and subsequent activation through $p38^{MAPK}$ in breast cancer cells [170]. In a similar manner, exposure to arsenite, a molecule with high affinity towards thiols, induced $p38^{MAPK}$-dependent Foxo3a activation, which in turn activated the transcription of Bim (EL), a pro-apoptotic protein, in rat pheochromocytoma cells, [171]. Interestingly, arsenite was also reported to mediate FoxO phosphorylation/inactivation through the stimulation of insulin cascade signaling in human keratinocytes and hepatoma cells, meaning that arsenite-driven modulation of FoxO proteins might be cell-dependent [172, 173].

FoxO activity can also be modulated by ROS-mediated post-translational modifications, which can be related to their lysine residues; more predominantly through acetylation and ubiquitination. Herein, we will mainly focus on a few aspects of modulation of FoxO activity through acetylation and ubiquitination. For a comprehensive review, see [155]. So far seven distinct acetylation sites in human FoxO1 and FoxO3a as well as five acetylation sites in human FoxO4 and FoxO6 have been identified, which are predominantly localized within the highly conserved nuclear localization signal motif and thus the acetylation state may affect cytoplasmic/nuclear shuttling, which in turn will modulate transcriptional activity of FoxO [34, 155, 174]. Interestingly, in a complex system of molecular mechanisms acetylation may both stimulate or inhibit the FoxO transcriptional activity, depending on FoxO isoforms and their binding partners, FoxO target genes and cell types used in the individual studies [175-177].

It was initially reported that p300-dependent acetylation of FoxO proteins enhances FoxO transcriptional activity. Recruitment of p300 to the promoter regions of target genes enhanced gene transcription by recruiting the basal transcriptional machinery and by easing

chromatin remodeling [178, 179]. In contrast, it was later reported that p300-driven acetylation inhibits FoxO transcription activity [180].

In addition to the acetylation of lysine residues, ubiquitination may also occur in the same lysines, leading to a deacetylation-related ubiquitination of FoxO. In line with that, mono-ubiquitination leads to FoxO4 nuclear retention and thus enhanced transcriptional activity [181]. In addition, Wang et al. reported that deacetylation of FoxO3a by Sirt1 or Sirt2 triggers Skp2-triven FoxO3a ubiquitination and subsequent proteasomal degradation [182]. Interestingly, when FoxO1 is exclusively phosphorylated at the serine residue S256 by Akt, then Skp2 ubiquitinates FoxO1, leading to subsequent proteasomal degradation [183].

1.7.2 FoxO target genes involved in antioxidant defense

FoxO proteins are not just modulated by ROS-driven processes but can also interfere with antioxidant defense, through the regulation of various target genes. In humans, Mn-SOD (SOD-2), an enzyme which catalyzes dismutation of superoxide to generate oxygen and hydrogen peroxide, is regulated by FoxO3a [184]. Additionally, Foxo3 modulates oxidative stress through the regulation of Cu, Zn-SOD (SOD-1) in murine erythroblasts [185]. Further hydrogen peroxide dismutation is mediated by catalase, which is also regulated by FoxO3a [186]. In addition, hydrogen peroxide reduction to water driven by Trx and GSH, reactions which are catalyzed by Prx3 and Prx5, in case of Trx-driven reduction, or GPx-1, in case of GSH. Interestingly, Prx3, Prx5 and GPx were reported to be regulated by FoxO proteins [185, 187, 188].

Furthermore, hydrogen peroxide may be reduced to generate the highly aggressive hydroxyl radical, in the presence of Fe^{2+} or Cu^{+}, which may be prevented by chelation, for instance by ferritin and metallothioneins, respectively [155]. As already shown, *C. elegans metallothionein-1* and *ftn-1* belong to the Class I DAF-16 target genes (Table 1) [62]. In mammals, AMPK-induced FoxO3a phosphorylation/activation upregulates mRNA levels of metallothionein [189]. Furthermore, ceruloplasmin, the major plasma copper protein which acts as ferroxidase to oxidize Fe^{2+} to Fe^{3+} and also allows for transport of Fe^{3+} by transferrin, is regulated by FoxO [190-192].

Lastly, selenoprotein P, the major plasma selenoprotein which predominatly acts as transporter of selenium from the liver to extrahepatic tissues through blood, and which is encoded by *SEPP1* gene, is regulated by a protein complex of peroxisomal proliferator activated receptor-γ coactivator 1a (PGC-1a)/FoxO1a/hepatocyte nuclear factor 4 alpha (HNF-4a) [193-197]. In addition to the traditional role of selenoprotein P, it can also act as a hydroperoxidase activity and thus may prevent low-density lipoprotein oxidation [198, 199].

1.8 Aims

A growing body of evidence supports the hypothesis that an unbalanced redox state of cells may affect FoxO activity, through post-translational modifications, interaction with coregulators, alterations in subcellular localization, protein synthesis and stability [155]. At the organismal level, such as in *C. elegans*, mild oxidative stress inhibits the DAF-2 signaling pathway and thus increases stress resistance, which in turn may promote longevity. The majority of phenotypes mediated by *daf-2*-deficiency are driven by activating DAF-16, the FoxO homolog in *C. elegans*. An approach to interfere with the redox state is by using agents affecting the thiol status of cells and/or organisms. Thiol modulating agents, such as diethyl maleate (DEM) or diamide may interact with protein cysteine residues or low-molecular-thiol such as GSH [200, 201]. Although thiol (cysteine) residues of FoxO were previously shown to be essential for stress-induced interaction with co-factors that eventually affect FoxO activity, the potential GSH contribution in modulating FoxO activity was never directly investigated [177, 202, 203].

Therefore, the current work had the following aims:

a) To assess whether DEM-induced thiol reduction may affect stress resistance and in turn decelerate ageing in *C. elegans*.
b) To examine the underlying mechanism mainly focusing on DAF-16 contributions and whether genetic GCL depletion, the enzyme catalyzing the rate-limiting step in glutathione synthesis, may alter the expression level of DAF-16 target genes and other related genes, which may potentially be affected [204].
c) To investigate the contribution of FoxO1 cysteine residues on key aspects of FoxO1 activity, such as cytoplasmic/nuclear shuttling, DNA binding, and transactivation activity, under physiological conditions.
d) To address the potential contribution of S-glutathionylation to the regulation of FoxO1 DNA binding under stressful conditions.

2. Material and methods

2.1 Materials

2.1.1 *In vivo* and *in vitro* models, cell culture material and employed agents

C. elegans strains were obtained by from Caenorhabditis Genetics Center (CGC, University of Minnesota, USA), which is supported by the National Institutes of Health-Office of Research Infrastructure Programs: wild-type Bristol N2; EU31 [skn-1(zu135)]; CF1038 [daf-16(mu86)]. *E. coli* strains OP50 and OP50i were also received from CGC. *E.coli* HT115 *gcs-1* clones were derived from an Ahringer library (Source BioScience, Nottingham, UK) [205].

Human embryonic kidney (HEK293) and human hepatoma (HepG2) were obtained from the German collection of microorganisms and cell cultures (DSMZ, Braunschweig, Germany). Cell culture medium (low glucose Dulbecco's modified Eagle's medium; Cat. No. D6046), 1x 0.05 % Trypsin/EDTA (Cat. No. T3924), Penicillin/Streptomycin (Cat. No. P4333), MEM non-essential amino acids (Cat. No. M7145) and PBS (Cat. No. D8537) were acquired from Sigma-Aldrich (Munich, Germany). FBS Superior (Cat. No. S0615) was obtained by Biochrom (Berlin, Germany). TurboFect (R0531, Thermo Fisher Scientific) and GenJet (Cat. No. SL100489, tebu-bio) transfection reagents were employed for transfecting HEK293 and HepG2 cells, respectively.

Thiol modulating agents, such as diamide (Cat. No. D3648), diethyl maleate (DEM) (Cat. No. D97703) and N-ethylmaleimide (NEM) (Cat. No. E1271) were obtained from Sigma-Aldrich. All compounds were dissolved and/or diluted in DMSO. In each case, DMSO was 0.1% v/v unless stated otherwise.

2.1.2 Plasmids

Plasmids encoding WT FoxO1 or a FoxO1 cysteine-deficient mutant (FoxO1-ΔCys1-7) containing biotinylation and a V5 tag were generated by Keshav Gopal (Klotz group). WT FoxO1 and FoxO1-ΔCys1-7 tagged with GFP were previously generated in the Klotz lab. Variants of the cysteine-deficient FoxO1 mutant were then generated by subclones of an EcoRI/XbaI fragment of FoxO1. WT FoxO1 and FoxO1-ΔCys1-7 tagged with EGFP were generated as depicted in Figure 6. SelP-Luc was previously generated in the Klotz lab [193], as well as FoxO1-Luc (unpublished). G6Pase-Luc was a kind gift from Dr. Andreas Barthel [206]. FHRE-Luc construct and pCI Neo were obtained from Addgene [207]. Renilla

luciferase control plasmid was obtained from Promega (pRL-SV40). Glutaredoxin cloning in the pBud vector was performed as depicted in Figure 7. Glutaredoxin variants were generated by a site-directed mutagenesis kit.

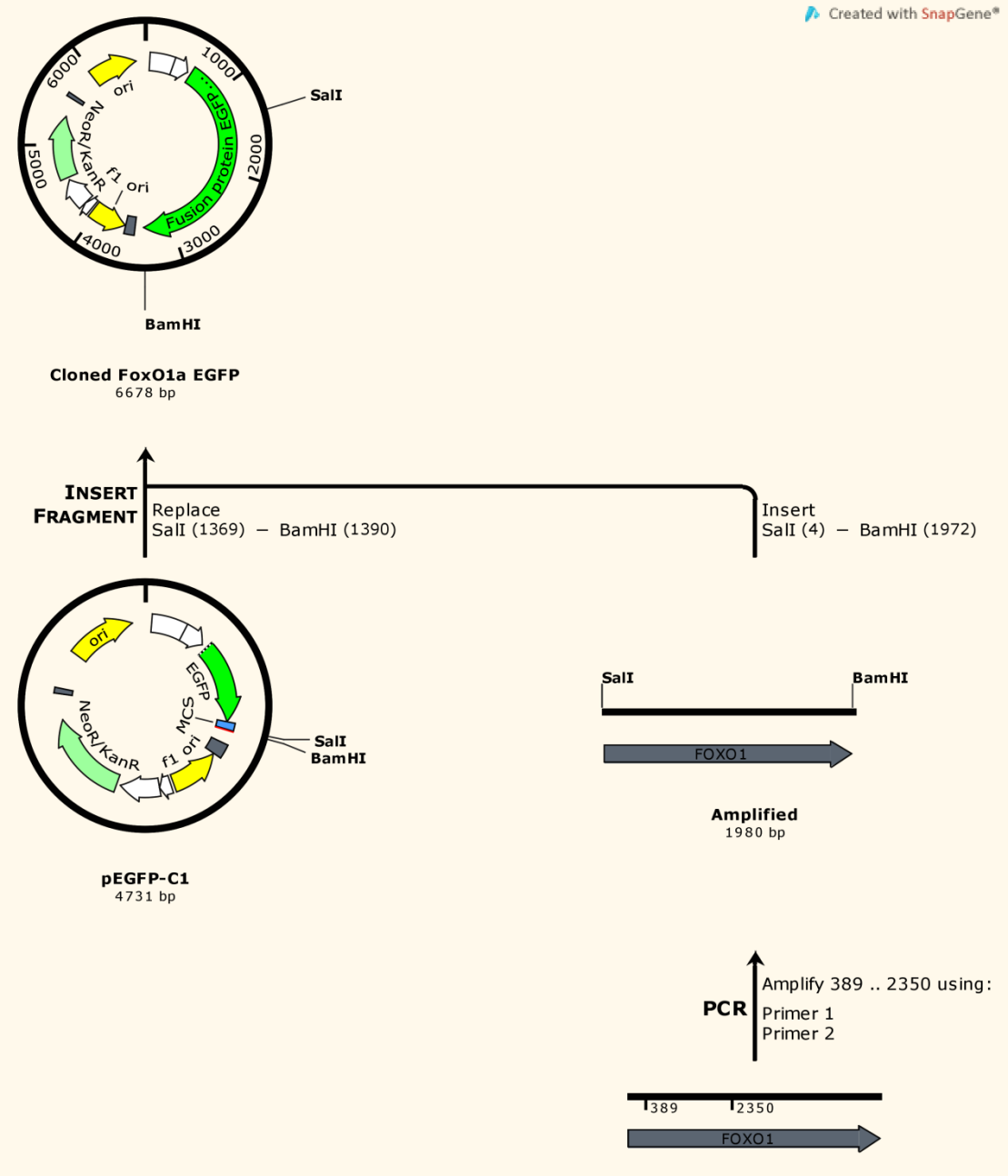

Fig. 6
Schematic cloning of FoxO1 in the pEGFP-C1 vector. FoxO1 was reversibly transcript from a FoxO1 template (FoxO1-V5; "amplify 389 .. 2350") using the following primers CTTGTCGACGCCGAGGCGCCTCAGGTG (primer 1) and CCCGGATCCGCCTCACACCCAGCTATGTGT (primer 2). After isolation from an agarose gel the amplicon was digested with SalI and BamHI. The same restriction enzymes were then employed for digestion of the pEGFP-C1 vector (Clontech). Eventually, the two fragments were ligated. Numbers next to restriction enzymes names represent the positions that the enzymes digested either the vector or the amplicon.

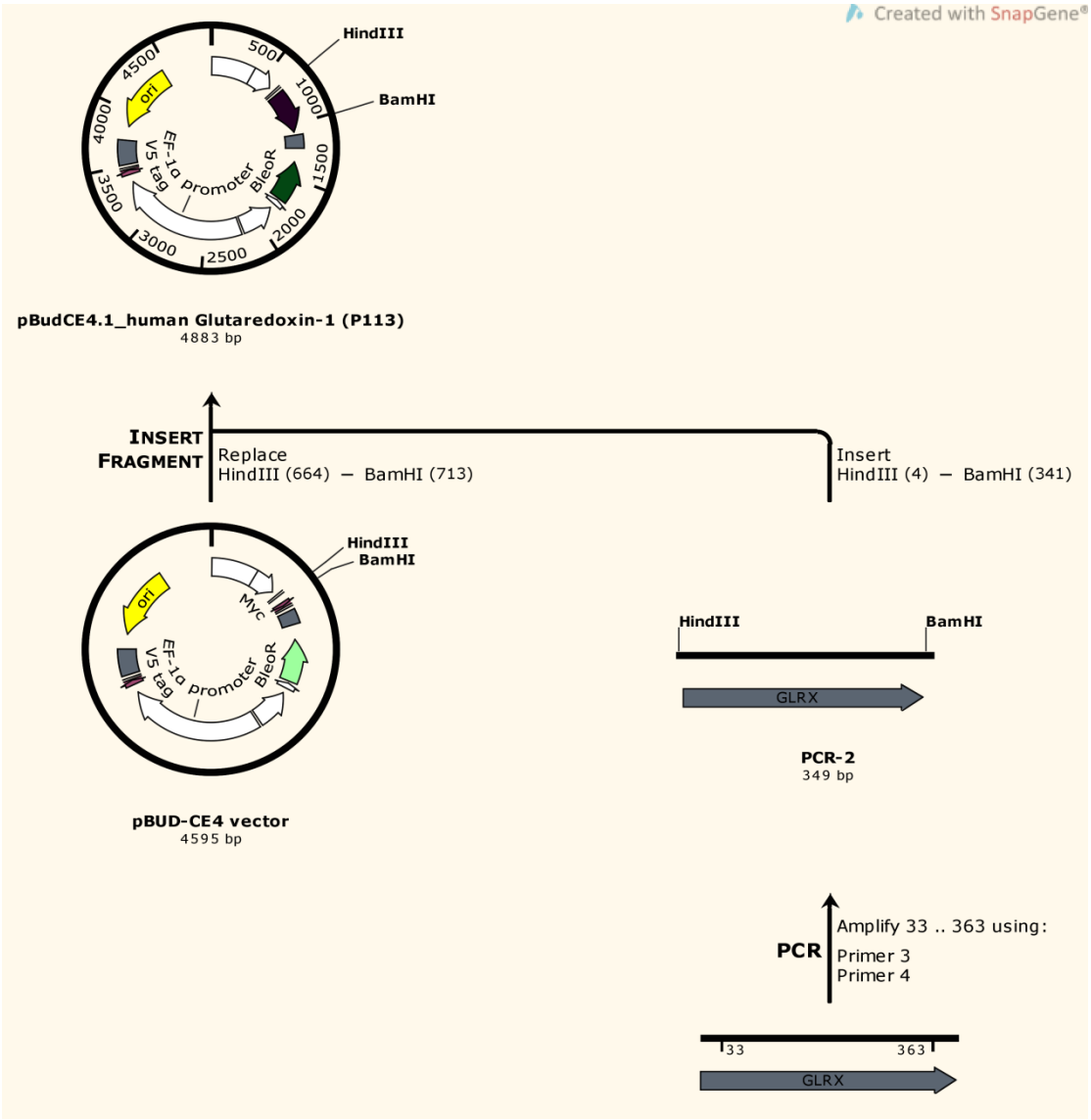

Fig. 7
Schematic cloning of glutaredoxin in the pBUD-CE4 vector. Glutaredoxin was reversibly transcript from a cDNA template ("amplify 33 .. 363") using the following primers GCGAAGCTTGCAGCCCATCGCCATGGCT (primer 1) and CGCGGATCCCTGCAGAGCTCCAATCTGC (primer 2). After isolation from an agarose gel, the amplicon was digested with HindIII and BamHI. The same restriction enzymes were then employed for digestion of the pBud-CE4 vector (Thermo Fisher Scientific). Eventually, the two fragments were ligated. Numbers next to restriction enzymes names represent the positions that the enzymes digested either the vector or the amplicon.

Table 5: FoxO1 and glutaredoxin plasmids

Plasmids	Vector	Assay
WT FoxO1 FoxO1 cysteine-deficient mutants	pcDNA3.2/capTEV-NT/V5-DEST	Luciferase Western blotting RT-qPCR
WT FoxO1 FoxO1-ΔCys-1-7	pcDNA/DEST53	EMSA
WT FoxO1 FoxO1-ΔCys-1-7	pEGFP-C1	Localization
Glutaredoxin Glutaredoxin cysteine-deficient mutants	pBUD-CE4	Western blotting EMSA

2.1.3 General materials

Table 6: Kits

Kit	Provider	Catalog Number
4x SuperSignal West PICO	Thermo Fisher Scientific	34080X4
BCA Protein Assay	Thermo Fisher Scientific	23227SPCL
Chemiluminescent Nucleic Acid Detection Module Kit	Thermo Fisher Scientific	89880
Dual-Luciferase® Reporter Assay System	Promega	E1960
LightShift EMSA Optimization and Control Kit	Thermo Fisher Scientific	EN0521
Nuclear Extract Kit	Active Motif	40010
Phusion Site-Directed Mutagenesis	Thermo Fisher Scientific	F541
RNase-free DNase set	QIAGEN	79254
RNeasy Mini Kit	QIAGEN	74104
SuperSignal West Femto Max	Thermo Fisher Scientific	34096

Table 7: Antibodies

Antibody	Species	Provider	Catalog Number
Anti-V5 Epitope Tag	Rabbit (pc)	Merck-Millipore	AB3792
b-Actin (13E5)	Mouse (mc)	Cell Signaling	3700
Pierce Glutathione (D8)	Mouse (mc)	Thermo Fisher Scientific	MA1-7620
Myc-Tag (9B11)	Mouse (mc)	Cell Signaling	2275
anti-mouse IgG-HRP (sec.)	-	Santa Cruz Biotechnology	sc-2005
anti-rabbit IgG-HRP (sec.)	-	Santa Cruz Biotechnology	sc-2004

(pc) polyclonal and (mc) monoclonal antibody; (sec.) secondary antibody

Table 8: Sequences of primers for reverse transcriptase quantitative-PCR

Gene	Species	Primer's Sequence in 5' → 3' direction
act-1	*C. elegans*	ATCAAGATCATCGCCCCACC (fwd) GCCGGACTCGTCGTATTCTT (rev)
ctl-1	*C. elegans*	TCGTTCATGCCAAGGGAGC (fwd) GATCCCGATTCTCCAGCGAC (rev)
ctl-2	*C. elegans*	GAAGGTGTTGGATACCGGGG (fwd) GGATGAGTGCCTTGACACGA (rev)
egl-1	*C. elegans*	AGATCAGCAGCATCGGCTAC (fwd) CATGGGCCGAGTAGGACATC (rev)
gcs-1	*C. elegans*	TGTGAACGTCGATGAAGCCA (fwd) TCCACGGAAGATTGGTGTGG (rev)
gei-7	*C. elegans*	CTGCCATCTCCGTGGTATCC (fwd) ACCCATGTTCCATCGTGTCC (rev)
gst-4	*C.elegans*	GCCCGTGATGATTTCTTGGC (fwd) GCCCAAGTCAATGAGTCTCCA (rev)
gst-10	*C.elegans*	ATCCAACGAGCAAGAGGCAA (fwd) ACTTCACTAGAGCCTCCGGG (rev)
sod-3	*C.elegans*	CCACCTGTGCAAACCAGGAT (fwd) TGCAAGTAGTAGGCGTGCTC (rev)
trx-1	*C.elegans*	ATGTCGATGAAGCGGAAGAT (fwd) TTTGACGCAGTTCGTCCTC (rev)
trxr-1	*C.elegans*	CAAGCGACAGCCGAGACAA (fwd)

		ACTCGCTGCTACTCCCATAGA (rev)
trx-2	*C.elegans*	CTCAACCGTCGGGTTAACTG (fwd) TCGATCGAATCTTCTCCATGT (rev)
mtl-1	*C.elegans*	TCATGGCTTGCAAGTGTGAC (fwd) CACAGCAGTACTTCTCACAACACTT (rev)
g6pc	*H. sapiens*	TTCCCTGTAACCTGTGAGACTG (fwd) AGATGGAAAGAGTAGATGTGACCAT (rev)
selP	*H. sapiens*	GGAGCTGCCAGAGTAAAGCA (fwd) ACATTGCTGGGGTTGTCAC (rev)
foxo1	*H. sapiens*	TTCCTTCATTCTGCACACGA (fwd) TGAAAGACATCTTTGGACTGCTT (rev)
HPRT-1	*H. sapiens*	GGGGACATAAAAGTAATTGGTGGAG (fwd) CTGACCAAGGAAAGCAAAGTCTG (rev)

(fwd) forward and (rev) reverse primer

Table 9: Chemicals and/or Reagents

Chemical and/or Reagent	Provider	Catalog Number
2-Mercaptoethanol	Sigma-Aldrich	M3148
2-Vinylpyridine 97%	Sigma-Aldrich	132292
3-(4,5-dimethylthiazol-2-yl)-2,5-diphenyltetrazolium bromide (MTT)	Sigma-Aldrich	M2128
5-Sulfosalicylic acid dihydrate	Sigma-Aldrich	S2310
5,5-dithio-bis-(2-nitrobenzoic acid) DTNB (Ellman's Reagent)	Carl Roth	6334.2
100x Halt Phosphatase Inhibitor Cocktail	Thermo Fisher Scientific	78420
100x Halt Protease Inhibitor Cocktail	Thermo Fisher Scientific	87786
Acrylamide/Bisacrylamide Rotiphorese® Gel 30	Carl Roth	3029.1
Agar-Agar BioScience	Carl Roth	6494.4
Agar Bacteriology grade	AppliChem	A0949
Ammonium acetate	Carl Roth	T872.1
Ampicillin sodium salt	Sigma-Aldrich	A9518
Boric acid	Carl Roth	6943.1
Bromophenol blue	Carl Roth	A512.1
BSA (fatty acid free)	Sigma-Aldrich	A8806
Calcium chloride dihydrate	AppliChem	A3587
Cholesterol	Sigma-Aldrich	C3045
Dimethyl sulfoxide (DMSO)	Carl Roth	A994.1
Ethanol (96%)	VWR	20821.310
Ethylenediamine tetraacetic acid disodium salt dehydrate (EDTA)	Carl Roth	8043.2
Glutathione Reductase from baker's yeast (S. cerevisiae)	Sigma-Aldrich	G3664
Glycerin	Carl Roth	7530.4
di-Potassium hydrogen phosphate	Carl Roth	P749.1
Glycine	Carl Roth	0079.4
IPTG dioxane-free	Thermo Fisher Scientific	R0392
Isopropanol	Carl Roth	CP41.4
HybondTM-NX	Amersham Biosciences	RPN303 T
Hydrochloric acid 25 %	Carl Roth	6331.3
LB Broth Base (Lennox L Broth Base)	Invitrogen	00006232
L-Glutathione reduced	Sigma-Aldrich	G6529
L-Glutathione oxidized	Sigma-Aldrich	G4376

Magnesium sulphate heptahydrate	Carl Roth	P027.1
Methanol	VWR	20864.320
Milk powder	Carl Roth	T145.3
Sodium chloride	Carl Roth	3957.2
NADPH tetrasodium salt	Carl Roth	AE14.3
NP-40/Igepal CA-630	Sigma-Aldrich	I7771
Pepton	Carl Roth	8952.2
Potassium dihydrogen phosphate	Carl Roth	3904.1
PVDF membrane 0.2 µm	Roche	03 010 040 001
PVDF membrane 0.45 µm	Carl Roth	T830.1
Nystatin 2-hydrate	AppliChem	A3811
SDS pellets	Carl Roth	CN30.3
Sodium-deoxycholate	Sigma-Aldrich	D6750
SsoAdvanced™ Universal SYBR® Green Supermix	BioRad	172-5275
Streptavidin Magnetic Beads	New England Biolabs	S1420S
Streptomycin sulfate	AppliChem	A1852
Triethanolamine	Carl Roth	6300.1
Tris	Carl Roth	5429.3
Tris-HCl	Carl Roth	9090.3
Tween-20	Sigma-Aldrich	P1379
TRIzol® Reagent	Life Technologies	155966026
Yeast extract	Sigma-Aldrich	70161

2.1.4 Buffers and solutions

C. elegans-related general buffers and maintenance

Calcium phosphate buffer (pH 6.0): 200 mM K_2HPO_4, 800 mM KH_2PO_4

Nystatin: 10 mM nystatin, 3.75 M ammonium acetate, 50% v/v ethanol

S-basal (pH 6.0): 100 mM NaCl, 0.1 w/v K_2HPO_4, 0.6 w/v mM KH_2PO_4

NGM plates: 17% w/v Agar-Agar, 2.5% w/v Pepton, 3% w/v NaCl, 0.05% v/v of 1 M CaCl2, 0.1% v/v of 5 mg/ml of Cholesterol, 0.1% v/v of 1 M MgSO4, 2.5% v/v of Calcium phosphate buffer, 0.5% v/v of Nystatin

DYT (bacterial growth medium): 16% w/v Pepton, 5% w/v NaCl, 10% w/v Yeast extract

LB medium: 20% w/v LB Broth Base

LB-agar plates: LB medium, 12% w/v Agar

MTT assay

MTT Solution: 5 mg/ml MTT in PBS

Solubilization reagent: 37% HCl/Isopropanol at a ratio 1/1000, (HCl 0.01 N/Isopropanol)

Western blotting analysis

RIPA buffer: 50 mM Tris-HCl (pH 8.0), 150 mM NaCl, 1% v/v NP-40/Igepal CA-630, 0.5% w/v Na-deoxycholate, 0.1% w/v SDS
2x Laemmli buffer: 125 mM Tris-HCl (pH 6.8), 20%v/v Glycerin, 4%w/v SDS, 10%v/v β-mercaptoethanol, 0.01%w/v Bromophenol blue
Separation Gel buffer: 1.5 M Tris-HCl (pH 8.8), 0.4%w/v SDS
Stacking Gel buffer: 0.5 M Tris-HCl (pH 6.8), 0.4%w/v SDS
10x Running buffer (pH 8.3): 1.92 M glycine, 250 mM Tris, 1%w/v SDS
10x Transfer buffer (pH 8.3): 1.92 M glycine, 250 mM Tris
1x Transfer buffer (working solution): 1x Transfer buffer, 20%v/v methanol
10x Tris-buffered saline (TBS) (pH 7.5): 1 M Tris (pH 7.6), 1.5 M NaCl
1x TBS-T (working solution): 1x TBS, 0.1%v/v Tween 20
Blocking solution: 5%w/v milk in 1x TBS
Primary antibody: 0.5% w/v milk or BSA in 1x TBS-T, primary antibody diluted 1:1000
Secondary antibody: 0.5% w/v milk in 1x TBS-T, secondary antibody diluted 1:5000

Electrophoretic mobility shift assay (EMSA)

5x TBE buffer: 450 mM Tris, 450 mM boric acid, 10 mM EDTA

2.2 Methods

2.2.1 *C. elegans* maintenance and synchronization

Nematodes were grown and maintained at 20°C on nematode growth medium (NGM) agar plates spotted with *E. coli* OP50 as food source, as described elsewhere [1]. For maintenance, at least five L4 larval stage nematodes were transferred routinely every fifth (in case of *skn-1*-deficient mutants every seventh) day. Synchronization of worms was performed by washing out maintenance plates with double-distilled H_2O, followed by centrifugation (1300x*g*, 1 minute, room temperature) to separate the eggs from the nematodes. The last step was performed at least twice. The obtained eggs were then transferred to fresh NGM agar plates and allowed to hatch. 64 hours post-hatching, nematodes were transferred to fresh NGM agar plates containing the respective compounds and processed for the respective assay, as described elsewhere.

2.2.2 Life span assays

Life span analyses were performed at 20°C. Age-synchronized, 64 hours old nematodes were manually transferred to NGM agar plates spotted with *E. coli* OP50 and supplemented with the respective compound or solvent. In case of life span analyses with heat-inactivated bacteria, *E. coli* OP50 were inactivated for 45 minutes at 65°C. For the first 10 days, worms were transferred daily to avoid overcrowding and for separation of adults nematodes from their offspring. Only in case of *skn-1*-deficient strain, nematodes were transferred only on day 7 and day 10. Following the reproductive period, nematodes were transferred every second day. From the beginning of day 12 and onwards, nematodes were transferred to NGM agar plates containing 200 µg/ml of streptomycin, the respective compound or solvent, and covered with the streptomycin-resistant *E. coli* strain OP50i to avoid contamination. Worms showing no movement, no reaction to gentle stimulation and no pharyngeal pumping were scored as dead. Worms lost or disintegrated due to internal hatchings were censored. Experiments were performed in quintuplicates for at least two independent times, unless stated otherwise.

2.2.3 DTNB assay

Age-synchronized, 64 hours old wild-type worms were washed with S-basal, followed by centrifugation (200x*g*, 1 minute, room temperature). That step was repeated twice and thereafter nematodes were transferred to NGM agar plates containing the respective compounds and spotted with *E. coli* OP50 for up to 3 hours. Nematodes were then washed out of the plates, centrifuged (200x*g*, 1 minute, room temperature) once and pellets were shock-frozen in liquid nitrogen. Shock-frozen pellets were lysed by grinding in liquid nitrogen and adding 250 µL of S-basal containing proteinase inhibitors. After sonication (7 cycles, 70% power, 5 seconds), the lysed pellets were centrifuged (12000x*g*, 5 minutes, 4°C) and supernatants containing thiols were collected. Amounts of thiols were assessed by convention of Ellman's reagent, 5,5′-dithiobis (2-nitrobenzoic acid) (DTNB), to TNB^{2-} [208]. Absorbance of thionitrobenzoate released was measured at 412 nm, related to GSH standards and normalized to protein content of each lysate. Protein content of lysates was assessed using Bradford solution [209]. Absorbance was measured with a CLARIOstar plate reader (BMG LABTECH, Baden-Württemberg, Germany).

2.2.4 RNA extraction and RT-qPCR in *C. elegans*

Age-synchronized, 64 hours old wild-type worms were distributed to NGM agar plates supplemented with the respective compounds and spotted with *E. coli* OP50. In case of *gcs-1*-specific RNA interference (RNAi) experiments, nematodes were distributed to NGM agar plates containing 1 mM isopropyl-β-D-thiogalactoside (IPTG), 100 µg/ml ampicillin and, if necessary, 12.5 µg/ml tetracycline and spotted with *E. coli* HT115 containing L4440 empty vector or L4440 carrying a *gcs-1* cDNA fragment. Nematodes were then washed daily, without centrifugation, and transferred to fresh NGM agar plates containing the respective compounds, until the day of harvesting as indicated. Worm pellets were collected and shock-frozen in liquid nitrogen.

Total RNA was isolated using TRIzol reagent and thereafter DNA hydrolysis on-column was performed using RNEasy Mini Kit and RNase-Free DNase (QIAGEN). RNEasy Mini kit was used according to the manufacturer's instructions; incubation with DNase was performed according to the manufacturer's instructions, with minor modifications (mixture of 5 µl of RNase-free DNase I and 35 µl of RNase-free Buffer RDD was employed for 30 minutes at room temperature). The RNA content was assessed spectrophometically using a SPECTROstar^{NANO} plate reader (BMG LABTECH). 500 ng of RNA was reversely transcribed using RevertAid Reverse Transcriptase (Thermo Scientific) according to the manufacturer's instructions. The resulting cDNA template was diluted 1:2 in RNase-free water and then subjected to qPCR analysis using SsoAdvanced Universal SYBR Green Supermix (5 µl SYBR Green, 0.2 µl of a 5 µM forward primer, 0.2 µl of a 5 µM reverse primer, and 1µl of the diluted cDNA template for 40 cycles at an annealing temperature of 60°C) and a CFX Connect cycler (BioRad Laboratories, Kabelsketal, Gernamy). The employed pairs of primers are described in table 7.

2.2.5 Bacterial growth assay

From Lysogeny broth (LB) containing agar plates freshly streaked with *E. coli*, a single colony was picked and inoculated in a glass tube containing 5 ml of LB medium overnight at 37°C under constant shaking of 150 rpm. Next day, from the initial inoculum an appropriate amount to achieve an optical density of 0.5 (OD 600 nm) was pipetted in an Erlenmeyer flask containing 50 ml of LB medium and bacteria grew at 37°C under constant shaking of 150 rpm for 5 hours. Respective compound or solvent was administrated in the lag or just before the exponential phase. Optical density (OD 600 nm) was measured every 20 minutes in cuvettes using SPECTROstar^{NANO} plate reader (BMG LABTECH).

2.2.6 Maintenance of cell cultures and seeding

HEK293 and HepG2 cells were held at 37°C in a humidified atmosphere with 5% v/v CO_2 and cultured in low glucose Dulbecco's modified Eagle's medium (DMEM) supplemented with 10% v/v fetal calf serum and 1% v/v penicillin/streptomycin (100 units/ml and 0.1 mg/ml, respectively). In case of HepG2 cells, medium was additionally supplemented with 1% v/v non-essential amino acids. Cell lines were routinely split as soon as they have reached approx. 90-100% confluence. Upon 90-100% confluence, cells were washed once with prewarmed PBS and trypsinized either for 1 (for HEK293 cells) or 5 (for HepG2 cells) minutes. Trypsinization was performed at 37 °C in a humidified atmosphere with 5% v/v CO_2 and cells were then resuspended in the respective prewarmed DMEM. A certain amount of cell suspension was transferred to a new flask containing the respective prewarmed fresh DMEM and placed back to the incubator.

Fully confluent 75 cm^2 flasks containing HEK293 or HepG2 cells were trypsinized as described above and cells were then resuspended to a final volume of 10 ml of the respective prewarmed DMEM. Cells were then seeded: (a.) in the wells of a 6-well plate in a final volume of 1 ml/well for localization experiments, luciferase reporter assays, expression of target genes, viability assay and western blotting analysis, (b.) in 60 mm dishes in a final volume of 5 ml/dish for GSH determination, and (c.) in 100 mm dishes in a final volume of 10 ml/dish for EMSAs and streptavidin pull downs, and thereafter were placed back in the incubator. In case of transfected cells, HEK293 were transfected with TurboFect, at a ratio 1/2 (1 µg of plasmid/2 µl of reagent). HepG2 cells were transfected with GenJet at a ratio 1/3 (1 µg of plasmid/3 µl of reagent). In both cases, incubation was performed according to the manufacturer's instructions.

2.2.7 Localization assay

Upon approx. 70% confluence post-seeding, HEK293 cells were transfected with 1 µg of plasmids encoding WT FoxO1-EGFP or FoxO1-ΔCys1-7-EGFP. Similarly, HepG2 cells were transfected with 2 µg of plasmids encoding WT FoxO1-EGFP or FoxO1-ΔCys1-7-EGFP. In both cases, a 24-hour incubation was performed according to the manufacturers' instructions. Following the incubation, analysis of each treatment was performed as followed: treatment was performed with the respective compound or solvent for up to 30 minutes in 1 ml of a prewarmed fresh serum-free DMEM followed by DMEM aspiration and subcellular localization of FoxO1-EGFP was assessed immediately on the plates; for one individual treatment representative pictures were obtained within less than 5 minutes. As soon as the acquiring of pictures for one treatment was complete, then another treatment was analyzed as

described above right after the 24-hour incubation. In both HEK293 and HepG2 cells, at least 200 cells were assessed and scored according to the predominant subcellular localization of the EGFP signal in "cytoplasm or nucleus or cytopslasm/nucleus using fluorescence microscopy (NIS-Elements microscope, Nikon; GFP filter, in excitation 475-495nm, and emission 520-560nm).

2.2.8 Luciferase assay

As soon as HEK293 cells reached 70% confluence post-seeding, they were transfected with 0.6 µg of the respective luciferase promoter constructs, 0.1 µg of renilla luciferase control plasmid and 0.6 µg of the respective FoxO1 expression plasmids or control plasmid. HepG2 cells were transfected with 0.9 µg of the respective luciferase promoter constructs, 0.15 µg of renilla luciferase control plasmid and 0.9 µg of respective FoxO expression variant plasmids or control plasmid. FoxO1 expression plasmids contained a biotin and a V5 tag. In both cases a 24-hour incubation was performed according to manufacturers' instructions. Following the incubation cells were lysed on ice with lysis buffer provided by a Dual-Luciferase® Reporter Assay System kit (Promega), according to the manufacturer's instructions. 10 µl of each sample was then analyzed in a 96-well plate according manufacturer's instructions, with minor modifications (50 µl of Luciferase Assay Reagent II, 50 µl of Stop & Glo® Reagent were added by pipetting). Luminescence was assessed within less than 2 minutes after the addition of the respective reagent using a CLARIOstar plate reader (BMG LABTECH).

2.2.9 RNA extraction and RT-qPCR in human cell lines

Upon approx. 70% confluence post-seeding, HEK293 cells were transfected with 1 µg of plasmids encoding WT FoxO1 or FoxO1-ΔCys1-7. Similarly, HepG2 cells were transfected with 2 µg of plasmids encoding WT FoxO1-EGFP or FoxO1-ΔCys1-7. Plasmids were tagged with biotin and V5. In both case a 24-hour incubation was performed according to the manufacturers' instructions. Following the incubation, total RNA was isolated using RNEasy Mini Kit (QIAGEN), according to the manufacturer's instructions. DNA hydrolysis using RNase-Free DNase (QIAGEN) was performed according to the manufacturer's instructions, with minor modifications (mixture of 5 µl of RNase-free DNase I and 35 µl of RNase-free Buffer RDD was employed for 30 minutes at room temperature). The RNA content was assessed spectrophotometrically using a SPECTROstar^{NANO} plate reader (BMG LABTECH). 500 ng of RNA was reversely transcribed using RevertAid Reverse Transcriptase (Thermo Scientific) according to manufacturer's instructions. The resulting cDNA template was

diluted 1:2 in RNase-free water and then subjected to qPCR analysis using SsoAdvanced Universal SYBR Green Supermix (5 µl SYBR Green, 0.2 µl of a 5 µM forward primer, 0.2 µl of a 5 µM reverse primer, and 1µl of the diluted cDNA template for 40 cycles at an annealing temperature of 60°C) and a CFX Connect cycler (BioRad Laboratories). The employed pairs of primers are described in table 7.

2.2.10 MTT assay

Upon 90-100% confluence post-seeding, HEK293 cells were treated with the respective compound or solvent for up to 30 minutes in 1 ml of a prewarmed fresh serum-free DMEM. Following the incubation, serum-free DMEM was replaced, without intermediate washing, with 1 ml prewarmed fresh serum-free DMEM containing 0.25 mg/ml of 3-(4,5-dimethylthiazol-2-yl)-2,5-diphenyltetrazolium bromide (MTT) and incubated for 2 hours in the incubator. To solubilize the resulting blue formazan precipitate, 6 ml of solubilization solution was added, followed by 30 minutes incubation on a shaker. Absorbance of the blueish solution was measured using a CLARIOstar plate reader (BMG LABTECH), at a wavelength of 570 nm. MTT conversion to the formazan was taken as representative of cell viability.

2.2.11 Glutathione determination

After seeding in 60 mm dishes and as soon as cells reached 90-100% confluence, HEK293 cells were then treated with the respective compound or solvent for up to 30 minutes in 5 ml of a prewarmed fresh serum-free DMEM. Following the treatment, cells were washed once with prewarmed PBS, harvested in 250 µl of ice-cold 0.01N HCl and stored at -20°C. Next day, cells were thawed on ice and supernatants were collected after centrifugation (1200x*g*, 10 minutes, 4°C). Total glutathione and glutathione disulfide amounts were then assessed enzymatically as described in [210] using a CLARIOstar plate reader (BMG LABTECH). Prior to that step, BCA Protein Assay kit was employed for protein determination. For glutathione determination, proteins were precipitated from the supernatant with 5% w/v 5-sulfosalicylic acid (original stock solution 20% w/v) of on ice. GSSG levels were assessed after blocking thiols with 2-vinylpyridine, using 5,5′-dithionitrobenzoic acid in the presence of NADPH and glutathione reductase.

2.2.12 Western blotting and pull down with streaptvidin beads

Upon 90-100% confluence post-seeding, HEK293 cells were treated with the respective compound or solvent for up to 30 minutes in 1 ml of a prewarmed fresh serum-free DMEM. Following the incubation, cells were washed once with prewarmed PBS and lysed in RIPA buffer supplemented with a protease and phosphatase inhibitor cocktail and 25 mM N-ethylmaleimide (NEM). Cell lysates were then sonicated (5 cycles, 70% power, 5 seconds) and supernatants were collected after centrifugation (12000x*g*, 5 minutes, 4°C). Protein determination was assessed using BCA protein assay kit according to the manufacturer's instructions. In case of transfected cells, upon approx. 70% confluence post-seeding, cells were transfected with 1 µg of FoxO1 variant plasmids or with 2 µg of either Grx-1 variant plasmids or empty pBudCE4.1 vector and incubated for 24 hours in the incubator. For transfection, a vector containing a biotinylation signal and a V5 tag (pcDNA3.2/capTEV-NT/V5-DEST) or a vector containing a myc tag (pBudCE4.1) in case of FoxO1 or Grx-1 variants were employed, respectively. Following a 24-hour incubation, transfected cells were processed as described above. In case of experiments requiring post-treatment recovery, serum-free DMEM containing the respective compound was replaced with prewarmed fresh DMEM, without an intermediate washing, and cells were incubated for the respective periods of time in the incubator.

20 µg of protein were mixed with the appropriate volume of 2x or 5x Lämmli buffer with or without β-mercaptoethanol, according to the requirements of the individual experiments and boiled at 95°C for 5 minutes. Lysates were analyzed by sodium dodecyl sulfate-polyacrylamide gel electrophoresis (SDS-PAGE) using 10% gels. Electrophoresis was performed at 80 to 100 V and thereafter the separated proteins were transferred to a PVDF membrane with 0.45 µm pores using wet (tank) blotting. Transfer was carried out at constant voltage of 100 V for 2 ½ hours at 4°C. The PVDF membrane was incubated in 5% milk dissolved in TBS (blocking solution) for 1 hour on a shaker at room temperature. Following blocking, the membrane was probed with primary antibody overnight at 4°C. The next day, the membrane was washed thrice for 5 minutes with TBS-T and incubated with the secondary antibody for at least 1 hour and again washed thrice for 5 minutes with TBS-T. All steps were carried out on a shaker at room temperature. Then, the membrane was incubated with an enhanced chemiluminescence reagent (ECL) for 1 minute and subsequent development using a ChemiDoc™ MP Image System (BioRad). Following development, the membrane was washed for at least 1 hour with TBS-T and reprobed with another primary antibody overnight at 4°C for yet another detection, as previously described. In case of detection of Grx-1 variants, 18% gels and PVDF membrane with 0.2 µm pores were employed. Transfer was performed at constant voltage of 90 V for 2 hours at 4°C.

In case of a pull down with streptavidin magnetic beads, 25 µl of the beads were added to 100 µl of a total protein lysates in RIPA buffer and the mixture was then incubated under constant rotation at 4°C overnight. Following the overnight incubation, biotinylation signal-containing proteins were pulled down according to the manufacturer's instructions (Streptavidin Magnetic Beads, New England Biolabs). Pulled down proteins were then analyzed using western blotting, as previously described.

2.2.13 Electrophoretic mobility shift assays (EMSA)

Upon approx. 70% confluence post-seeding, 5 ml of the initial 10 ml of DMEM in the dish were removed and cells were transfected with 5 µg of plasmids encoding FoxO1 variants and incubated for 24 hours in the incubator. Thereafter, transfected cells were treated with the respective compound or solvent for up to 30 minutes in 15 ml of a prewarmed fresh serum-free DMEM. Thereafter, treatment was removed and nuclear extracts were generated using a cell fractionation kit (Nuclear Extract Kit, Active Motif) according to the manufacturer's instructions. Protein content of the nuclear extracts was assessed using a BCA protein assay kit according to the manufacturer's instructions. For transfection with plasmids encoding FoxO1 or Grx-1 variants, 5 µg of each of the respective plasmid was employed. In case that co-transfection of WT FoxO1 with either Grx-1 variant plasmids or empty pBudCE4.1 vector was required, 3 µg of WT FoxO1 and 7 µg of Grx-1 variants were used. For transfection, a vector containing a GFP tag (pcDNA/DEST53) or a vector containing a myc tag (pBudCE4.1) in case of WT FoxO1 or Grx-1 variants were employed, respectively. In addition, in experiments requiring post-treatment recovery, serum-free DMEM containing the respective compound was replaced with prewarmed fresh DMEM, without an intermediate washing step, and cells were incubated for the respective time points in the incubator.

A mixture containing 1 µl 10x binding buffer, 0.5 µl of each of the following components, poly (dIdC), glycerol, NP-40, KCl (all reagents were part of the LightShift EMSA Optimization and Control Kit, Thermo), 2 µg of protein nuclear extract, 24 pmol of competitor in case it was required for the experiment, and double distilled H_2O in a final volume of 9.2 µl was incubated for 10 minutes at room temperature according to the manufacturer's instructions (LightShift EMSA Optimization and Control Kit, Thermo). Following the 10-minute incubation, 80 fmol (original stock solution 100 fmol/µl) of a biotinylated probe were added and the mixture was incubated for another 30 minutes. The biotinylated probe was a double stranded DNA with the following sequence: 5'-CAAAACAACAAAACAACAAAACAA-3', 5'-TTGTTTTGTTGTTTTGTTGTTTTG-3'. Thereafter, 2.5 µl of the loading dye was added. Samples were analyzed using a native 4.2% polyacrylamide gel, which was pre-run at constant 100 V for 1 hour. Electrophoresis was

performed at constant 30 mA for up to 5 hours on ice. Following electrophoresis, transferring to a pre-equilibrated hybond membrane (HybondTM-NX, Cat. No. CRPN303 T, Amersham Biosciences) was at constant 100 V for 15 minutes on ice. Post-transfer, crosslinking of the membrane was performed under ultraviolet light (312 nm, VL-6.LM bulb, Biotechnologie GmbH) in approx. 2 cm distance for 10 minutes and the membrane was then processed for detection using a Chemiluminescent Nucleic Acid Detection Module Kit (Thermo) according to the manufacturer's instructions. Development of the membrane was performed using the ChemiDoc^{TM} MP Image System (BioRad).

Ms. Maria Landrock, M. Sc., contributed to viability assay (twice), GSH determination (twice), the western blotting analysis of the WT FoxO1 and FoxO-ΔCys1-7 (twice) and the establishment of the electrophoretic mobility shift assay (EMSA).

3. Results

3.1 DEM treatment leads to depletion of total thiols in *C. elegans*

Initially, effects of different DEM concentrations on the thiol status in *C. elegans* were assessed (Fig. 8). DEM is an α,β-unsaturated carbonyl compound able to form adducts with thiols and to serve as a substrate for glutathione S-transferases, meaning that it can deplete but not necessarily oxidize GSH [200].

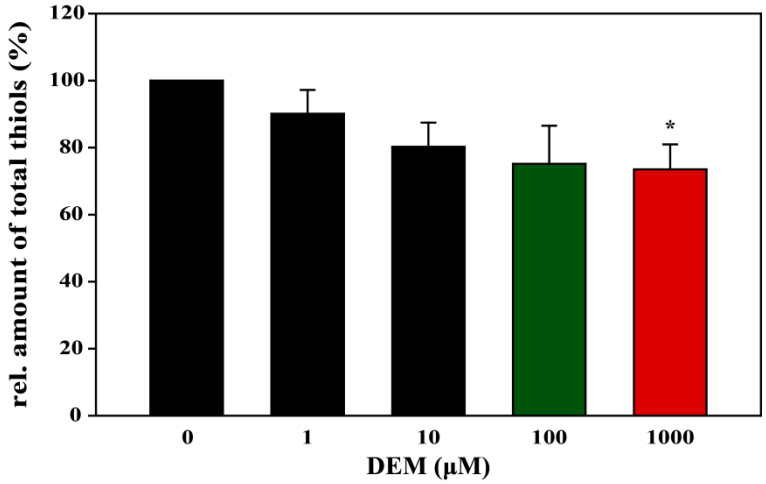

Figure 8:
DEM-induced depletion of total thiols in *C. elegans*. Age-synchronized, 64 hours old wild-type worms were transferred to NGM agar plates containing the respective DEM concentration or solvent (DMSO 0.1% v/v). Following a 3-hour incubation, the total amount of thiols was assessed using DTNB. Thiol/protein level ratios were calculated and normalized against the control (0 µM DEM), which was set to 100%. Data are presented as means +SEM from 3 independent experiments. *$p<0.05$ as compared to control; Student´s t-test.

Although exposure to low DEM concentrations (up to 10 µM) led to a non-significant depletion of total thiols, an approximate 25% decrease in thiol content was detected upon exposure of worms to higher DEM concentrations (up to 1 mM). No real concentration-dependent pattern in thiol depletion was detected at 100 µM DEM and above, but treatment with 1 mM DEM induced statistically significant thiol depletion (Fig. 8). As DEM was able to deplete thiols in *C. elegans*, we further investigated the effect of DEM exposure on *C. elegans* life span.

3.2 Mild thiol depletion may enhance *C. elegans* life span

To test for the effect of thiol depletion on *C. elegans* life span, worms were exposed to different DEM concentrations and the consequence for life span was assessed (Fig 9).

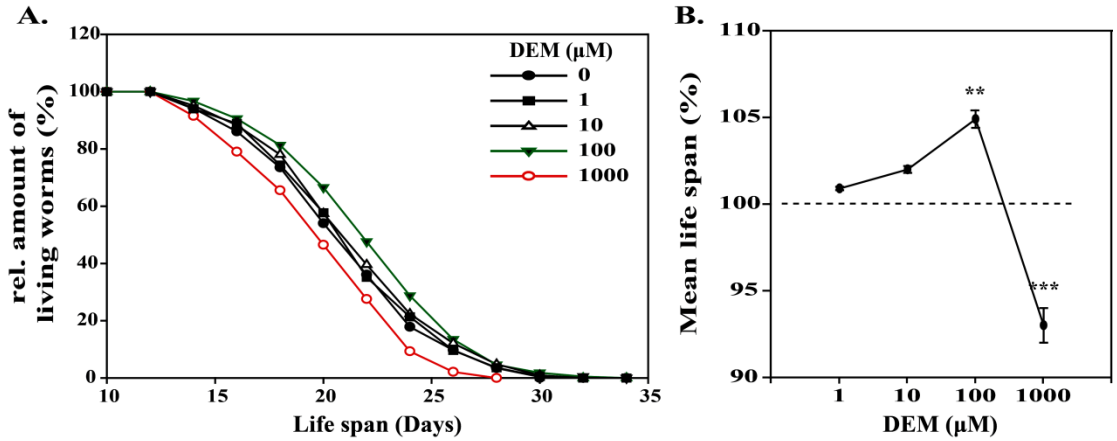

Figure 9:
Effects of DEM treatment on *C. elegans* life span. (A) Representative life span curve of an individual experiment and (B) overall mean life span of three experiments are depicted. Age-synchronized, 64 hours old wild-type nematodes were transferred to NGM agar plates containing the respective DEM concentration or solvent (DMSO 0.1% v/v), and their survival rates was monitored at 20°C. Experiments were carried out in quintuplicates and were performed thrice. (A) 100 µM (green) $p<0.01$ and 1 mM (red) $p<0.001$ as compared to control (0 µM black); log-rank test. (B) Data are presented as means ±SEM from 3 independent experiments; control (DMSO 0.1%v/v treatment) was set to 100%; **$p<0.01$ as compared to control; ***$p<0.001$ as compared to control; Student´s t-test.

In line with the observed thiol alterations (Fig. 8), administration of low DEM concentrations (up to 10 µM) did not significantly affect life span. However, exposure of worms to 100 µM DEM significantly increased both mean and maximum life span. In contrast to the 100 µM-mediated deceleration of ageing, exposure to 1 mM DEM shortened nematode life span, leading to a non-linear impact of thiol depletion on *C. elegans* life span (Fig. 9). It should be noted that, because no significant difference in overall thiols (Fig. 8) was detected between 100 µM and 1 mM DEM (concentrations that caused alterations of *C. elegans* life span), total amounts of thiols might not be the most suitable marker to determine effects that thiol modulating agents could potentially have on *C. elegans* viability. As *C. elegans* was held and grown on bacteria, and as bacterial viability is known to affect *C. elegans* life span, we tested whether the observed effect might be due to an interaction of DEM with the thiols of bacteria. We therefore analyzed bacterial growth in the presence of DEM (Fig. 10) and determined *C. elegans* life spans using heat-inactivated bacteria (Fig. 11).

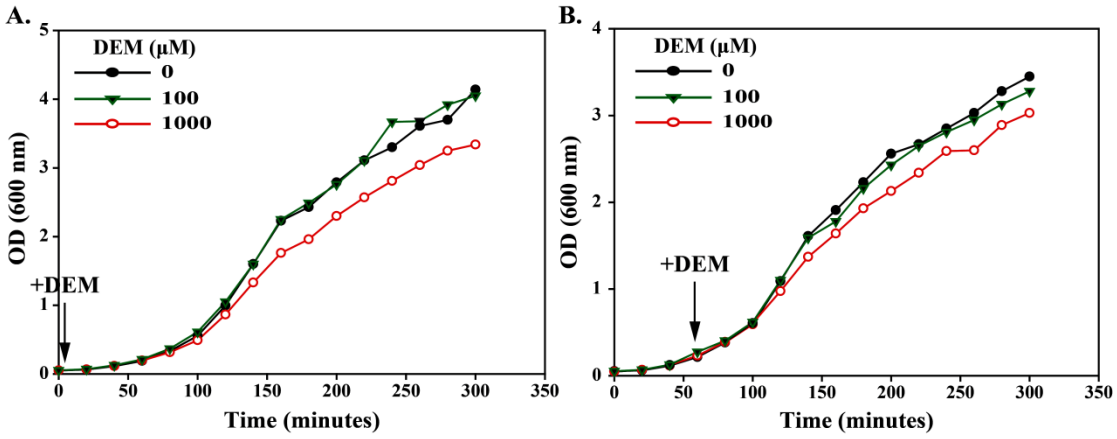

Figure 10:
Effect of DEM exposure on OP50 *E. coli* growth. The effect of 100 µM (green) and 1 mM (red) DEM or solvent (DMSO 0.1% v/v; black line) when administrated in (A) the lag or (B) just before the exponential phase of growing bacterial inocula (OP50 *E. coli*) was studied at 37°C. Each graph is representative of an individual experiment; each experiment was performed twice and same results were acquired.

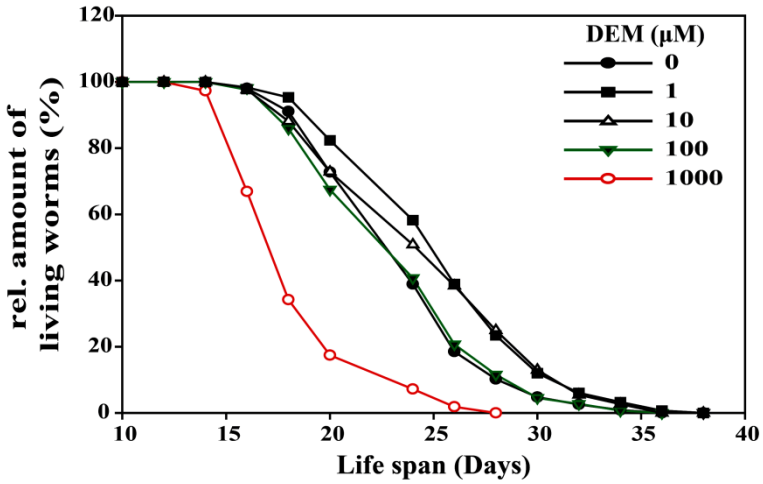

Figure 11:
Effect of DEM exposure on *C. elegans* life span, upon feeding with heat-inactivated bacteria. The life span curves of an individual experiment are depicted. Age-synchronized, 64 hours old wild-type nematodes were transferred to NGM agar plates containing the respective DEM concentration or solvent (DMSO 0.1% v/v), and their survival rates was monitored at 20°C. Experiment was carried out in quintuplicates and was performed twice; same results were acquired. 100 µM DEM (green) n.s and 1 mM DEM (red) $p<0.001$ as compared to control (black 0 µM DEM); log-rank test.

Administration of 100 µM DEM either in the lag (Fig. 10A) or just before the exponential phase (Fig. 10B) did not affect bacterial growth. In contrast, exposure to 1 mM DEM inhibited bacterial growth. Moreover, in worms fed with heat-inactivated bacteria, exposure to DEM at concentrations as low as 10 µM increased both mean and maximum life span; but treatment with 1 mM DEM significantly diminished life span. Exposure to 100 µM did not significantly affect *C. elegans* life span (Fig. 11). We hypothesized that DEM was not actively taken up by bacteria and thus more of the compound was potentially available for the worms, which might explain the somewhat shifted hormetic effect, since less than 100 µM DEM might be required to promote deceleration of ageing. Since low DEM concentrations

did not affect bacteria, implying that worms were not held under an "artificial" caloric restriction at these DEM concentrations, we further investigated the mechanism underlying the life span modulating effect of DEM. For the upcoming experiments, we mainly focused on DEM concentrations causing alterations in *C. elegans* life span (100 µM or 1 mM DEM), while worms were fed with living bacteria.

3.3 Low-dose-DEM elicited *C. elegans* life span extension through DAF-16 and SKN-1

To identify the mechanism underlying the DEM-driven effect *C. elegans* life span extension, the potential contribution of DAF-16 and SKN-1 was investigated (Fig. 12). We hypothesized that the DEM-mediated effects in *C. elegans* life span might be triggered by increased stress resistance. DAF-16 and SKN-1, *C. elegans* homologues of FoxO and Nrf-2 respectively, are two transcription factors of major importance in the regulation of stress resistance and longevity. Therefore, we employed two distinct strains in which either *daf-16* or *skn-1* were inactivated [155, 204].

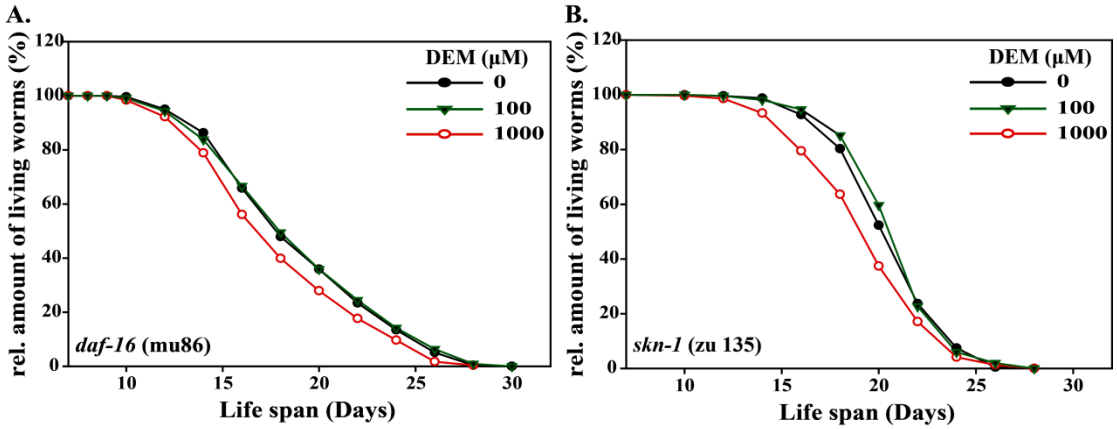

Figure 12:
Contributions of DAF-16 and SKN-1 to DEM-mediated effects on *C.elegans* life span. Representative life span curve of an individual experiment of (A) *daf-16* (mu86)-deficient and (B) *skn-1* (zu 135)-deficient mutants are depicted. Age-synchronized, 64 hours old type nematodes were transferred to NGM agar plates containing 100 µM (green) or 1 mM (red) DEM concentration or solvent (DMSO 0.1% v/v; black), and their survival rates was assessed at 20°C. Experiments were carried out in quintuplicates. Experiments with 100 µM DEM were performed (A) thrice and (B) twice; 1 mM DEM was only analyzed in one experiment in both cases. (A.) 100 µM DEM n.s and 1 mM DEM $p<0.01$ as compared to control (black); log-rank test. (B.) 100 µM, n.s and 1 mM $p<0.001$ as compared to control; log-rank test.

The increase in life span induced by 100 µM DEM in wild type worms was abolished, whereas the toxic effect (1 mM DEM) was not alleviated in the *daf-16*-deficient mutant (Fig. 12A). A similar observation was obtained in the *skn-1*-deficient mutant (Fig. 12B). Therefore, the 100 µM-induced effect of DEM, but not the one elicited by 1 mM, might require both transcription factors to be mediated. To further evaluate the obtained result, the expression levels of various DAF-16 and/or SKN-1 target genes in *C. elegans* were analyzed.

3.4 Low-dose-DEM dose caused upregulation of DAF-16 and SKN-1 target genes

We analyzed the expression of genes known to be modulated by DAF-16 and SKN-1, mainly focusing on genes which could contribute to antioxidant defense and stress response (Fig. 13). Target genes, such as *ctl-1*, *sod-3*, *gei-1* (also known as *icl-1*) are known to be regulated by DAF-16 [60, 62]. Moreover, *gcs-1*, *gst-4*, and *gst-10* are mainly regulated by SKN-1 [76]. Since both DAF-16 and SKN-1 are downstream targets of insulin/IGF-1, they often share target genes, such as *ctl-2* [60, 81]. As DEM-driven thiol depletion and oxidative stress might induce DNA damage, we also studied the mRNA levels of *egl-1*, a gene regulated by CEP-1, the *C. elegans* p53 homolog [211].

In line with the results obtained by the *daf-16* or *skn-1*-deficient mutants, upregulation of DAF-16 or SKN-1 target genes was detected in nematodes treated with 100 µM DEM. In contrast, no significant alteration was observed upon exposure to 1 mM DEM (Fig. 13). The majority of peak mRNA levels was detected after 3-7 days of 100 µM DEM treatment, which is in line with an adaptive response being induced by low DEM concentrations, resulting in upregulation of antioxidant genes as well as genes involved in GSH metabolism. In contrast to the upregulation of both DAF-16 and SKN-1 target genes upon treatment with 100 µM DEM, exposure to 1 mM strongly upregulated *egl-1* mRNA levels (Fig. 13H). Exposure to 1 mM DEM seemed to cause damage to an extent that induction of DAF-16/SKN-1-dependent genes was no longer possible and thus signaling processes related to programmed cell death were stimulated.

In addition to the reduction in total thiols, DEM successfully depleted GSH following a 5-day exposure [204]. According to the time course, DEM seemed to initially create adducts with protein thiols and thereafter with GSH, meaning that the use of DEM might not be the optimal approach to identify potential contributions of GSH to regulation of *C. elegans* life span. To further elucidate the role of GSH, we genetically manipulated GSH biosynthesis.

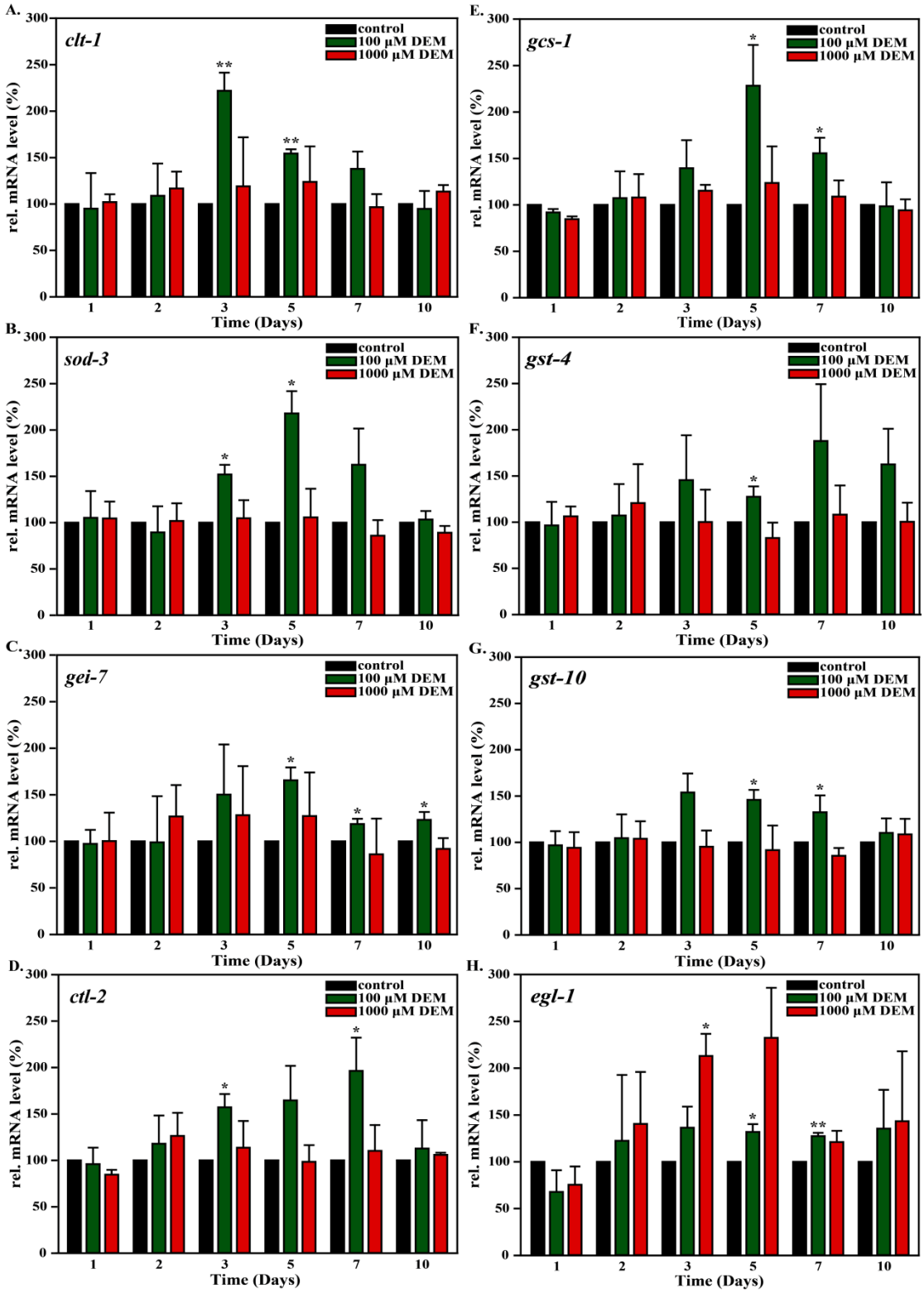

Figure 13:
Expression of DAF-16 and SKN-1 target genes in *C.elegans* exposed to DEM. Relative mRNA level of (A.-C.) predominantly DAF-16-regulated genes, (E.-G.) predominantly SKN-1-regulated genes (D.) *ctl-2* is regulated by both transcription factors, and (H.) *egl-1*, a p53-regulated gene, are depicted. Age-synchronized, 64 hours old wild-type nematodes were exposed to 100 µM (green), 1000 µM (red) DEM concentration or solvent (DMSO 0.1% v/v, black), for the indicated time points at 20°C. Thereafter nematodes were harvested and RNA was isolated. The mRNA levels were determined using RT-qPCR and normalized over *act-1* mRNA levels (a housekeeper gene); DMSO control was then set to 100. Data are means of 3 independent experiments + SEM (*p<0.05 as compared to control; **p<0.01 as compared to control; Student´s t-test).

3.5 Regulation of redox-related genes upon attenuation of GSH biosynthesis

To attenuate GSH *de novo* biosynthesis, we directly knocked out *gcs*-1 mRNA, using an RNAi approach. In *C. elegans*, g*cs-1* encodes for the catalytic subunit of GCS-1, the rate-limiting enzyme in GSH biosynthesis. In addition to a significant GSH reduction, administration of *gcs-1*-specific RNAi to L4 adult nematodes throughout the entire life span enhanced stress resistance which in turn led to a significant increase in mean and maximum life span [204]. To test whether the DEM-like effects of GSH depletion had similar downstream targets, *ctl-1*, *sod-3*, and *gst-4* regulation was investigated. Moreover, the potential contribution of genes encoding either members of the thioredoxin-dependent redox system, such as *trx-1*, *trxr-1*, and *trxr-2* or proteins highly enriched with cysteine residues, such as metallothioneins (*mtl-1*), was also assessed (Fig. 14) [212, 213].

Initially, and as expected, administration of *gcs-1*-specific RNAi successfully downregulated *gcs-1* expression as compared to nematodes fed with the empty control vector L4440 (Fig. 14A). Inhibition of *gcs-1* did not significantly affect the expression level of DAF-16 target genes, such as *sod-3*, and *ctl-1* (Fig 14B and C). In contrast, remarkable upregulation in the expression of genes encoding for proteins that could potentially complement the action of GSH, such as thioredoxins or metallothioneins, which in turn could contribute to antioxidant protection and redox regulation of cellular processes was detected (Fig. 14E-H).

Although, low-dose-DEM mediated (a.) depletion of glutathione (data not shown) and (b.) elevation in the expression of DAF-16 and SKN-1 transcriptional targets evolved in *C. elegans* antioxidant defense (Fig. 13), a direct manipulation of GSH, causing an approximate 50% depletion (data not shown), DAF-16 transcriptional activity was not significantly affected (Fig 14B and C). Since DEM can also form adducts with cysteine residues of proteins, leading to depletion of overall thiols (Fig. 8), we further investigated whether direct manipulation of cysteine residues of FoxO1, the mammalian DAF-16 homolog, may affect several aspects of FoxO1, such as cytoplasmic-nuclear shuttling, DNA binding, and transactivation activity.

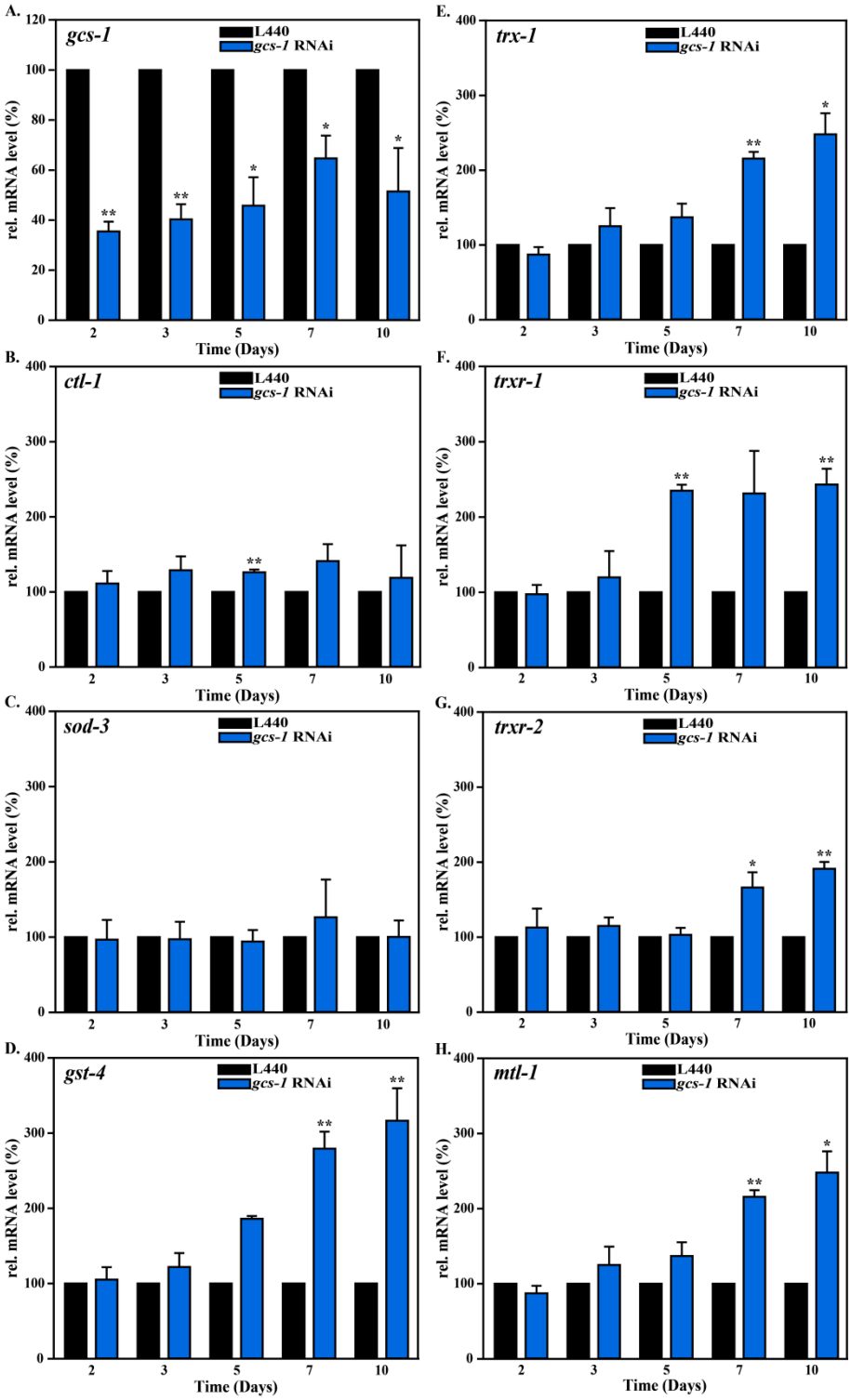

Figure 14:
Expression of DAF-16 and SKN-1 target genes and other redox-modulated genes following *gcs-1* depletion in *C.elegans*. Relative mRNA levels of (B.-D.) predominantly DAF-16 or SKN-1-regulated genes, (E.-H.) redox-modulated genes/thioredoxin system genes and *mtl-1* (A.) *gcs-1* expression, are depicted. Age-synchronized, 64 hours old wild-type nematodes were incubated for the indicated time points on agar plates, supplemented with 100 µg/ml ampicillin and 1 mM IPTG and spotted with *E. coli* HT115 containing empty vector L4440 (black) or vector containing a *gcs-1* cDNA fragment (blue). Respective mRNA levels were assessed by RT-qPCR and normalized over *act-1* mRNA levels as a housekeeper; empty vectors were set to 100. Data are means of 3 independent experiments +SEM (*p<0.05 as compared to L440; **p<0.01 as compared to L440; Student´s t-test).

3.6 Contribution of FoxO1 cysteine residues in its activity under basal conditions

In an attempt to mimic the DEM interaction with cysteine residues of proteins, we genetically manipulated FoxO1 cysteine residues (all cysteines were mutated to serines) through site-directed mutagenesis. FoxO1 harbors seven cysteine residues, of which two (Cys23 and Cys612) are highly conserved among the FoxO isoforms (Fig. 7). Similar to its *C. elegans* homolog, FoxO1 is a transcription factor shuttling between the cytoplasm and the nucleus. In addition to cytoplasmic-nuclear shuttling, DNA binding and transactivation activity may interfere with FoxO1 activity and therefore these aspects were tested in a cysteine-deficient mutant under basal conditions in HEK293 and HepG2 transfected cells.

3.6.1 Neither localization nor DNA binding were affected in cysteine-deficient FoxO1

FoxO1 DNA binding was analyzed through EMSA. HEK293 cells were transfected with plasmids encoding either wild type FoxO1 (WT FoxO1)-GFP or cysteine-deficient FoxO1 (FoxO1-ΔCys1-7)-GFP (Fig. 15). Moreover, HEK293 and HepG2 cells were transfected with plasmids encoding either WT FoxO1-EGFP or FoxO1-ΔCys1-7-EGFP, and subsequently their cytoplasmic-nuclear shuttling was assessed (Fig. 16).

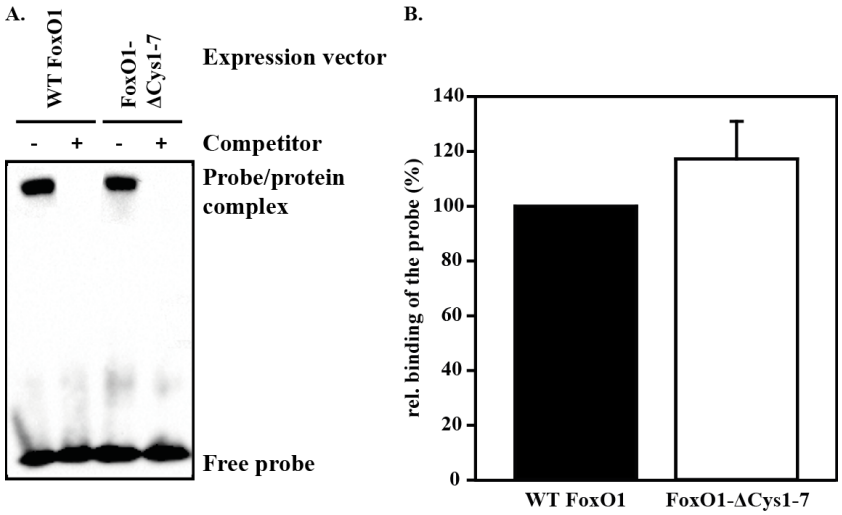

Figure 15:
Basal FoxO1 DNA binding in HEK293 transfected cells. (A) Representative EMSA depicting either WT FoxO1 or FoxO1 ΔCys1-7 DNA binding and (B) statistical analysis of four individual experiments. Nuclear extracts of HEK293 cells transfected with WT FoxO1-GFP or FoxO1-ΔCys1-7-GFP were generated using cell fractionation kit and thereafter DNA binding of FoxO1 was assessed using EMSAs. The competitor represents an unlabeled with biotin probe. (B) Data are presented as means +SD from 4 independent experiments.

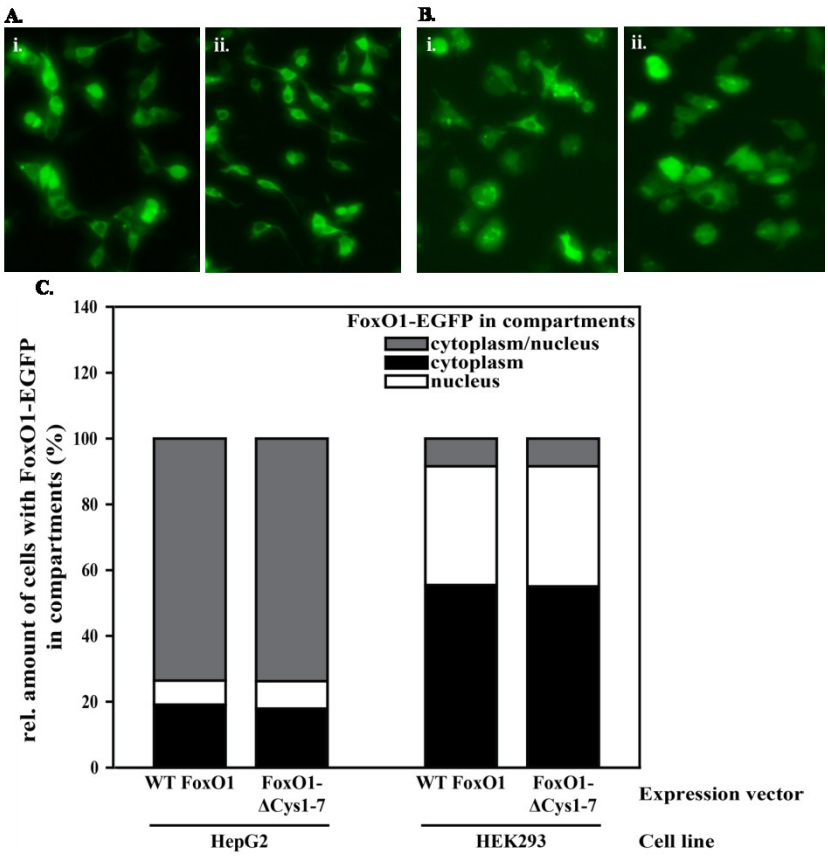

Figure 16:
Basal FoxO1 localization in HEK293 and HepG2 transfected cells. Examples of cells with basal FoxO1-EGFP distribution in compartments in (A.) HEK293 and (B.) HepG2 cells. WT FoxO1-EGFP and FoxO1-ΔCys1-7-EGFP are represented in "i." and "ii.", respectively. (C.) Analysis of basal FoxO1-EGFP distribution among compartments. HEK293 or HepG2 cells were transfected with WT FoxO1-EGFP or FoxO1-ΔCys1-7-EGFP and basal FoxO1-EGFP distribution in compartments was assessed using fluorescence microscope. (C.) Data are presented as fractions of 100% of 3 independent experiments. In all cases, SD was lower than 5% of the relative amount of cells, as were set to 100%.

Initially, as determined using EMSAs, FoxO1 cysteine deficiency did not significantly impair FoxO1 DNA binding in HEK293 cells, in which different FoxO1-GFP forms were overexpressed (Fig. 15). That observation is in line with the absence of cysteine residues in the FoxO1 DNA binding domain (Fig. 7). The overall distribution of FoxO1 in compartments was somewhat different between the two cell lines. In HEK293 cells, FoxO1 was predominantly localized in the cytoplasm, whereas FoxO1 was ubiquitously distributed in HepG2 cells (Fig. 16). A potential explanation might be the constitutive phosphorylation of Akt only in HEK293 cells, which in turn could cause FoxO1 cytoplasmic retention under basal conditions (data not shown). Despite the differential FoxO1 distribution between the two cell lines, FoxO1-ΔCys1-7 followed the same distribution pattern as WT FoxO1 (Fig. 14). As neither nucleocytoplasmic distribution nor DNA binding of FoxO1 was altered by FoxO1 cysteine deficiency, yet another aspect of FoxO1, its transactivation activity, was studied.

3.6.2 Basal transactivation activity of FoxO1 depends on its Cys612 residue

To investigate basal FoxO1 transactivation activity, the stimulation of FoxO1-responsive promoter constructs in cells overexpressing either WT FoxO1-V5 or FoxO1-ΔCys1-7-V5 tagged with biotin was assessed by luciferase reporter assay (Fig. 17). Promoter constructs which are known to be activated by FoxO1, such as FHRE-Luc, G6Pase-Luc, SelP-Luc and FoxO1-Luc, were employed [174, 193, 206, 207].

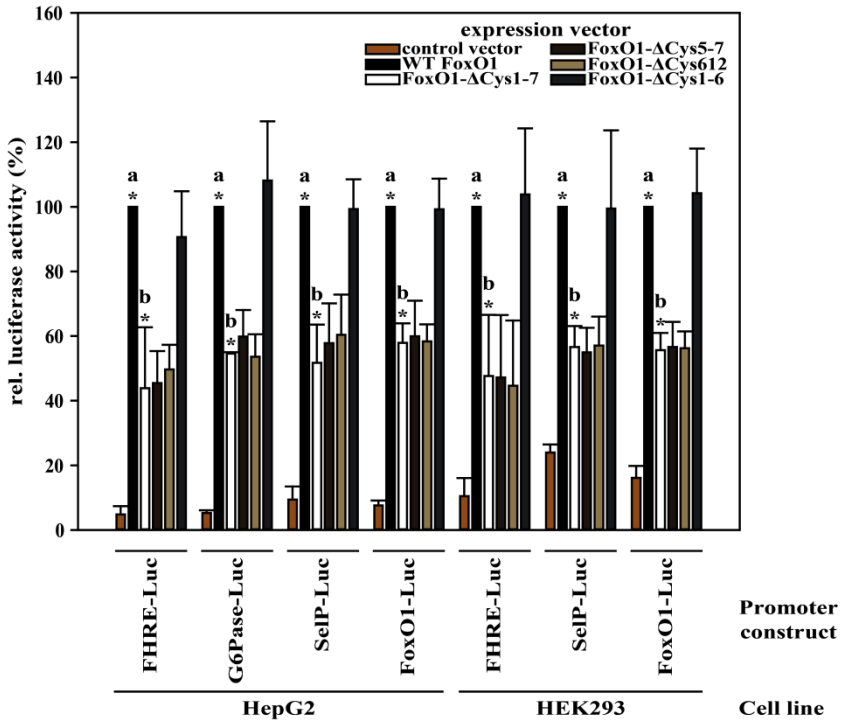

Figure 17:
Stimulation of FoxO1-responsive promoters in HEK293 and HepG2 cells, transfected with different FoxO1 forms. HEK293 or HepG2 cells were co-transfected with different FoxO1-related promoter constructs and various expression vectors as indicated. Cells were then lysed and processed for detecting stimulation of FoxO1-responsive promoters using luciferase reporter assay. Promoter constructs were conjugated with a firefly luciferase and as internal control renilla luciferase was employed. Firefly luciferase/renilla luciferase ratio was calculated and then WT FoxO1 was set to 100. As a "control vector", pCI Neo was employed. All FoxO1 expression vectors were tagged with biotin and V5. G6Pase Luc was not assessed in HEK293 cells due to low *g6pc* expression levels. Data are presented as means +SD from 3 independent experiments. *a, $p<0.001$ as compared to control vector; *b, $p<0.001$ as compared to WT FoxO1; One-way Anova with Student-Newman-Keuls post-test.

Although overexpression of FoxO1-ΔCys1-7 successfully stimulated FoxO1-responsive promoters as compared to cells transfected with an control vector, and in contrast to the intact nucleocytoplasmic distribution (Fig. 16) and DNA binding (Fig. 15), stimulation of FoxO1-responsive promoters in cells overexpressing FoxO1-ΔCys1-7 was less prominent as compared to those transfected with WT FoxO1 (Fig. 17). To elucidate which cysteine is responsible for the impaired transactivation activity, additional Cys-deficient mutants were employed. In summary, overexpression of a mutant harboring a mutation only in Cys612 (FoxO1-ΔCys612) mimicked the Cys-deficiency-induced loss of FoxO1 transactivation

activity. Moreover, mutation of the first six cysteine residues (FoxO1-ΔCys1-6) was without effect on FoxO1 transactivation activity (Fig. 17). Transfection efficiency was even regardless of the expression vector (Fig. 18). Cys612 located in the FoxO1 transactivation domain, which might explain its requirement for full activity (Fig. 7).

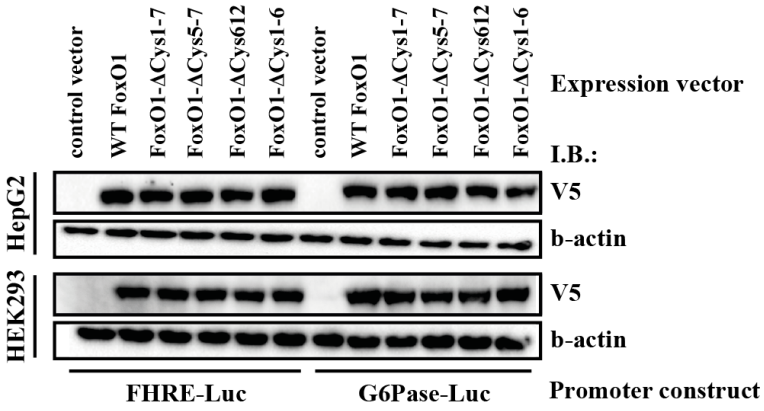

Figure 18:
Transfection efficiency of various FoxO1 constructs in HEK293 and HepG2 cells. Representative transfection efficiency of FoxO1 forms in HEK293 and HepG2 cells. V5 antibody was used to detect exogenous FoxO1; b-actin was employed as a housekeeping protein. HEK293 or HepG2 cells were transfected with different FoxO1 forms and thereafter the stimulation of FoxO1-responsive promoters was assessed using luciferase reporter assay. The same lysates obtained for the luciferase reporter assay were then analyzed by SDS-PAGE gel and transfection efficiency was studied using western blotting analysis. As a "control vector", pCI Neo was employed. All FoxO1 expression vectors were tagged with biotin and V5. Western blotting analysis was performed twice, using lysates obtained from different experiments.

To assess whether loss of FoxO1 transactivation activity mediated by FoxO1 cysteine deficiency (Fig. 15) had an effect on FoxO1 activity, the expression levels of FoxO1 target genes, such as *g6pc*, *selP*, and *foxo1*, were studied (Fig. 19) [174, 193, 206]. To avoid "noise" caused by overepression of the exogenous FoxO1, specific primers for the 3'-UTR region were designed for detection FoxO1 mRNA.

In line with the results obtained using the luciferase reporter assay, elevated expression levels of FoxO1 target genes due to FoxO1 overexpression was more prominent in cells transfected with WT FoxO1 as compared to those transfected with FoxO1-ΔCys1-7. Among all seven cysteines, mutation in the last FoxO1 cysteine residue (FoxO1-ΔCys612) induced effects similar to FoxO1-ΔCys1-7, whereas mutation of the other six FoxO1 cysteine residues (FoxO1-ΔCys1-6) had no effect on FoxO1 transactivation activity (Fig. 19).

In summary, cysteine deficiency in FoxO1 affected neither its localization nor its DNA binding. In contrast, a single mutation in Cys612 of FoxO1 caused impairment of basal transactivation activity, which in turn led to impaired regulation of FoxO1 target genes. Since cysteine residues are known to mediate oxidative stress-induced interactions with co-factors such as CBP/p300, which reversibly interacts with FoxO1 and FoxO4 upon exposure to hydrogen peroxide, we investigated whether diamide-induced severe oxidative stress could

potentially trigger similar redox-sensitive interactions [177, 203]. Despite both hydrogen peroxide and diamide both depleting and oxidizing GSH, diamide seems to mediate more severe stressful conditions, which in turn could activate different signaling pathways, such as pathways towards apoptosis, as compared to hydrogen peroxide [214].

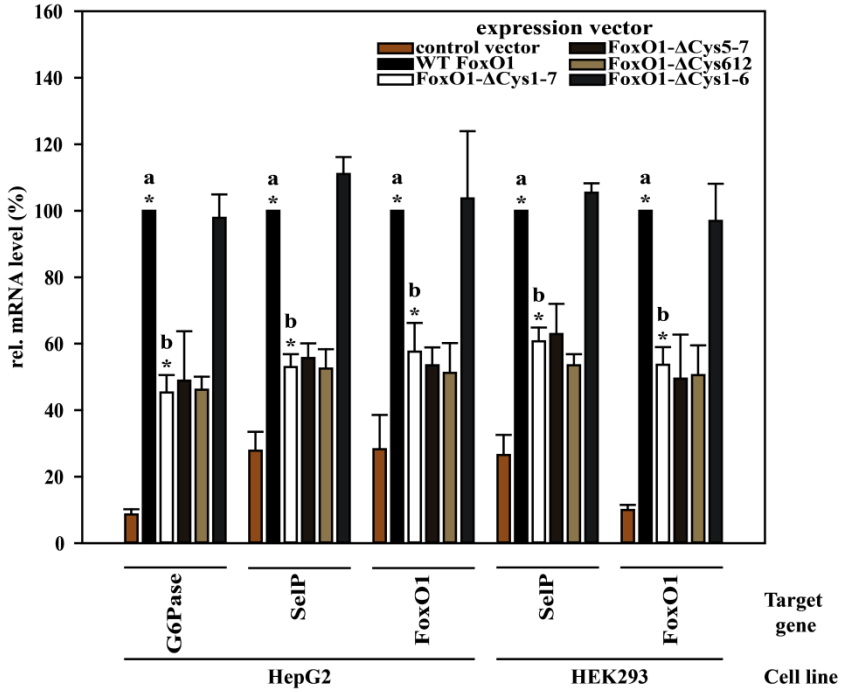

Figure 19:
Expression of FoxO1 target genes in HEK293 and HepG2 cells, transfected with different FoxO1 forms. HEK293 or HepG2 cells were transfected with different FoxO1 forms and thereafter the expression level of FoxO1 target genes was assessed using RT-qPCR. The respective mRNA level was normalized to HPRT1, which was used as a housekeeping gene, and thereafter the ratio obtained for WT FoxO1 was set to 100. As a "control vector", pCI Neo was used. All FoxO1 expression vectors were tagged with biotin and V5. The expression of *g6pc* was not assessed due to low overall expression level in HEK293 cells. Data are presented as means +SD from 3 independent experiments. *a, $p<0.001$ as compared to control vector; *b, $p<0.001$ as compared to WT FoxO1; One-way Anova with Student-Newman-Keuls post-test.

3.7 Viability reduction, depletion/oxidation of GSH, and FoxO1 nuclear accumulation induced by diamide

Diamide is a well-known thiol oxidizing agent, which was reported to deplete and oxidize GSH [201]. To test whether GSH was indeed depleted/oxidized, HEK293 cells were treated with different diamide concentrations for 30 minutes and thereafter GSH levels were measured (Fig. 20).

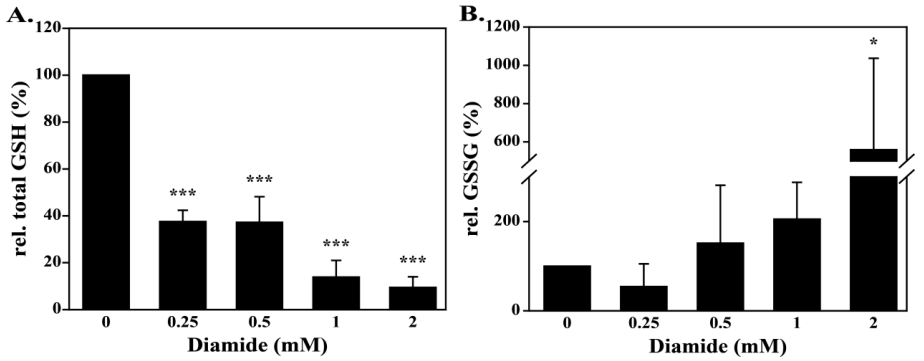

Figure 20:
GSH and GSSG levels upon diamide treatment in HEK293 cells. HEK293 cells were treated with different diamide concentrations for 30 minutes and thereafter (A.) total GSH and (B.) GSSG was measured enzymatically. As a control DMSO 0.1% v/v was employed. In case of diamide 2 mM, DMSO concentration was 0.2% v/v. GSH or GSSG/protein level ratios were calculated and normalized against the control, which was set to 100%. Data are presented as means +SD from 4 independent experiments. *p<0.05 as compared to control; ***p<0.001 as compared to control; Student´s t-test.

Diamide successfully oxidized GSH to GSSG in a somewhat concentration-dependent way (Fig. 20). Interestingly, GSH was also depleted; presumably because of active GSH/GSSG secretion or formation of protein mixed-disulfides (S-glutathionylated proteins). Since the 2GSH to GSSG ratio was altered due to diamide treatment, the cellular state was altered. Imbalances in redox state could trigger cell death through ROS accumulation and we therefore investigated whether diamide was tolerated by HEK293 cells within the same concentration and time frame (Fig. 21).

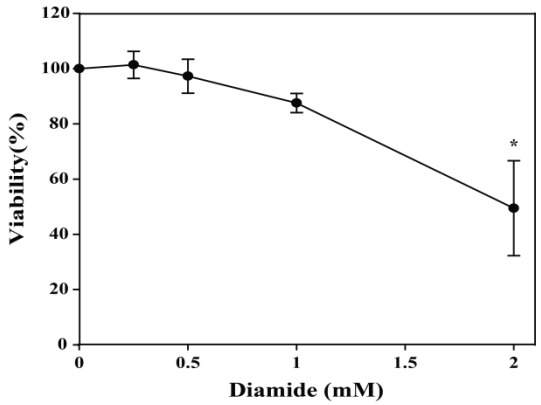

Figure 21:
Viability of HEK293 cells upon diamide treatment. HEK293 cells were treated with different diamide concentrations for 30 minutes and thereafter cell viability was assessed by MTT conversion. As a control, DMSO 0.1% v/v was employed. In case of diamide 2 mM, DMSO concentration was 0.2% v/v. DMSO control was set to 100. Data are presented as means ±SD from 4 independent experiments. *p<0.05 as compared to control; Student´s t-test.

Although exposure to diamide reduced viability in a concentration-dependent way in HEK293 cells, approximately 90% of the cells were still alive upon 1 mM diamide treatment (Fig. 21). Therefore, for the upcoming experiments the employed diamide concentration was as high as 1 mM. As a transcription factor, FoxO1 shuttles between the cytoplasm and

nucleus to regulate the transcription of its target genes. During oxidative stress, FoxO1 is predominately localized in the nucleus to promote the upregulation of genes related to antioxidant defense. To address that general observation and whether cysteine deficiency may alter that FoxO1 process, FoxO1 localization was assessed using HEK293 of HepG2 cells transfected with plasmids encoding either WT FoxO1-EGFP or FoxO1-ΔCys1-7-EGFP (Fig. 22).

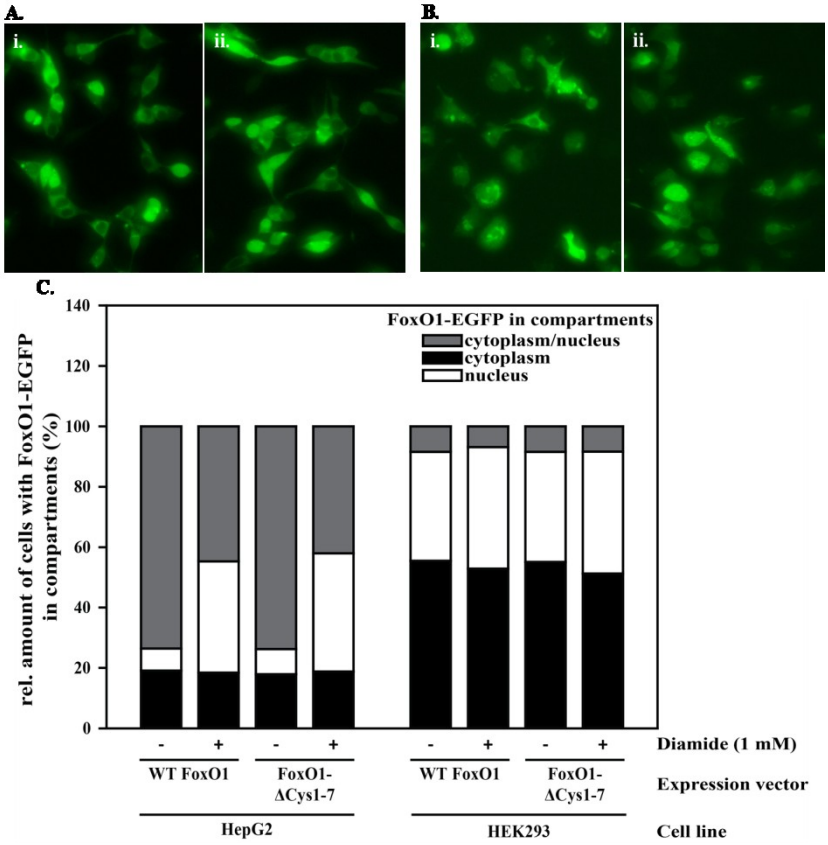

Figure 22:
FoxO1 localization upon diamide treatment in HEK293 or HepG2 transfected cells. Examples of cells with WT FoxO1-EGFP distribution in compartments in (A.) HEK293 and (B.) HepG2 cells. Control and 1 mM diamide treatment are depicted in "i." and "ii.", respectively. (C.) Analysis of FoxO1-EGFP distribution among compartments. HEK293 or HepG2 cells were transfected with WT FoxO1-EGFP or FoxO1-ΔCys1-7-EGFP, treated with DMSO (0.1% v/v) or 1 mM diamide and thereafter FoxO1-EGFP distribution in compartments was assessed using fluorescence microscope. (C.) Data are presented as fractions of 100% of 3 independent experiments. In all case, SD was lower than 5% of the relative amount of cells, as were set to 100%.

In line with the above statement, 1 mM diamide treatment promoted FoxO1-EGFP nuclear accumulation in HepG2 cells; it did so regardless of the presence or absence of FoxO1 cysteine residues. In contrast, the same treatment did not significantly alter FoxO1-EGFP distribution in HEK293. A potential explanation might be that in comparison to a minor 4% nucleic FoxO1-EGFP in HepG2 cells under physiological conditions, approximately 40% of FoxO1-EGFP was already located in the nucleus in HEK293 under the same conditions. As a consequence, the nuclear FoxO1-EGFP in HEK293 cells was already

sufficient to promote upregulation of genes involved in antioxidant defense and therefore no additional FoxO1-EGFP nuclear accumulation was detected in HEK293 cells. Since in both cell lines FoxO1-EGFP nuclear accumulation was detected upon 1 mM diamide treatment, we investigated DNA binding ability of FoxO1 under the same conditions.

3.8 C612-independent attenuation of FoxO1 DNA binding upon diamide treatment in HEK293 cells

Using EMSAs, we assessed (a.) the general DNA binding ability of FoxO1 upon exposure to 1 mM diamide and (b.) FoxO1 cysteine residues may affect it. HEK293 cells were transfected with WT FoxO1-GFP or various cysteine-deficient mutants plasmids, including FoxO1-ΔCys1-7, FoxO1-ΔCys1-6, and FoxO1-ΔCys612 (Fig. 23).

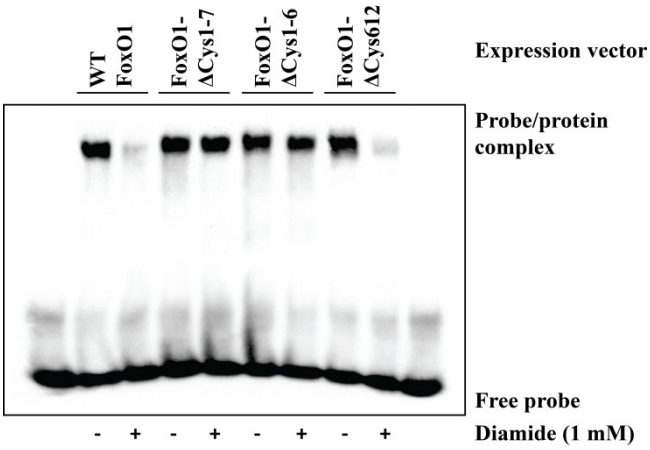

Figure 23:
FoxO1 DNA binding in HEK293 transfected cells treated with diamide. Representative DNA binding of various FoxO1 forms in HEK293 cells upon 1 mM diamide treatment. HEK293 cells were transfected with WT FoxO1-GFP or cysteine deficient FoxO1-GFP mutants. We then treated with DMSO (0.1% v/v) or 1 mM diamide for 30 minutes, nuclear extracts were generated using a cell fractionation kit and thereafter DNA binding of FoxO1 was studied using EMSAs. Western blotting analysis was performed twice, using lysates obtained by different experiments.

Exposure of cells to 1 mM diamide led to attenuated WT FoxO1 DNA binding, whereas no loss of binding was observed with FoxO1-ΔCys1-7. Surprisingly, FoxO1 DNA binding remained almost intact in FoxO1-ΔCys1-6, but was impaired wit FoxO1-ΔCys612 under 1 mM diamide treatment (Fig. 23). Thus diamide-induced attenuation of FoxO1 DNA binding was Cys612-independent which was in contrast to Cys612-dependent loss of basal FoxO1 transactivation activity (Fig. 17). To further elucidate the underlying mechanism causing the WT FoxO1 DNA binding attenuation, we tested whether S-glutationylation could be involved. To investigate that hypothesis we initially assessed whether (a.) diamide could promote S-glutathionylation (Fig. 24) and (b.) impaired WT FoxO1 DNA binding could be restored by reversing S-glutathionylation (Fig. 26).

3.9 Diamide-induced protein S-glutathionylation in HEK293 cells

Protein S-glutathionylation is a reversible post-translational modification occurring under oxidative/nitrosative stress, but rarely also under physiological conditions. Upon oxidative/nitrosative stress, GSH may form a disulfide bridge with a cysteine residue of a protein and thus protect the redox sensitive cysteines from irreversible oxidation which in turn could lead to protein degradation (Chapter 1.6.2.2.1). As a thiol oxidizing agent, diamide could presumably have induced protein S-glutathionylation to affect FoxO1, and we thus tested that hypothesis (Fig. 24) [214].

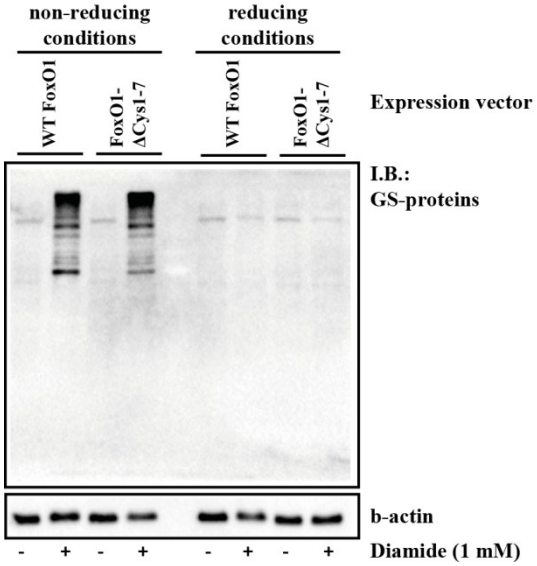

Figure 24:
Induction of S-glutathionylation upon diamide treatment in HEK293 transfected cells. Representative western blot related to diamide-promoted protein S-glutathionylation in HEK293 cells transefected with either WT FoxO1 or FoxO1-ΔCys1-7. Cells were treated with DMSO (0.1% v/v) or 1 mM diamide and lysed in RIPA buffer. Lysates were then analyzed by SDS-PAGE both under non-reducing and reducing conditions. Under reducing conditions, formation of protein S-glutathionylation was abolished. As loading control, the housekeeping protein b-actin was employed. FoxO1 expression vectors were tagged with biotin and V5. The data are representative of 5 independent experiments.

Indeed, exposure to 1 mM diamide promoted protein S-glutathionylation in transfected HEK293 cells, as detected under non-reducing conditions. As expected, the detected signal vanished in the presence of a reducing agent, such as β-mercaptoethanol (Fig. 22). As already mentioned, induction of protein S-glutathionylation might explain GSH depletion (Fig. 19), without excluding the probability of active secretion of GSH/GSSG. Since diamide treatment induced protein S-glutathionylation, we then tried to reverse the post-translational modification. To achieve that, two different approaches were tested: (a.) simple recovery and (b.) Grx-1 overexpression.

3.10 Attenuation of FoxO1 DNA binding by diamide is mediated by S-glutathionylation in HEK293 cells

An important asset of S-glutathionylation is the reversibility of this modification by Grxs. To examine whether diamide-induced S-glutathionylation is reversible and could be recovered by endogenous Grxs, HEK293 cells were left to recover in the absence of diamide. To elucidate whether Grxs accelerated reversion of S-glutathionylation, we overexpressed Grx-1, a key Grx capable of reversing S-glutathionylation (Fig. 25). Grxs were reported to utilize the monothiol pathway to promote deglutathionylation [102]. To verify that, two Grx-1 mutants were generated in which either Cys23 (Grx-1-ΔCys23) or Cys26 (Grx-1-ΔCys26) was mutated to serine.

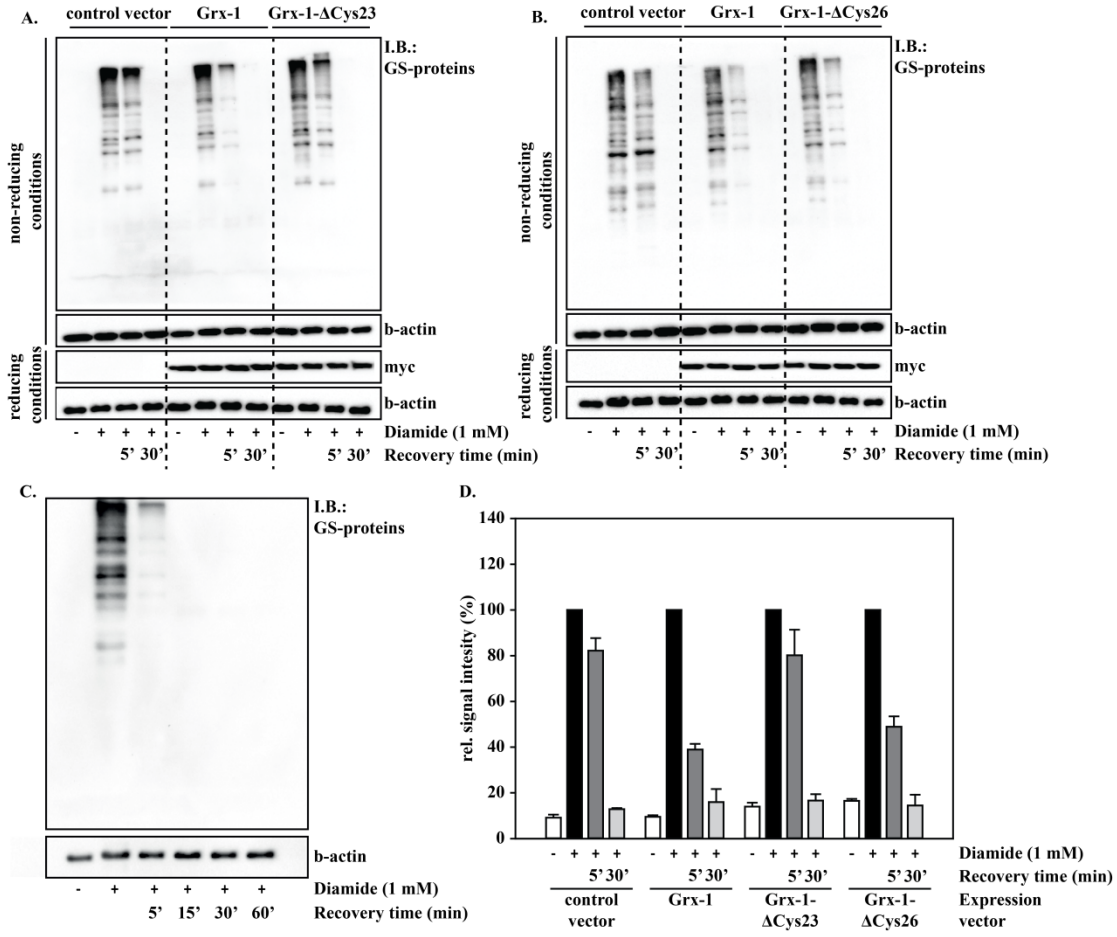

Figure 25:
Reversibility of protein S-glutathionylation in HEK293 cells. (A. B.) Representative western blotting analysis of HEK293 cells transfected with empty vector or variants of Grx-1; (A.) Grx-1-ΔCys23 and (B.) Grx-1-ΔCys26. (C.) Representative western blotting analysis of HEK293 cells recovering in absence of diamide (D.) Densitometric analysis of (A.) and (B.) Following a 30-minute exposure to DMSO (0.1% v/v) or 1mM diamide, cells were left to recover in absence of the compound for up to (A. B.) 30 minutes or (C.) 60 minutes. Cells were then lysated, analyzed by SDS-PAGE and S-glutathionylation induction was assessed using western blotting analysis. Grx-1 variants were tagged with myc. (A.) and (B.) were performed twice. (C.) was repeated thrice. (D.) Densitometric signal of an entire line was normalized to b-actin, a housekeeping protein. Thereafter, the ratio acquired for 1 mM diamide was set to 100. Data are presented as mean +max of 2 independent experiments.

Protein S-glutathionylation was indeed rapidly reversed; after just five minutes of simple recovery the majority of the proteins were back to their physiological non-S-glutathionylated form (Fig. 25C). Overexpression of Grx-1 somewhat accelerated deglutathionylation as compared to cells overexpressing the control vector. In line with previous reports, in cells transfected with Grx-1-ΔCys23 [103, 106], Grx-1 overexpression-induced acceleration of deglutathionylation was attenuated, meaning that Cys23 (Fig. 25A) was the important Grx-1 cysteine residue in inducing reversibility of S-gluathionylation. Therefore, we investigated whether attenuation in DNA binding of WT FoxO1 was potentially mediated by S-glutathionylation (Fig. 26).

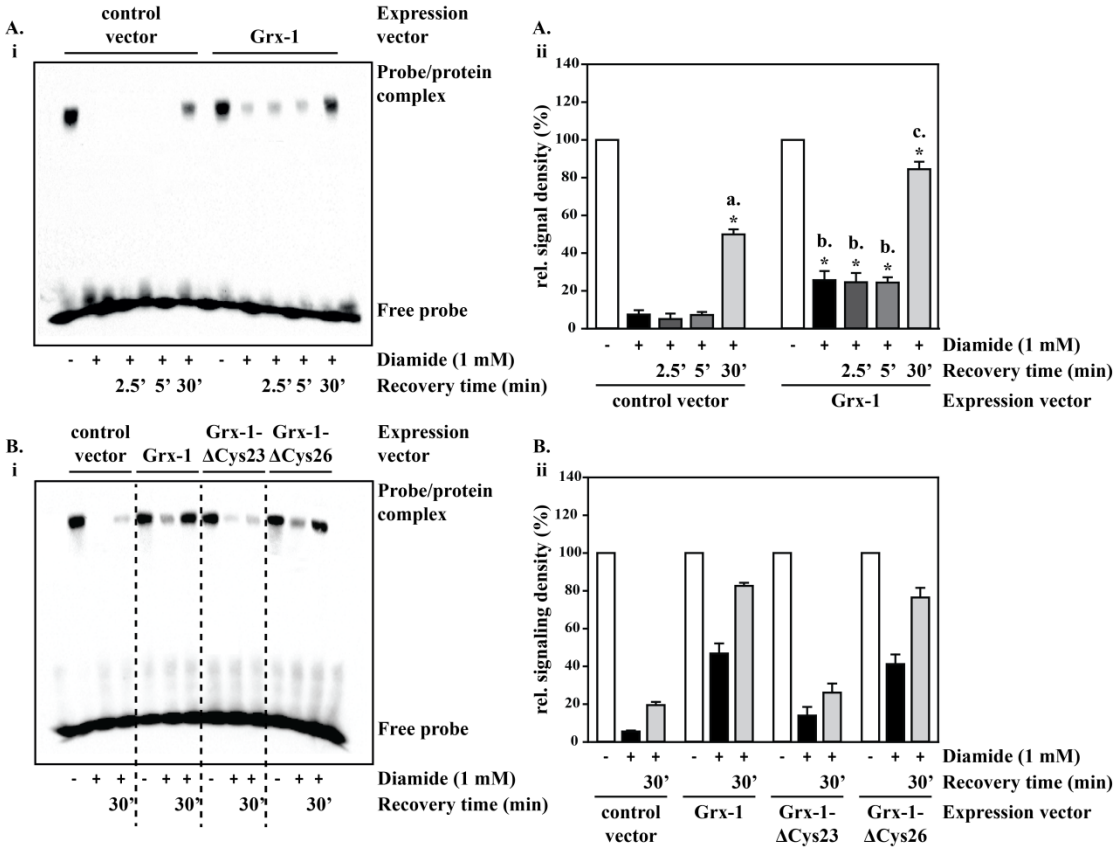

Figure 26:
Contribution of S-gluathionylation to attenuated DNA binding of WT FoxO1. (i.) Representative EMSA blot of HEK293 cells co-transfected with WT FoxO1 and either control vector or Grx-1 variants. (ii.) Densitometric analysis of EMSAs. HEK293 cells were transfected with WT FoxO1 and (A.) control vector or Grx-1 and (B.) control vector and Grx-1 variants. After exposure to DMSO (0.1% v/v) or 1 mM diamide, cells were recovered for up to 30 minutes and thereafter nuclear extracts were generated a using cell fractionation kit. DNA binding of FoxO1 was then analyzed using EMSA. WT FoxO1 was labeled with GFP; Grx-1 variants were tagged with myc (ii.) Band density was assessed and control (DMSO) was then set to 100. Data are presented as (A.) mean +SD of 3 and (B.) mean +max of 2 individual experiments. (A. ii.) *a, $p<0.001$ as compared to 1 mM diamide; *b, $p<0.001$ as compared to control; *c, $p<0.001$ as compared to 1 mM diamide and $p<0.001$ as compared to 30' recovery of the control vector; One-way Anova with Student-Newman-Keuls post-test.

Initially, DNA binding of WT FoxO1 was restored after 30 minutes recovery in HEK293 cells transfected with the control vector. Grx-1 overexpression not only somewhat alleviated the diamide-induced attenuation of WT FoxO1 DNA binding but additionally accelerated the

recovery of the impaired DNA binding of WT FoxO1 as compared to control vector (Fig. 26A). In addition to the observation that mutation of Cys23 of Grx-1 (Grx-1-ΔCys23) reversed the Grx-1-mediated acceleration in DNA binding recovery; mutation in Cys26 of Grx-1 (Grx-1-ΔCys26) did not affect the Grx-1-induced effect (Fig. 26B), implying that S-gluathionylation might be the key modification causing the attenuation. Since protein S-gluathionylation was found to be involved in the DNA binding attenuation of WT FoxO1, we further asked whether FoxO1 is potentially S-glutathionylated (Fig. 27).

3.11 Is FoxO1 a potential direct target of GSH under diamide-induced oxidative stress?

As revealed through EMSAs, the diamide-induced attenuation of WT FoxO1 DNA binding was mediated by S-glutathionylation. We therefore investigated whether GSH may directly bind to a random FoxO1 cysteine residue and induce FoxO1 S-gluathionylation. To address that, a pull down of biotinylated FoxO1 using streptavidin beads in cell lysates obtained from HEK293 cells transfected with biotinylation signal-containing WT FoxO1 or FoxO1-ΔCys1-7 was employed followed by GS-protein detection (Fig. 27).

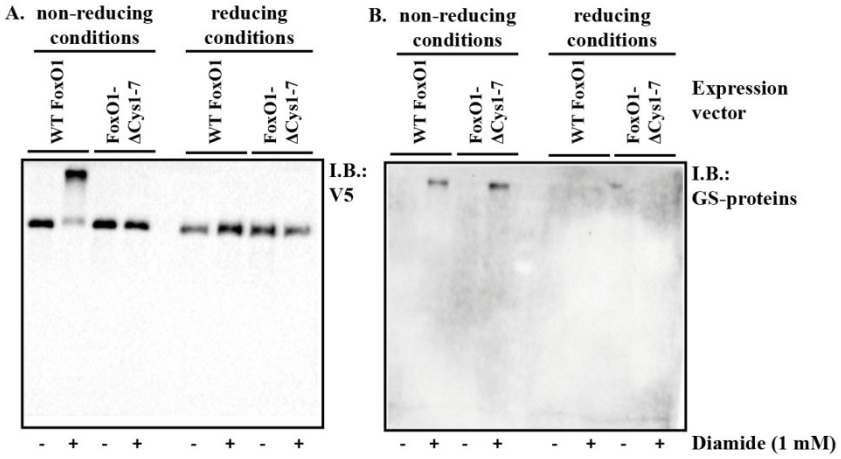

Figure 27:
Diamide-driven protein complex that contains WT FoxO1. Representative western blots of (A.) detection of exogenous FoxO1 variants or (B.) detection of GS-proteins after streptavidin pull down are depicted. HEK293 cells were transfected with WT FoxO1 or FoxO1-ΔCys1-7, tagged with biotin and V5. Thereafter, the transfected cells were exposed to DMSO (0.1% v/v) or 1 mM diamide for 30 minutes and lysed in RIPA buffer. Streptavidin beads were employed in 100 µg of total protein and biotinylated FoxO1 was pulled down. Lysates were then analyzed by SDS-PAGE and the status of biotinylated FoxO1 was assessed using western blotting analysis. Western blotting was performed twice with different lysates.

Upon diamide treatment WT FoxO1, but not FoxO1-ΔCys1-7, was in a protein complex with an unknown co-factor under non-reducing conditions. Reducing conditions abolished diamide-induced protein complex, which in line with the observation related to FoxO1-ΔCys1-7, led to the hypothesis that diamide-mediated WT FoxO1 interaction with an unknown factor was dependent on cysteine residues of FoxO1 (Fig. 27A). That observation is

somewhat in line with previous reports of FoxO1 being in protein complex upon exposure to hydrogen peroxide [203]. Immunoblotting of S-glutathionylated proteins revealed that the protein complex is potentially S-gluathionylated. Surprisingly, an additional band was detected in case of FoxO1-ΔCys1-7 (Fig. 27B). One possible explanation might be that streptavidin beads could potentially pull down endogenous biotinylated proteins, such as acetyl-coA carboxylase, which could be either directly S-glutathionylated or in a protein complex with an S-glutathionylated co-factor.

4. Discussion

The tripeptide, GSH, is the major cellular non-enzymatic ROS scavenger and the ratio of its redox couple [2GSH]/[GSSG] is frequently employed to assess the cellular redox state [100, 109]. Although the pivotal role of GSH in ROS elimination and the ROS-mediated modulation of FoxOs are well reported, a direct correlation between GSH and FoxO modulation has not been investigated. Herein, we attempted to elucidate such an interaction both *in vivo* and *in vitro*. Exposure of *C. elegans* with a thiol-modulating agent (DEM) revealed that total thiol amounts were successfully reduced. On top of that, to investigate whether glutathione may modulate FoxO transcription factors, depletion of *gcs-1* was employed in *C. elegans*. In an attempt to mimic the DEM interaction with the protein thiol (cysteine) residues, cysteine residues of our protein of interest, FoxO1, were mutated. However, depletion of *gcs-1* may not simulate modifications that require GSH molecules, such as S-gluathionylation, a post-translational modification in which GSH forms a disulfide bridge with a cysteine residue of a protein. Therefore, we employed a thiol oxidizing agent, diamide, *in vitro*.

4.1 DEM-mediated alteration of thiol status affects *C. elegans* life span

C. elegans, a model organism frequently employed in study of ageing, was used for our *in vivo* experiments. Thiol modulating compounds were previously shown to affect *C. elegans* life span. One of the compounds, plumbagin, induced a life span extension when applied at low concentrations but had a lethal effect at higher concentrations [215]. Plumbagin-induced biological actions have been proposed to be related to alterations in cellular thiols, rather than in ROS accumulation [216]. Similarly to the effect of plumbagin, mild DEM-induced thiol depletion led to a hormetic effect on *C. elegans* life span (Fig. 9B). Low DEM concentrations, up to 100 μM, may initiate an adaptive response, which in turn elevated stress resistance and promoted life span extension in *C. elegans* (Fig. 9A). In contrast, higher DEM concentrations may have caused extensive ROS accumulation, inducing severe oxidative stress and subsequently life span shortening in *C. elegans* (Fig. 9A).

4.2 DEM-induced hormetic effect mediated by DAF-16 and SKN-1

Two transcription factors involved in adaptive processes induced upon oxidative stress where found to mediate the DEM-induced deceleration of *C. elegans* ageing; DAF-16 and SKN-1. In *daf-16* or *skn-1*-deficient strains, the 100 μM DEM-mediated effect was abolished, leading to the assumption that both transcription factors are required to enhance *C. elegans*

life span (Fig. 12). In line with that, exposure of wild type nematodes to 100 µM DEM induced upregulation of *ctl-1*, *sod-3*, and *gei-1*, which are predominantly regulated by DAF-16 (Fig. 11A-C) [60, 62]. In addition, the expression level of SKN-1 regulated genes, more specifically *gcs-1*, *gst-4*, and *gst-10*, was also elevated (Fig. 13E-G) [76]. The enhanced expression level of the above-mentioned genes, *ctl-1*, *sod-3*, *gcs-1*, *gst-4*, and *gst-10*, including the increased *ctl-2* expression level, which is transcriptionally regulated by both DAF-16 and SKN-1, may explain the adaptive response upon treatment with 100 µM DEM, since all the above target genes play a pivotal role in antioxidant defense. In contrast, administration of 1 mM DEM did not significantly alter the expression level of genes regulated by DAF-16 or SKN-1, but led to upregulation of *egl-1*, a target gene regulated by a p53-orthologue, which could serve as indicator for initiation of the apoptotic process in *C. elegans* (Fig. 13H) [211]. In contrast to the observed general pattern of gene regulation, treatment with 1 mM DEM induced more profound DAF-16 nuclear accumulation as compared to 100 µM DEM, meaning that DAF-16 might be inactive despite translocating to the nucleus upon exposure to 1 mM DEM [204]. A potential explanation of an inactive DAF-16 form trapped into the nucleus could be the nuclear export machinery malfunction driven by DEM treatment, which has previously reported in mammalian cells [217]. Although alterations were detected with regard to DAF-16 and SKN-1, DEM treatment with concentrations between 100 µM and 1 mM led to non-concentration dependent thiol or GSH depletion, meaning that the DEM-mediated hormetic effect should not entirely depend on thiols or GSH depletion (Fig. 28).

The term “hormesis” was first introduced in 1943 by Southam et al. and can be defined as “beneficial effects of low doses of substances or interventions known to be toxic at higher doses” [218]. Although the term was introduced long ago, hormesis was first used as mechanism underlying decelaration of *C. elegans* ageing around 1994 [219]. In later years, there was a hypothesis that exposure to mild oxidative stress could activate DAF-16, which in turn could initiate the transcriptional regulation of genes encoding antioxidant defense enzymes, such as SOD and catalases. Activation of antioxidant enzymes could eventually mediate an adaptive response which in turn would initiate less susceptibility to subsequent intense stress and therefore enhance *C. elegans* life span. Indeed, a growing body of evidence reports that DAF-16 is activated upon mild oxidative stress and thus DAF-16 was demonstrated to be involved in hormesis-mediated life span extension. For instance, *daf-16* was shown to be required for a hormesis-induced deceleration of ageing in nematodes in which thermotolerance was mediated by pre-treatment with sub-lethal heat [219, 220]. By activating DAF-16, low-doses of juglone elevated stress resistance and in turn increased life span in *C. elegans* [221, 222]. Lastly, low-doses of the green tea flavonoid, epigallocatechin

gallate did not significantly generate hydrogen peroxide but enhanced *C. elegans* life span while upregulating the expression of *sod-3* [223].

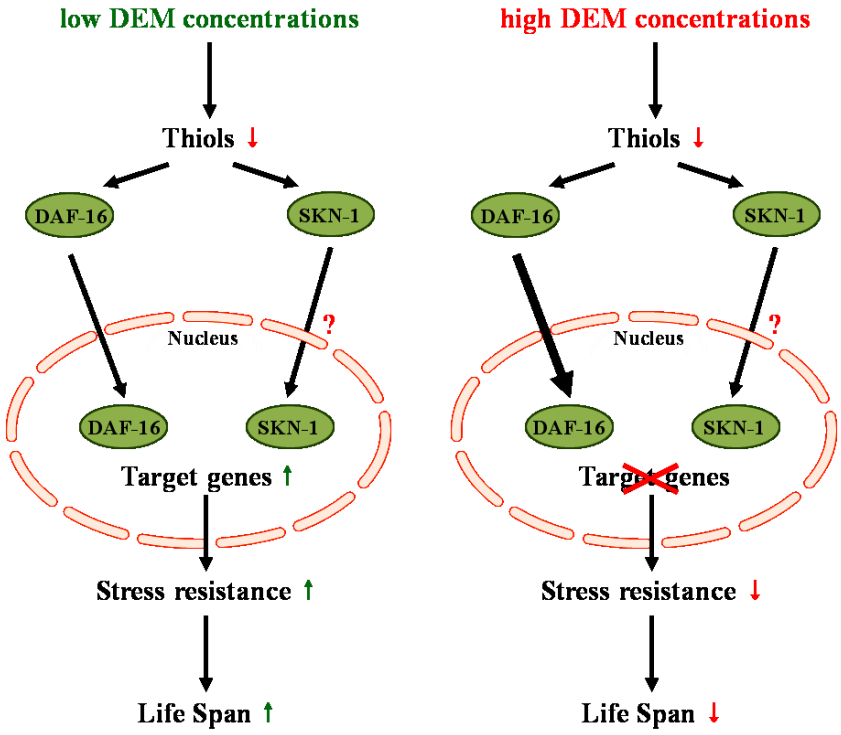

Figure 28:
Non-linear effect mediated by DEM on *C. elegans* life span. DEM-induced mild thiol depletion promotes hormetic effect in *C. elegans*. Low DEM concentrations enhance stress resistance and in turn deceleration in ageing of *C. elegans*. DEM-mediated adaptive response was promoted by elevated expression levels of genes predominantly regulated by DAF-16 or SKN-1. In contrast, high DEM concentrations did not significantly induce upregulation of DAF-16 and/or SKN-1 target genes and thus severe induction of stress promoted acceleration of *C. elegans* ageing.

4.3 Genetic manipulation of *gcs-1* results in upregulation of genes of the thioredoxin-dependent-redox system

As previously mentioned, mild GSH depletion mediated by either exposure to low DEM concentrations or by *gcs-1* depletion extended *C. elegans* life span [204]. That observation was in contrast to previous reports in which direct supplementation with a GSH derivative or low juglone concentration, leading to elevated GSH level, may increase life span and stress resistance through DAF-16 activation in *C. elegans* [221, 222]. Depletion of *gcs-1* starting at L4 larvae stage induced profound upregulation of genes related to thioredoxin-dependent redox system, such as *trx-1*, *trxr-1*, and *trxr-2* (Fig. 14E-G) [212]. In addition to enhanced gene expression of the thioredoxin system, *gst-4* and *mtl-1* levels were also elevated (Fig. 14D and H) [76, 213]. Upregulation of genes contributing in maintenance of redox status could mediate a protective response in mild GSH depletion, which in turn may increase life span of nematodes with impaired *gcs-1* expression. In contrast to the life span-extending

effect induced by low DEM concentrations, *gcs-1* knockout did not statistically significantly alter either DAF-16 nucleocytoplasmic shuttling or regulation of DAF-16 target genes, meaning that GSH depletion may not directly contribute to deceleration of *C. elegans* ageing with regard to DAF-16 modulation [204]. However, it should be noted that genetic GSH depletion may not successfully simulate GSH-driven post-translational modifications in which the GSH is required, such as in S-glutathionylation.

4.4 Cys612-dependent loss of basal transactivation activity of FoxO1

Cysteine residues of FoxO proteins were previously demonstrated to have an important role in regulation of FoxO activity under stressful conditions, predominantly induced by exposure to hydrogen peroxide. Initially, hydrogen peroxide-induced acetylation of FoxO4 was shown to be induced by cysteine-dependent interaction with CBP/p300 [177]. In addition, FoxO4 nucleocytoplasmic shuttling mediated by hydrogen peroxide was reported to be promoted by cysteine-dependent interaction with Transportin-1. Interestingly, the underlying mechanism was highly conserved in *C. elegans* [224]. In a similar manner, nuclear import receptors, Importin-7 and Importin-8, formed a cysteine-dependent interaction with FoxO3a, promoting FoxO3a nuclear translocation upon exposure to hydrogen peroxide [202]. Recently, it was also proposed that, similar to FoxO4 acetylation, cysteine-dependent interaction of FoxO1 with CBP/p300 might promote hydrogen peroxide-driven FoxO1 acetylation. The above-mentioned interaction was potently blocked by thioredoxin [203].

In an attempt to mimic DEM-mediated formation of adducts with cysteine residues of proteins, we genetically manipulated FoxO1 cysteine residues. In HEK293 or HepG2 cells transfected with WT FoxO1 or FoxO1-ΔCys1-7, neither FoxO1 nucleocytoplasmic distribution nor FoxO1 DNA binding was affected under basal conditions (Fig. 16 and Fig. 15 respectively). The observation regarding the cytoplasmic-nuclear shuttling was expected since cysteine residue-driven alterations in FoxO1 distribution through post-translational modifications, such as acetylation mediated by CBP/p300, usually required a stimulus, such a hydrogen peroxide, to initiate the entire process. In addition, no cysteine residue is located in the DNA binding domain of FoxO1 which could potentially induce attenuation of basal FoxO1 DNA binding. However, loss of FoxO1 basal transactivation activity was detected and was shown to be mediated by a single mutation in Cys612 (FoxO-ΔCys612) (Fig. 17), which is located in the transactivation domain of FoxO1. Interestingly, Cys612 is highly conserved among FoxO isoforms and is responsible for cysteine-dependent interactions induced in FoxO3a and FoxO4 upon exposure to hydrogen peroxide [177, 184] Although the underlying mechanism remains elusive, we hypothesize that mutation in Cys612 somewhat mimics cysteine oxidation which could potentially diminish FoxO1 transactivation activity (Fig. 29).

Such incident has been reported in case of p53, in which direct cysteine oxidation can block DNA binding and transactivation activity [225, 226]. In line with the loss of FoxO1 transactivation activity, upregulation of FoxO1 target genes stimulated by transfection of FoxO1 forms was less prominent in cells transfected with FoxO1-ΔCys612 as compared to WT FoxO1 (Fig. 19). Albeit FoxO1-ΔCys612 overexperssion stimulated the expression of FoxO1 target genes less efficiently as compared to the WT FoxO1, overexperssion of FoxO1-ΔCys612 significantly elevated the expression levels of the target genes as compared to the control vector (Fig. 17). That significant elevation was dependent on some residual transactivation activity, accompanied with the unaffected DNA binding of the FoxO1-ΔCys1-7 (Fig. 15).

4.5 Cys612-independent attenuation of WT FoxO1 DNA binding upon diamide treatment

Hydrogen peroxide is one of the most frequently employed ROS forms to investigate FoxO regulation induced by ROS-mediated interactions. Herein, we employed a thiol oxidizing agent, diamide, to test whether FoxO1 activity is affected under stressful conditions. Diamide was reported to promote more severe oxidative stress and enhanced protein S-glutathionylation as compared to hydrogen peroxide [214]. Exposure to 1 mM diamide induced WT FoxO1 DNA binding attenuation, which was less prominent in FoxO1-ΔCys1-7. It should be noted that diamide-driven attenuation was independent of Cys612 (Fig. 23). Interestingly, the FoxO1 DNA binding domain does not harbor any cysteine residues. Reversing diamide-induced S-glutathionylation through (a.) recovery in the absence of diamide or (b.) Grx-1 overexpression recovered DNA binding of FoxO1 (Fig. 25). More importantly, the observed recovery was independent of Cys26, but dependent on Cys23 of Grx-1 (Fig. 25B) which is in line with the monothiol mechanism of Grx-1 in mediating degluathionylation, meaning that S-gluathionylation mediated the impaired FoxO1 DNA binding upon exposure to diamide [103, 106]. A similar mechanism in DNA binding inhibition driven by S-glutathionylation was reported in other transcription factors, such as in p53. [227]. It should be noted that all p53 cysteine residues are located in its DNA binding domain, which is in contrast to the absence of cysteine residues located in the FoxO1 DNA binding domain.

In addition to S-glutathionylation-induced DNA binding attenuation of FoxO1 upon exposure to diamide, WT FoxO1 was in a protein complex dependent on its cysteine residues (Fig. 26A). Preliminary data reveal that the creation of this protein complex is independent of Cys612 (data not shown), which is in line with the Cys612-independent attenuation in DNA binding of WT FoxO1 (Fig. 23). Cys612-independent interaction of WT FoxO1 with an

unknown factor upon diamide treatment was in contrast to the recently reported interaction of FoxO1 with CBP/p300 upon exposure to hydrogen peroxide [203]. Indeed, a pull down of biotinylation signal-containing WT FoxO1 failed to co-precipitate down CBP/p300 (data not shown), which led us to the hypothesis that diamide may mediate different interactions as compared to hydrogen peroxide. The diamide-driven protein complex seemed to be S-glutathionylated (Fig. 26B); however, we should also keep in mind that another endogenous biotinylated protein which is directly S-glutathionylated or in a protein complex with an S-glutathionylated co-factor might also be pulled down by streptavidin beads. Although the underlying mechanism is still not understood, glutathione could mediate redox regulation of FoxO1 through S-glutathionylation (Fig. 29).

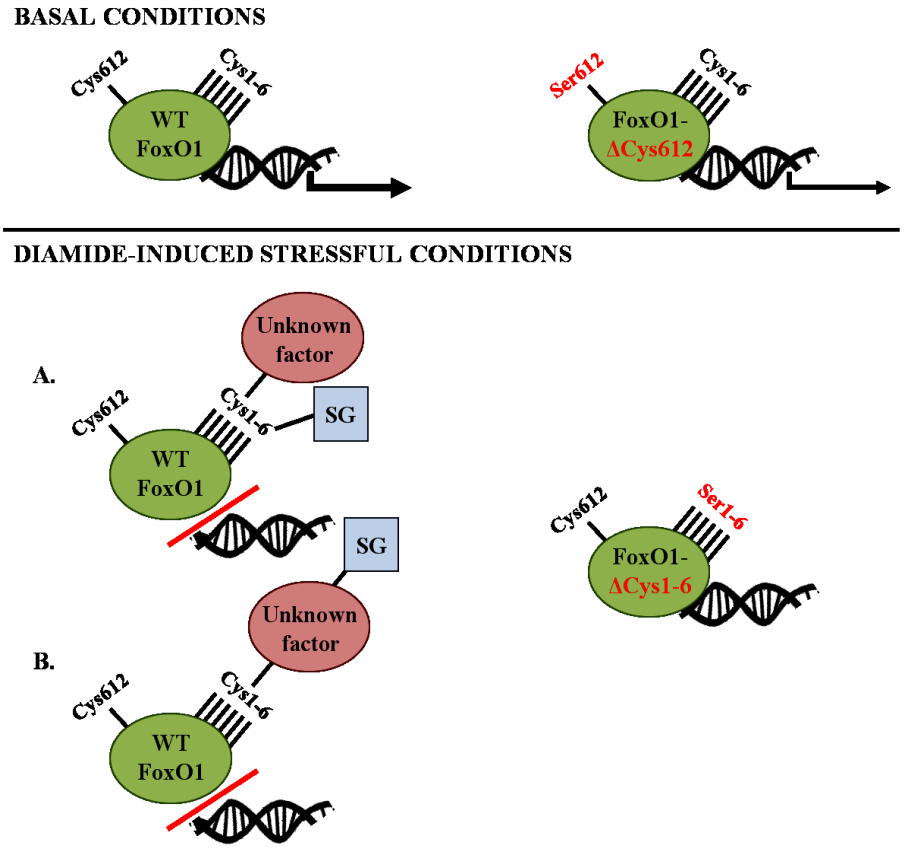

Figure 29:
Cysteine-driven regulation of FoxO1. Under basal conditions, mutation of Cys612 in FoxO1 impaired transactivation activity of FoxO1, which in turn promoted inefficient stimulation of the expression of FoxO1 target genes as compared to WT FoxO1. In contrast to the role of Cys612 on the loss of FoxO1 basal transactivation activity, a Cys612-independent interaction with either (A.) glutathione induced FoxO1 S-glutathionylation or (B.) an unknown S-gluathionylated factor promoted, attenuated WT FoxO1 DNA binding upon exposure to diamide.

4.6 Alterations in the redox status of proteins/kinases acting upstream of FoxO transcription factors mediated by the thioredoxin or glutaredoxin system

Although attenuated WT FoxO1 DNA binding was mediated by S-glutathionylation, which was hypothesized to act immediately on FoxO1 (Fig. 26), we should also consider the possibility that S-glutationylation or redox changes mediated by the thioredoxin system may affect the redox status of proteins/kinases which in turn could influence the activity of FoxO transcription factors.

For example, Trx overexpression was reported to mediate the phosphorylation of MKK4 and MKK7, which are upstream kinases of the JNK signaling cascade, inducing its activation. JNK activation initiated phosphorylation of cJun, Jun B, and Fra-1, which were then recruited in a protein complex with AP-1 and thus promoted AP-1 DNA binding [228]. JNK-mediated phosphorylation of FoxOs was demonstrated to have either activating or inactivating role in the case of FoxO4 or FoxO3a, respectively [161, 229].

As already mentioned, phosphorylation of Akt promotes phosphorylation/inactivation of FoxO transcription factors (Fig. 3). The redox state of Akt was reported to be regulated through glutaredoxin; hydrogen peroxide-driven oxidation of Akt was alleviated by Grx overexpression, leading to inhibition of apoptosis [230]. Therefore, regulation of Akt might also occur through S-glutathionylation. In addition, several other signaling proteins interfering with changes in Akt activity, such as PTEN, protein phosphatase 2 (PP2A), and apoptosis signal-regulating kinase 1 (ASK-1), were reported to be regulated by S-glutathionylation [147].

Lastly, the insulin signaling cascade, downstream of which FoxO transcription factors are regulated, was shown to be negatively regulated by protein tyrosine phosphatases (PTP)-1B [231]. A growing body of evidence shows that reversible oxidation at Cys215 of the active site of PTP1B mediated by S-glutathionylation initiates the inactivation of PTP1B [232, 233]. For instance, such an interaction may explain the accelerated recovery of WT FoxO1 DNA binding upon Grx-1 overexpression. Overexpression of Grx-1 could initiate S-gluathionylation reversibility, which in turn could mediate PTP-1B reactivation. Upon PTP-1B reactivation, insulin pathway would be inhibited and thus would allow WT FoxO1 to successfully bind to DNA.

5. Conclusion

FoxO transcription factors were previously demonstrated to be regulated by stressful stimuli eliciting elevation in ROS levels [155]. Although ROS-driven modulation of FoxOs is well documented, the role of glutathione on FoxO transcription factor activity was never directly investigated before. *In vivo* mild depletion of glutathione by targeting *gcs-1*, the enzyme catalyzing the rate-limiting step in glutathione synthesis, did not affect the regulation of DAF-16 target genes, such as *sod-3* and *ctl-1*, which was in line with the predominant cytoplasmic retention of DAF-16 in *C. elegans*.

In contrast to the results obtained by *gcs-1* depletion in *C. elegans*, *in vitro* GSH depletion/oxidation mediated by diamide attenuated WT FoxO1 DNA binding. Interestingly, overexpression of Grx-1 accelerated the recovery of WT FoxO1 to bind in DNA, indicating that interference with glutathione mediated the diamide-driven attenuation of WT FoxO1 DNA binding. In addition, employment of Grx-1 mutants (Grx-1-ΔCys23 and Grx-1-ΔCys26) revealed that S-glutathionylation was responsible for the observed attenuation. As already mentioned above, a possible explanation for the acquired contradictory results between the *in vivo* and *in vitro* approaches could be rest to the inability of *gcs-1* inhibition to mimic processes that require oxidized GSH, such as in the case of S-glutathioynlation.

In summary, this work has established that GSH levels affect FoxO activation and S-glutathionylation contributes to the regulation of FoxO activity. Nevertheless, several questions are still unanswered, such as: Is WT FoxO1 directly S-glutathionylated or is the attenuation in FoxO1 DNA binding through a cysteine-dependent interaction with an unknown S-glutathionylated co-factor? Which FoxO1 cysteine residue is important for the diamide-induced consequences? Could Grx-1-driven acceleration in WT FoxO1 DNA binding recovery be mediated by S-glutathionylation occurring in another protein, such as Akt or PTP-1B, regulating FoxO1 activity? Is the attenuation exclusively mediated by diamide treatment? Whatever the outcome, it has been firmly established here that glutathione may interfere with the redox regulation of FoxO1.

6. References

1. Brenner, S., The genetics of Caenorhabditis elegans. *Genetics* **1974,** 77, (1), 71-94.
2. Olsen, A.; Vantipalli, M. C.; Lithgow, G. J., Using Caenorhabditis elegans as a model for aging and age-related diseases. *Annals of the New York Academy of Sciences* **2006,** 1067, 120-8.
3. Barriere, A.; Felix, M. A., Isolation of C. elegans and related nematodes. *WormBook : the online review of C. elegans biology* **2014**, 1-19.
4. Golden, J. W.; Riddle, D. L., The Caenorhabditis elegans dauer larva: developmental effects of pheromone, food, and temperature. *Developmental biology* **1984,** 102, (2), 368-78.
5. Klass, M. R., Aging in the nematode Caenorhabditis elegans: major biological and environmental factors influencing life span. *Mechanisms of ageing and development* **1977,** 6, (6), 413-29.
6. Sulston, J.; Hodgkin, J., *Methods*. 1988.
7. Edgar, R. S.; Wood, W. B., The nematode Caenorhabditis elegans: a new organism for intensive biological study. *Science* **1977,** 198, (4323), 1285-6.
8. Sulston, J. E., Neuronal cell lineages in the nematode Caenorhabditis elegans. *Cold Spring Harbor symposia on quantitative biology* **1983,** 48 Pt 2, 443-52.
9. Sulston, J. E.; Albertson, D. G.; Thomson, J. N., The Caenorhabditis elegans male: postembryonic development of nongonadal structures. *Developmental biology* **1980,** 78, (2), 542-76.
10. Bucher, E. A.; Seydoux, G., Gastrulation in the nematode Caenorhabditis elegans. *Seminars in Developmental Biology* **1994,** 5, (2), 121-130.
11. Sulston, J. E.; Schierenberg, E.; White, J. G.; Thomson, J. N., The embryonic cell lineage of the nematode Caenorhabditis elegans. *Developmental biology* **1983,** 100, (1), 64-119.
12. Ambros, V., Control of developmental timing in Caenorhabditis elegans. *Current Opinion in Genetics & Development* **2000,** 10, (4), 428-433.
13. Sulston, J. E.; Horvitz, H. R., Post-embryonic cell lineages of the nematode, Caenorhabditis elegans. *Developmental biology* **1977,** 56, (1), 110-156.
14. Johnson, T. E.; Mitchell, D. H.; Kline, S.; Kemal, R.; Foy, J., Arresting development arrests aging in the nematode Caenorhabditis elegans. *Mechanisms of ageing and development* **1984,** 28, (1), 23-40.
15. Riddle, D. L.; Albert, P. S., Genetic and Environmental Regulation of Dauer Larva Development. In *C. elegans II*, 2nd ed.; Riddle, D. L.; Blumenthal, T.; Meyer, B. J.; Priess, J. R., Eds. Cold Spring Harbor (NY), 1997.

16. Cassada, R. C.; Russell, R. L., The dauerlarva, a post-embryonic developmental variant of the nematode Caenorhabditis elegans. *Developmental biology* **1975,** 46, (2), 326-342.
17. Byerly, L.; Cassada, R. C.; Russell, R. L., The life cycle of the nematode Caenorhabditis elegans. *Developmental biology* **1976,** 51, (1), 23-33.
18. Hodgkin, J., Primary sex determination in the nematode C. elegans. *Development* **1987,** 101 Suppl, 5-16.
19. Consortium, C. e. S., Genome sequence of the nematode C. elegans: a platform for investigating biology. *Science* **1998,** 282, (5396), 2012-8.
20. Spieth, J.; Lawson, D., Overview of gene structure. *WormBook : the online review of C. elegans biology* **2006**, 1-10.
21. Blumenthal, T., Trans-splicing and operons in C. elegans. *WormBook : the online review of C. elegans biology* **2012**, 1-11.
22. Jones, D.; Crowe, E.; Stevens, T. A.; Candido, E. P., Functional and phylogenetic analysis of the ubiquitylation system in Caenorhabditis elegans: ubiquitin-conjugating enzymes, ubiquitin-activating enzymes, and ubiquitin-like proteins. *Genome biology* **2002,** 3, (1), RESEARCH0002.
23. Hu, C. W.; Chen, J. L.; Hsu, Y. W.; Yen, C. C.; Chao, M. R., Trace analysis of methylated and hydroxymethylated cytosines in DNA by isotope-dilution LC-MS/MS: first evidence of DNA methylation in Caenorhabditis elegans. *The Biochemical journal* **2015,** 465, (1), 39-47.
24. Berninsone, P. M., Carbohydrates and glycosylation. *WormBook : the online review of C. elegans biology* **2006**, 1-22.
25. Troemel, E. R.; Chou, J. H.; Dwyer, N. D.; Colbert, H. A.; Bargmann, C. I., Divergent seven transmembrane receptors are candidate chemosensory receptors in C. elegans. *Cell* **1995,** 83, (2), 207-18.
26. Han, M.; Sternberg, P. W., let-60, a gene that specifies cell fates during C. elegans vulval induction, encodes a ras protein. *Cell* **1990,** 63, (5), 921-31.
27. Sundaram, M. V., Vulval development: the battle between Ras and Notch. *Current biology : CB* **2004,** 14, (8), R311-3.
28. Ullrich, A.; Bell, J. R.; Chen, E. Y.; Herrera, R.; Petruzzelli, L. M.; Dull, T. J.; Gray, A.; Coussens, L.; Liao, Y. C.; Tsubokawa, M.; et al., Human insulin receptor and its relationship to the tyrosine kinase family of oncogenes. *Nature* **1985,** 313, (6005), 756-61.
29. Taniguchi, C. M.; Emanuelli, B.; Kahn, C. R., Critical nodes in signalling pathways: insights into insulin action. *Nature reviews. Molecular cell biology* **2006,** 7, (2), 85-96.

30. Pinero Gonzalez, J.; Carrillo Farnes, O.; Vasconcelos, A. T.; Gonzalez Perez, A., Conservation of key members in the course of the evolution of the insulin signaling pathway. *Bio Systems* **2009,** 95, (1), 7-16.

31. Riddle, D. L.; Swanson, M. M.; Albert, P. S., Interacting genes in nematode dauer larva formation. *Nature* **1981,** 290, (5808), 668-71.

32. Li, J.; Tewari, M.; Vidal, M.; Lee, S. S., The 14-3-3 protein FTT-2 regulates DAF-16 in Caenorhabditis elegans. *Developmental biology* **2007,** 301, (1), 82-91.

33. Chiang, W. C.; Ching, T. T.; Lee, H. C.; Mousigian, C.; Hsu, A. L., HSF-1 regulators DDL-1/2 link insulin-like signaling to heat-shock responses and modulation of longevity. *Cell* **2012,** 148, (1-2), 322-34.

34. Obsil, T.; Obsilova, V., Structure/function relationships underlying regulation of FOXO transcription factors. *Oncogene* **2008,** 27, (16), 2263-75.

35. Lin, K.; Dorman, J. B.; Rodan, A.; Kenyon, C., daf-16: An HNF-3/forkhead family member that can function to double the life-span of Caenorhabditis elegans. *Science* **1997,** 278, (5341), 1319-22.

36. Ogg, S.; Paradis, S.; Gottlieb, S.; Patterson, G. I.; Lee, L.; Tissenbaum, H. A.; Ruvkun, G., The Fork head transcription factor DAF-16 transduces insulin-like metabolic and longevity signals in C. elegans. *Nature* **1997,** 389, (6654), 994-9.

37. Kwon, E. S.; Narasimhan, S. D.; Yen, K.; Tissenbaum, H. A., A new DAF-16 isoform regulates longevity. *Nature* **2010,** 466, (7305), 498-502.

38. Robida-Stubbs, S.; Glover-Cutter, K.; Lamming, D. W.; Mizunuma, M.; Narasimhan, S. D.; Neumann-Haefelin, E.; Sabatini, D. M.; Blackwell, T. K., TOR signaling and rapamycin influence longevity by regulating SKN-1/Nrf and DAF-16/FoxO. *Cell metabolism* **2012,** 15, (5), 713-24.

39. Landis, J. N.; Murphy, C. T., Integration of diverse inputs in the regulation of Caenorhabditis elegans DAF-16/FOXO. *Developmental dynamics : an official publication of the American Association of Anatomists* **2010,** 239, (5), 1405-12.

40. Greer, E. L.; Dowlatshahi, D.; Banko, M. R.; Villen, J.; Hoang, K.; Blanchard, D.; Gygi, S. P.; Brunet, A., An AMPK-FOXO pathway mediates longevity induced by a novel method of dietary restriction in C. elegans. *Current biology : CB* **2007,** 17, (19), 1646-56.

41. Alam, H.; Williams, T. W.; Dumas, K. J.; Guo, C.; Yoshina, S.; Mitani, S.; Hu, P. J., EAK-7 controls development and life span by regulating nuclear DAF-16/FoxO activity. *Cell metabolism* **2010,** 12, (1), 30-41.

42. Zhang, Y.; Xu, J.; Puscau, C.; Kim, Y.; Wang, X.; Alam, H.; Hu, P. J., Caenorhabditis elegans EAK-3 inhibits dauer arrest via nonautonomous regulation of nuclear DAF-16/FoxO activity. *Developmental biology* **2008,** 315, (2), 290-302.

43. Ohkura, K.; Suzuki, N.; Ishihara, T.; Katsura, I., SDF-9, a protein tyrosine phosphatase-like molecule, regulates the L3/dauer developmental decision through hormonal signaling in C. elegans. *Development* **2003,** 130, (14), 3237-48.

44. Patel, D. S.; Fang, L. L.; Svy, D. K.; Ruvkun, G.; Li, W., Genetic identification of HSD-1, a conserved steroidogenic enzyme that directs larval development in Caenorhabditis elegans. *Development* **2008,** 135, (13), 2239-49.

45. Lehtinen, M. K.; Yuan, Z.; Boag, P. R.; Yang, Y.; Villen, J.; Becker, E. B.; DiBacco, S.; de la Iglesia, N.; Gygi, S.; Blackwell, T. K.; Bonni, A., A conserved MST-FOXO signaling pathway mediates oxidative-stress responses and extends life span. *Cell* **2006,** 125, (5), 987-1001.

46. Li, W.; Gao, B.; Lee, S. M.; Bennett, K.; Fang, D., RLE-1, an E3 ubiquitin ligase, regulates C. elegans aging by catalyzing DAF-16 polyubiquitination. *Developmental cell* **2007,** 12, (2), 235-46.

47. Ghazi, A.; Henis-Korenblit, S.; Kenyon, C., Regulation of Caenorhabditis elegans lifespan by a proteasomal E3 ligase complex. *Proceedings of the National Academy of Sciences of the United States of America* **2007,** 104, (14), 5947-52.

48. Oh, S. W.; Mukhopadhyay, A.; Svrzikapa, N.; Jiang, F.; Davis, R. J.; Tissenbaum, H. A., JNK regulates lifespan in Caenorhabditis elegans by modulating nuclear translocation of forkhead transcription factor/DAF-16. *Proceedings of the National Academy of Sciences of the United States of America* **2005,** 102, (12), 4494-9.

49. Li, J.; Ebata, A.; Dong, Y.; Rizki, G.; Iwata, T.; Lee, S. S., Caenorhabditis elegans HCF-1 functions in longevity maintenance as a DAF-16 regulator. *PLoS biology* **2008,** 6, (9), e233.

50. Takahashi, Y.; Daitoku, H.; Hirota, K.; Tamiya, H.; Yokoyama, A.; Kako, K.; Nagashima, Y.; Nakamura, A.; Shimada, T.; Watanabe, S.; Yamagata, K.; Yasuda, K.; Ishii, N.; Fukamizu, A., Asymmetric arginine dimethylation determines life span in C. elegans by regulating forkhead transcription factor DAF-16. *Cell metabolism* **2011,** 13, (5), 505-16.

51. Essers, M. A.; de Vries-Smits, L. M.; Barker, N.; Polderman, P. E.; Burgering, B. M.; Korswagen, H. C., Functional interaction between beta-catenin and FOXO in oxidative stress signaling. *Science* **2005,** 308, (5725), 1181-4.

52. Tissenbaum, H. A.; Guarente, L., Increased dosage of a sir-2 gene extends lifespan in Caenorhabditis elegans. *Nature* **2001,** 410, (6825), 227-30.

53. Chiang, W. C.; Tishkoff, D. X.; Yang, B.; Wilson-Grady, J.; Yu, X.; Mazer, T.; Eckersdorff, M.; Gygi, S. P.; Lombard, D. B.; Hsu, A. L., C. elegans SIRT6/7 homolog SIR-2.4 promotes DAF-16 relocalization and function during stress. *PLoS genetics* **2012,** 8, (9), e1002948.

54. Nasrin, N.; Ogg, S.; Cahill, C. M.; Biggs, W.; Nui, S.; Dore, J.; Calvo, D.; Shi, Y.; Ruvkun, G.; Alexander-Bridges, M. C., DAF-16 recruits the CREB-binding protein coactivator complex to the insulin-like growth factor binding protein 1 promoter in HepG2 cells. *Proceedings of the National Academy of Sciences of the United States of America* **2000,** 97, (19), 10412-7.

55. Wolff, S.; Ma, H.; Burch, D.; Maciel, G. A.; Hunter, T.; Dillin, A., SMK-1, an essential regulator of DAF-16-mediated longevity. *Cell* **2006,** 124, (5), 1039-53.

56. Dumas, K. J.; Delaney, C. E.; Flibotte, S.; Moerman, D. G.; Csankovszki, G.; Hu, P. J., Unexpected role for dosage compensation in the control of dauer arrest, insulin-like signaling, and FoxO transcription factor activity in Caenorhabditis elegans. *Genetics* **2013,** 194, (3), 619-29.

57. Xiao, R.; Zhang, B.; Dong, Y.; Gong, J.; Xu, T.; Liu, J.; Xu, X. Z., A genetic program promotes C. elegans longevity at cold temperatures via a thermosensitive TRP channel. *Cell* **2013,** 152, (4), 806-17.

58. Honjoh, S.; Yamamoto, T.; Uno, M.; Nishida, E., Signalling through RHEB-1 mediates intermittent fasting-induced longevity in C. elegans. *Nature* **2009,** 457, (7230), 726-30.

59. Furuyama, T.; Nakazawa, T.; Nakano, I.; Mori, N., Identification of the differential distribution patterns of mRNAs and consensus binding sequences for mouse DAF-16 homologues. *The Biochemical journal* **2000,** 349, (Pt 2), 629-34.

60. Murphy, C. T.; McCarroll, S. A.; Bargmann, C. I.; Fraser, A.; Kamath, R. S.; Ahringer, J.; Li, H.; Kenyon, C., Genes that act downstream of DAF-16 to influence the lifespan of Caenorhabditis elegans. *Nature* **2003,** 424, (6946), 277-83.

61. McElwee, J. J.; Schuster, E.; Blanc, E.; Thomas, J. H.; Gems, D., Shared transcriptional signature in Caenorhabditis elegans Dauer larvae and long-lived daf-2 mutants implicates detoxification system in longevity assurance. *The Journal of biological chemistry* **2004,** 279, (43), 44533-43.

62. Tepper, R. G.; Ashraf, J.; Kaletsky, R.; Kleemann, G.; Murphy, C. T.; Bussemaker, H. J., PQM-1 complements DAF-16 as a key transcriptional regulator of DAF-2-mediated development and longevity. *Cell* **2013,** 154, (3), 676-90.

63. Blackwell, T. K.; Bowerman, B.; Priess, J. R.; Weintraub, H., Formation of a monomeric DNA binding domain by Skn-1 bZIP and homeodomain elements. *Science* **1994,** 266, (5185), 621-8.

64. Rupert, P. B.; Daughdrill, G. W.; Bowerman, B.; Matthews, B. W., A new DNA-binding motif in the Skn-1 binding domain-DNA complex. *Nature structural biology* **1998,** 5, (6), 484-91.

65. Bishop, N. A.; Guarente, L., Two neurons mediate diet-restriction-induced longevity in C. elegans. *Nature* **2007,** 447, (7144), 545-9.

66. Tullet, J. M.; Hertweck, M.; An, J. H.; Baker, J.; Hwang, J. Y.; Liu, S.; Oliveira, R. P.; Baumeister, R.; Blackwell, T. K., Direct inhibition of the longevity-promoting factor SKN-1 by insulin-like signaling in C. elegans. *Cell* **2008,** 132, (6), 1025-38.

67. Inoue, H.; Hisamoto, N.; An, J. H.; Oliveira, R. P.; Nishida, E.; Blackwell, T. K.; Matsumoto, K., The C. elegans p38 MAPK pathway regulates nuclear localization of the transcription factor SKN-1 in oxidative stress response. *Genes & development* **2005,** 19, (19), 2278-83.

68. Taguchi, K.; Motohashi, H.; Yamamoto, M., Molecular mechanisms of the Keap1-Nrf2 pathway in stress response and cancer evolution. *Genes to cells : devoted to molecular & cellular mechanisms* **2011,** 16, (2), 123-40.

69. Hayes, J. D.; Dinkova-Kostova, A. T., The Nrf2 regulatory network provides an interface between redox and intermediary metabolism. *Trends in biochemical sciences* **2014,** 39, (4), 199-218.

70. Choe, K. P.; Przybysz, A. J.; Strange, K., The WD40 repeat protein WDR-23 functions with the CUL4/DDB1 ubiquitin ligase to regulate nuclear abundance and activity of SKN-1 in Caenorhabditis elegans. *Molecular and cellular biology* **2009,** 29, (10), 2704-15.

71. Leung, C. K.; Hasegawa, K.; Wang, Y.; Deonarine, A.; Tang, L.; Miwa, J.; Choe, K. P., Direct interaction between the WD40 repeat protein WDR-23 and SKN-1/Nrf inhibits binding to target DNA. *Molecular and cellular biology* **2014,** 34, (16), 3156-67.

72. Leung, C. K.; Wang, Y.; Deonarine, A.; Tang, L.; Prasse, S.; Choe, K. P., A negative-feedback loop between the detoxification/antioxidant response factor SKN-1 and its repressor WDR-23 matches organism needs with environmental conditions. *Molecular and cellular biology* **2013,** 33, (17), 3524-37.

73. Glover-Cutter, K. M.; Lin, S.; Blackwell, T. K., Integration of the unfolded protein and oxidative stress responses through SKN-1/Nrf. *PLoS genetics* **2013,** 9, (9), e1003701.

74. An, J. H.; Vranas, K.; Lucke, M.; Inoue, H.; Hisamoto, N.; Matsumoto, K.; Blackwell, T. K., Regulation of the Caenorhabditis elegans oxidative stress defense protein SKN-1 by glycogen synthase kinase-3. *Proceedings of the National Academy of Sciences of the United States of America* **2005,** 102, (45), 16275-80.

75. Hebeisen, M.; Roy, R., CDC-25.1 stability is regulated by distinct domains to restrict cell division during embryogenesis in C. elegans. *Development* **2008,** 135, (7), 1259-69.

76. Oliveira, R. P.; Porter Abate, J.; Dilks, K.; Landis, J.; Ashraf, J.; Murphy, C. T.; Blackwell, T. K., Condition-adapted stress and longevity gene regulation by Caenorhabditis elegans SKN-1/Nrf. *Aging cell* **2009,** 8, (5), 524-41.

77. Li, X.; Matilainen, O.; Jin, C.; Glover-Cutter, K. M.; Holmberg, C. I.; Blackwell, T. K., Specific SKN-1/Nrf stress responses to perturbations in translation elongation and proteasome activity. *PLoS genetics* **2011,** 7, (6), e1002119.

78. Paek, J.; Lo, J. Y.; Narasimhan, S. D.; Nguyen, T. N.; Glover-Cutter, K.; Robida-Stubbs, S.; Suzuki, T.; Yamamoto, M.; Blackwell, T. K.; Curran, S. P., Mitochondrial SKN-1/Nrf mediates a conserved starvation response. *Cell metabolism* **2012,** 16, (4), 526-37.

79. Staab, T. A.; Griffen, T. C.; Corcoran, C.; Evgrafov, O.; Knowles, J. A.; Sieburth, D., The conserved SKN-1/Nrf2 stress response pathway regulates synaptic function in Caenorhabditis elegans. *PLoS genetics* **2013,** 9, (3), e1003354.

80. Ewald, C. Y.; Landis, J. N.; Porter Abate, J.; Murphy, C. T.; Blackwell, T. K., Dauer-independent insulin/IGF-1-signalling implicates collagen remodelling in longevity. *Nature* **2015,** 519, (7541), 97-101.

81. Park, S. K.; Tedesco, P. M.; Johnson, T. E., Oxidative stress and longevity in Caenorhabditis elegans as mediated by SKN-1. *Aging cell* **2009,** 8, (3), 258-69.

82. Pickering, A. M.; Staab, T. A.; Tower, J.; Sieburth, D.; Davies, K. J., A conserved role for the 20S proteasome and Nrf2 transcription factor in oxidative stress adaptation in mammals, Caenorhabditis elegans and Drosophila melanogaster. *The Journal of experimental biology* **2013,** 216, (Pt 4), 543-53.

83. D'Autreaux, B.; Toledano, M. B., ROS as signalling molecules: mechanisms that generate specificity in ROS homeostasis. *Nature reviews. Molecular cell biology* **2007,** 8, (10), 813-24.

84. Kimura, K. D.; Tissenbaum, H. A.; Liu, Y.; Ruvkun, G., daf-2, an insulin receptor-like gene that regulates longevity and diapause in Caenorhabditis elegans. *Science* **1997,** 277, (5328), 942-6.

85. Lakowski, B.; Hekimi, S., The genetics of caloric restriction in Caenorhabditis elegans. *Proceedings of the National Academy of Sciences of the United States of America* **1998,** 95, (22), 13091-6.

86. Doonan, R.; McElwee, J. J.; Matthijssens, F.; Walker, G. A.; Houthoofd, K.; Back, P.; Matscheski, A.; Vanfleteren, J. R.; Gems, D., Against the oxidative damage theory of aging: superoxide dismutases protect against oxidative stress but have little or no effect on life span in Caenorhabditis elegans. *Genes & development* **2008,** 22, (23), 3236-41.

87. Van Raamsdonk, J. M.; Hekimi, S., Deletion of the mitochondrial superoxide dismutase sod-2 extends lifespan in Caenorhabditis elegans. *PLoS genetics* **2009,** 5, (2), e1000361.

88. Hunter, T.; Bannister, W. H.; Hunter, G. J., Cloning, expression, and characterization of two manganese superoxide dismutases from Caenorhabditis elegans. *The Journal of biological chemistry* **1997,** 272, (45), 28652-9.

89. Honda, Y.; Honda, S., The daf-2 gene network for longevity regulates oxidative stress resistance and Mn-superoxide dismutase gene expression in Caenorhabditis elegans. *FASEB journal : official publication of the Federation of American Societies for Experimental Biology* **1999,** 13, (11), 1385-93.

90. Yanase, S.; Ishi, N., Cloning of the oxidative stress-responsive genes in Caenorhabditis elegans. *Journal of radiation research* **1999,** 40, (1), 39-47.

91. Van Raamsdonk, J. M.; Hekimi, S., Superoxide dismutase is dispensable for normal animal lifespan. *Proceedings of the National Academy of Sciences of the United States of America* **2012,** 109, (15), 5785-90.

92. Petriv, O. I.; Rachubinski, R. A., Lack of peroxisomal catalase causes a progeric phenotype in Caenorhabditis elegans. *The Journal of biological chemistry* **2004,** 279, (19), 19996-20001.

93. Taub, J.; Lau, J. F.; Ma, C.; Hahn, J. H.; Hoque, R.; Rothblatt, J.; Chalfie, M., A cytosolic catalase is needed to extend adult lifespan in C. elegans daf-C and clk-1 mutants. *Nature* **2003,** 421, (6924), 764.

94. Jee, C.; Vanoaica, L.; Lee, J.; Park, B. J.; Ahnn, J., Thioredoxin is related to life span regulation and oxidative stress response in Caenorhabditis elegans. *Genes to cells : devoted to molecular & cellular mechanisms* **2005,** 10, (12), 1203-10.

95. Fierro-Gonzalez, J. C.; Gonzalez-Barrios, M.; Miranda-Vizuete, A.; Swoboda, P., The thioredoxin TRX-1 regulates adult lifespan extension induced by dietary restriction in Caenorhabditis elegans. *Biochemical and biophysical research communications* **2011,** 406, (3), 478-82.

96. Leiers, B.; Kampkotter, A.; Grevelding, C. G.; Link, C. D.; Johnson, T. E.; Henkle-Duhrsen, K., A stress-responsive glutathione S-transferase confers resistance to oxidative stress in Caenorhabditis elegans. *Free radical biology & medicine* **2003,** 34, (11), 1405-15.

97. Ayyadevara, S.; Engle, M. R.; Singh, S. P.; Dandapat, A.; Lichti, C. F.; Benes, H.; Shmookler Reis, R. J.; Liebau, E.; Zimniak, P., Lifespan and stress resistance of Caenorhabditis elegans are increased by expression of glutathione transferases capable of metabolizing the lipid peroxidation product 4-hydroxynonenal. *Aging cell* **2005,** 4, (5), 257-71.

98. Ayyadevara, S.; Dandapat, A.; Singh, S. P.; Siegel, E. R.; Shmookler Reis, R. J.; Zimniak, L.; Zimniak, P., Life span and stress resistance of Caenorhabditis elegans are differentially affected by glutathione transferases metabolizing 4-hydroxynon-2-enal. *Mechanisms of ageing and development* **2007,** 128, (2), 196-205.

99. Birben, E.; Sahiner, U. M.; Sackesen, C.; Erzurum, S.; Kalayci, O., Oxidative stress and antioxidant defense. *The World Allergy Organization journal* **2012,** 5, (1), 9-19.

100. Meister, A.; Anderson, M. E., Glutathione. *Annual review of biochemistry* **1983,** 52, 711-60.

101. Holmgren, A., Hydrogen donor system for Escherichia coli ribonucleoside-diphosphate reductase dependent upon glutathione. *Proceedings of the National Academy of Sciences of the United States of America* **1976,** 73, (7), 2275-9.

102. Lillig, C. H.; Berndt, C.; Holmgren, A., Glutaredoxin systems. *Biochimica et Biophysica Acta (BBA) - General Subjects* **2008,** 1780, (11), 1304-1317.

103. Johansson, C.; Lillig, C. H.; Holmgren, A., Human mitochondrial glutaredoxin reduces S-glutathionylated proteins with high affinity accepting electrons from either glutathione or thioredoxin reductase. *The Journal of biological chemistry* **2004,** 279, (9), 7537-43.

104. Lillig, C. H.; Berndt, C.; Vergnolle, O.; Lonn, M. E.; Hudemann, C.; Bill, E.; Holmgren, A., Characterization of human glutaredoxin 2 as iron-sulfur protein: a possible role as redox sensor. *Proceedings of the National Academy of Sciences of the United States of America* **2005,** 102, (23), 8168-73.

105. Yang, Y.; Jao, S.; Nanduri, S.; Starke, D. W.; Mieyal, J. J.; Qin, J., Reactivity of the human thioltransferase (glutaredoxin) C7S, C25S, C78S, C82S mutant and NMR solution structure of its glutathionyl mixed disulfide intermediate reflect catalytic specificity. *Biochemistry* **1998,** 37, (49), 17145-56.

106. Bushweller, J. H.; Aslund, F.; Wuthrich, K.; Holmgren, A., Structural and functional characterization of the mutant Escherichia coli glutaredoxin (C14----S) and its mixed disulfide with glutathione. *Biochemistry* **1992,** 31, (38), 9288-93.

107. White, C. C.; Viernes, H.; Krejsa, C. M.; Botta, D.; Kavanagh, T. J., Fluorescence-based microtiter plate assay for glutamate-cysteine ligase activity. *Analytical biochemistry* **2003,** 318, (2), 175-80.

108. Kaplowitz, N.; Aw, T. Y.; Ookhtens, M., The regulation of hepatic glutathione. *Annual review of pharmacology and toxicology* **1985,** 25, 715-44.

109. Watson, W. H.; Chen, Y.; Jones, D. P., Redox state of glutathione and thioredoxin in differentiation and apoptosis. *BioFactors* **2003,** 17, (1-4), 307-14.

110. Meredith, M. J.; Reed, D. J., Status of the mitochondrial pool of glutathione in the isolated hepatocyte. *The Journal of biological chemistry* **1982,** 257, (7), 3747-53.

111. Hwang, C.; Sinskey, A. J.; Lodish, H. F., Oxidized redox state of glutathione in the endoplasmic reticulum. *Science* **1992,** 257, (5076), 1496-502.

112. Ballatori, N.; Krance, S. M.; Notenboom, S.; Shi, S.; Tieu, K.; Hammond, C. L., Glutathione dysregulation and the etiology and progression of human diseases. *Biological chemistry* **2009,** 390, (3), 191-214.

113. Suthanthiran, M.; Anderson, M. E.; Sharma, V. K.; Meister, A., Glutathione regulates activation-dependent DNA synthesis in highly purified normal human T lymphocytes stimulated via the CD2 and CD3 antigens. *Proceedings of the National Academy of Sciences of the United States of America* **1990,** 87, (9), 3343-7.

114. Pallardo, F. V.; Markovic, J.; Garcia, J. L.; Vina, J., Role of nuclear glutathione as a key regulator of cell proliferation. *Molecular aspects of medicine* **2009,** 30, (1-2), 77-85.

115. Liu, R. M.; Gaston Pravia, K. A., Oxidative stress and glutathione in TGF-beta-mediated fibrogenesis. *Free radical biology & medicine* **2010,** 48, (1), 1-15.

116. Flohe, L., Glutathione peroxidase. *Basic life sciences* **1988,** 49, 663-8.

117. Manso, C.; Wroblewski, F., Glutathione reductase activity in blood and body fluids. *The Journal of clinical investigation* **1958,** 37, (2), 214-8.

118. Fernandez-Checa, J. C.; Kaplowitz, N.; Garcia-Ruiz, C.; Colell, A.; Miranda, M.; Mari, M.; Ardite, E.; Morales, A., GSH transport in mitochondria: defense against TNF-induced oxidative stress and alcohol-induced defect. *The American journal of physiology* **1997,** 273, (1 Pt 1), G7-17.

119. Lu, S. C., Glutathione synthesis. *Biochimica et biophysica acta* **2013,** 1830, (5), 3143-53.

120. Huang, Z. Z.; Chen, C.; Zeng, Z.; Yang, H.; Oh, J.; Chen, L.; Lu, S. C., Mechanism and significance of increased glutathione level in human hepatocellular carcinoma and liver regeneration. *FASEB journal : official publication of the Federation of American Societies for Experimental Biology* **2001,** 15, (1), 19-21.

121. Lu, S. C.; Ge, J. L., Loss of suppression of GSH synthesis at low cell density in primary cultures of rat hepatocytes. *The American journal of physiology* **1992,** 263, (6 Pt 1), C1181-9.

122. Diaz Vivancos, P.; Wolff, T.; Markovic, J.; Pallardo, F. V.; Foyer, C. H., A nuclear glutathione cycle within the cell cycle. *The Biochemical journal* **2010,** 431, (2), 169-78.

123. Holmgren, A., Regulation of ribonucleotide reductase. *Current topics in cellular regulation* **1981,** 19, 47-76.

124. Hall, A. G., Review: The role of glutathione in the regulation of apoptosis. *European journal of clinical investigation* **1999,** 29, (3), 238-45.

125. Franklin, C. C.; Krejsa, C. M.; Pierce, R. H.; White, C. C.; Fausto, N.; Kavanagh, T. J., Caspase-3-Dependent Cleavage of the Glutamate-L-Cysteine Ligase Catalytic Subunit during Apoptotic Cell Death. *The American journal of pathology* **2002,** 160, (5), 1887-94.

126. Garcia-Ruiz, C.; Fernandez-Checa, J. C., Redox regulation of hepatocyte apoptosis. *Journal of gastroenterology and hepatology* **2007,** 22 Suppl 1, S38-42.

127. Dalle-Donne, I.; Rossi, R.; Giustarini, D.; Colombo, R.; Milzani, A., S-glutathionylation in protein redox regulation. *Free Radical Biology and Medicine* **2007,** 43, (6), 883-898.

128. Martinez-Ruiz, A.; Lamas, S., Signalling by NO-induced protein S-nitrosylation and S-glutathionylation: convergences and divergences. *Cardiovascular research* **2007,** 75, (2), 220-8.

129. Giustarini, D.; Milzani, A.; Aldini, G.; Carini, M.; Rossi, R.; Dalle-Donne, I., S-nitrosation versus S-glutathionylation of protein sulfhydryl groups by S-nitrosoglutathione. *Antioxidants & redox signaling* **2005,** 7, (7-8), 930-9.

130. Mallis, R. J.; Buss, J. E.; Thomas, J. A., Oxidative modification of H-ras: S-thiolation and S-nitrosylation of reactive cysteines. *The Biochemical journal* **2001,** 355, (Pt 1), 145-53.

131. Mallis, R. J.; Hamann, M. J.; Zhao, W.; Zhang, T.; Hendrich, S.; Thomas, J. A., Irreversible thiol oxidation in carbonic anhydrase III: protection by S-glutathiolation and detection in aging rats. *Biological chemistry* **2002,** 383, (3-4), 649-62.

132. Dominici, S.; Valentini, M.; Maellaro, E.; Del Bello, B.; Paolicchi, A.; Lorenzini, E.; Tongiani, R.; Comporti, M.; Pompella, A., Redox modulation of cell surface protein thiols in U937 lymphoma cells: the role of gamma-glutamyl transpeptidase-dependent H2O2 production and S-thiolation. *Free radical biology & medicine* **1999,** 27, (5-6), 623-35.

133. Borges, C. R.; Geddes, T.; Watson, J. T.; Kuhn, D. M., Dopamine biosynthesis is regulated by S-glutathionylation. Potential mechanism of tyrosine hydroxylast inhibition during oxidative stress. *The Journal of biological chemistry* **2002,** 277, (50), 48295-302.

134. Eaton, P.; Wright, N.; Hearse, D. J.; Shattock, M. J., Glyceraldehyde phosphate dehydrogenase oxidation during cardiac ischemia and reperfusion. *Journal of molecular and cellular cardiology* **2002,** 34, (11), 1549-60.

135. Klatt, P.; Molina, E. P.; De Lacoba, M. G.; Padilla, C. A.; Martinez-Galesteo, E.; Barcena, J. A.; Lamas, S., Redox regulation of c-Jun DNA binding by reversible S-glutathiolation. *FASEB journal : official publication of the Federation of American Societies for Experimental Biology* **1999,** 13, (12), 1481-90.

136. Pineda-Molina, E.; Klatt, P.; Vazquez, J.; Marina, A.; Garcia de Lacoba, M.; Perez-Sala, D.; Lamas, S., Glutathionylation of the p50 subunit of NF-kappaB: a mechanism for redox-induced inhibition of DNA binding. *Biochemistry* **2001,** 40, (47), 14134-42.

137. Qanungo, S.; Starke, D. W.; Pai, H. V.; Mieyal, J. J.; Nieminen, A. L., Glutathione supplementation potentiates hypoxic apoptosis by S-glutathionylation of p65-NFkappaB. *The Journal of biological chemistry* **2007,** 282, (25), 18427-36.

138. Fratelli, M.; Goodwin, L. O.; Orom, U. A.; Lombardi, S.; Tonelli, R.; Mengozzi, M.; Ghezzi, P., Gene expression profiling reveals a signaling role of glutathione in redox regulation. *Proceedings of the National Academy of Sciences of the United States of America* **2005,** 102, (39), 13998-4003.

139. Dandrea, T.; Bajak, E.; Warngard, L.; Cotgreave, I. A., Protein S-glutathionylation correlates to selective stress gene expression and cytoprotection. *Archives of biochemistry and biophysics* **2002,** 406, (2), 241-52.

140. Sies, H.; Akerboom, T. P., Glutathione disulfide (GSSG) efflux from cells and tissues. *Methods in enzymology* **1984,** 105, 445-51.

141. Mawatari, S.; Murakami, K., Different types of glutathionylation of hemoglobin can exist in intact erythrocytes. *Archives of biochemistry and biophysics* **2004,** 421, (1), 108-14.

142. Rossi, R.; Dalle-Donne, I.; Milzani, A.; Giustarini, D., Oxidized forms of glutathione in peripheral blood as biomarkers of oxidative stress. *Clinical chemistry* **2006,** 52, (7), 1406-14.

143. Craghill, J.; Cronshaw, A. D.; Harding, J. J., The identification of a reaction site of glutathione mixed-disulphide formation on gammaS-crystallin in human lens. *The Biochemical journal* **2004,** 379, (Pt 3), 595-600.

144. Pastore, A.; Tozzi, G.; Gaeta, L. M.; Bertini, E.; Serafini, V.; Di Cesare, S.; Bonetto, V.; Casoni, F.; Carrozzo, R.; Federici, G.; Piemonte, F., Actin glutathionylation increases in fibroblasts of patients with Friedreich's ataxia: a potential role in the pathogenesis of the disease. *The Journal of biological chemistry* **2003,** 278, (43), 42588-95.

145. Wang, J.; Boja, E. S.; Tan, W.; Tekle, E.; Fales, H. M.; English, S.; Mieyal, J. J.; Chock, P. B., Reversible glutathionylation regulates actin polymerization in A431 cells. *The Journal of biological chemistry* **2001,** 276, (51), 47763-6.

146. Gravina, S. A.; Mieyal, J. J., Thioltransferase is a specific glutathionyl mixed disulfide oxidoreductase. *Biochemistry* **1993,** 32, (13), 3368-76.

147. Shelton, M. D.; Chock, P. B.; Mieyal, J. J., Glutaredoxin: role in reversible protein s-glutathionylation and regulation of redox signal transduction and protein translocation. *Antioxidants & redox signaling* **2005,** 7, (3-4), 348-66.

148. Lind, C.; Gerdes, R.; Schuppe-Koistinen, I.; Cotgreave, I. A., Studies on the mechanism of oxidative modification of human glyceraldehyde-3-phosphate dehydrogenase by glutathione: catalysis by glutaredoxin. *Biochemical and biophysical research communications* **1998,** 247, (2), 481-6.

149. Xiao, R.; Lundstrom-Ljung, J.; Holmgren, A.; Gilbert, H. F., Catalysis of thiol/disulfide exchange. Glutaredoxin 1 and protein-disulfide isomerase use different mechanisms to enhance oxidase and reductase activities. *The Journal of biological chemistry* **2005,** 280, (22), 21099-106.

150. Weigel, D.; Jurgens, G.; Kuttner, F.; Seifert, E.; Jackle, H., The homeotic gene fork head encodes a nuclear protein and is expressed in the terminal regions of the Drosophila embryo. *Cell* **1989,** 57, (4), 645-58.

151. Weigel, D.; Jackle, H., The fork head domain: a novel DNA binding motif of eukaryotic transcription factors? *Cell* **1990,** 63, (3), 455-6.

152. Kaestner, K. H.; Knochel, W.; Martinez, D. E., Unified nomenclature for the winged helix/forkhead transcription factors. *Genes & development* **2000,** 14, (2), 142-6.

153. Monsalve, M.; Olmos, Y., The complex biology of FOXO. *Current drug targets* **2011,** 12, (9), 1322-50.

154. Kim, D. H.; Perdomo, G.; Zhang, T.; Slusher, S.; Lee, S.; Phillips, B. E.; Fan, Y.; Giannoukakis, N.; Gramignoli, R.; Strom, S.; Ringquist, S.; Dong, H. H., FoxO6 integrates insulin signaling with gluconeogenesis in the liver. *Diabetes* **2011,** 60, (11), 2763-74.

155. Klotz, L. O.; Sanchez-Ramos, C.; Prieto-Arroyo, I.; Urbanek, P.; Steinbrenner, H.; Monsalve, M., Redox regulation of FoxO transcription factors. *Redox biology* **2015,** 6, 51-72.

156. Mahadev, K.; Zilbering, A.; Zhu, L.; Goldstein, B. J., Insulin-stimulated hydrogen peroxide reversibly inhibits protein-tyrosine phosphatase 1b in vivo and enhances the early insulin action cascade. *The Journal of biological chemistry* **2001,** 276, (24), 21938-42.

157. Meng, T. C.; Buckley, D. A.; Galic, S.; Tiganis, T.; Tonks, N. K., Regulation of insulin signaling through reversible oxidation of the protein-tyrosine phosphatases TC45 and PTP1B. *The Journal of biological chemistry* **2004,** 279, (36), 37716-25.

158. Mahadev, K.; Motoshima, H.; Wu, X.; Ruddy, J. M.; Arnold, R. S.; Cheng, G.; Lambeth, J. D.; Goldstein, B. J., The NAD(P)H oxidase homolog Nox4 modulates

insulin-stimulated generation of H2O2 and plays an integral role in insulin signal transduction. *Molecular and cellular biology* **2004,** 24, (5), 1844-54.

159. Yang, J. Y.; Zong, C. S.; Xia, W.; Yamaguchi, H.; Ding, Q.; Xie, X.; Lang, J. Y.; Lai, C. C.; Chang, C. J.; Huang, W. C.; Huang, H.; Kuo, H. P.; Lee, D. F.; Li, L. Y.; Lien, H. C.; Cheng, X.; Chang, K. J.; Hsiao, C. D.; Tsai, F. J.; Tsai, C. H.; Sahin, A. A.; Muller, W. J.; Mills, G. B.; Yu, D.; Hortobagyi, G. N.; Hung, M. C., ERK promotes tumorigenesis by inhibiting FOXO3a via MDM2-mediated degradation. *Nature cell biology* **2008,** 10, (2), 138-48.
160. Asada, S.; Daitoku, H.; Matsuzaki, H.; Saito, T.; Sudo, T.; Mukai, H.; Iwashita, S.; Kako, K.; Kishi, T.; Kasuya, Y.; Fukamizu, A., Mitogen-activated protein kinases, Erk and p38, phosphorylate and regulate Foxo1. *Cellular signalling* **2007,** 19, (3), 519-27.
161. Essers, M. A.; Weijzen, S.; de Vries-Smits, A. M.; Saarloos, I.; de Ruiter, N. D.; Bos, J. L.; Burgering, B. M., FOXO transcription factor activation by oxidative stress mediated by the small GTPase Ral and JNK. *The EMBO journal* **2004,** 23, (24), 4802-12.
162. Huang, H.; Regan, K. M.; Lou, Z.; Chen, J.; Tindall, D. J., CDK2-dependent phosphorylation of FOXO1 as an apoptotic response to DNA damage. *Science* **2006,** 314, (5797), 294-7.
163. Huo, X.; Liu, S.; Shao, T.; Hua, H.; Kong, Q.; Wang, J.; Luo, T.; Jiang, Y., GSK3 protein positively regulates type I insulin-like growth factor receptor through forkhead transcription factors FOXO1/3/4. *The Journal of biological chemistry* **2014,** 289, (36), 24759-70.
164. Woods, Y. L.; Rena, G.; Morrice, N.; Barthel, A.; Becker, W.; Guo, S.; Unterman, T. G.; Cohen, P., The kinase DYRK1A phosphorylates the transcription factor FKHR at Ser329 in vitro, a novel in vivo phosphorylation site. *The Biochemical journal* **2001,** 355, (Pt 3), 597-607.
165. Ott, C.; Jacobs, K.; Haucke, E.; Navarrete Santos, A.; Grune, T.; Simm, A., Role of advanced glycation end products in cellular signaling. *Redox biology* **2014,** 2, 411-29.
166. Tanaka, J.; Qiang, L.; Banks, A. S.; Welch, C. L.; Matsumoto, M.; Kitamura, T.; Ido-Kitamura, Y.; DePinho, R. A.; Accili, D., Foxo1 links hyperglycemia to LDL oxidation and endothelial nitric oxide synthase dysfunction in vascular endothelial cells. *Diabetes* **2009,** 58, (10), 2344-54.
167. Walter, P. L.; Kampkotter, A.; Eckers, A.; Barthel, A.; Schmoll, D.; Sies, H.; Klotz, L. O., Modulation of FoxO signaling in human hepatoma cells by exposure to copper or zinc ions. *Archives of biochemistry and biophysics* **2006,** 454, (2), 107-13.

168. Barthel, A.; Ostrakhovitch, E. A.; Walter, P. L.; Kampkotter, A.; Klotz, L. O., Stimulation of phosphoinositide 3-kinase/Akt signaling by copper and zinc ions: mechanisms and consequences. *Archives of biochemistry and biophysics* **2007,** 463, (2), 175-82.

169. Plum, L. M.; Brieger, A.; Engelhardt, G.; Hebel, S.; Nessel, A.; Arlt, M.; Kaltenberg, J.; Schwaneberg, U.; Huber, M.; Rink, L.; Haase, H., PTEN-inhibition by zinc ions augments interleukin-2-mediated Akt phosphorylation. *Metallomics : integrated biometal science* **2014,** 6, (7), 1277-87.

170. Ho, K. K.; McGuire, V. A.; Koo, C. Y.; Muir, K. W.; de Olano, N.; Maifoshie, E.; Kelly, D. J.; McGovern, U. B.; Monteiro, L. J.; Gomes, A. R.; Nebreda, A. R.; Campbell, D. G.; Arthur, J. S.; Lam, E. W., Phosphorylation of FOXO3a on Ser-7 by p38 promotes its nuclear localization in response to doxorubicin. *The Journal of biological chemistry* **2012,** 287, (2), 1545-55.

171. Cai, B.; Xia, Z., p38 MAP kinase mediates arsenite-induced apoptosis through FOXO3a activation and induction of Bim transcription. *Apoptosis : an international journal on programmed cell death* **2008,** 13, (6), 803-10.

172. Hamann, I.; Klotz, L. O., Arsenite-induced stress signaling: modulation of the phosphoinositide 3'-kinase/Akt/FoxO signaling cascade. *Redox biology* **2013,** 1, 104-9.

173. Hamann, I.; Petroll, K.; Hou, X.; Anwar-Mohamed, A.; El-Kadi, A. O.; Klotz, L. O., Acute and long-term effects of arsenite in HepG2 cells: modulation of insulin signaling. *Biometals : an international journal on the role of metal ions in biology, biochemistry, and medicine* **2014,** 27, (2), 317-32.

174. Calnan, D. R.; Brunet, A., The FoxO code. *Oncogene* **2008,** 27, (16), 2276-88.

175. Motta, M. C.; Divecha, N.; Lemieux, M.; Kamel, C.; Chen, D.; Gu, W.; Bultsma, Y.; McBurney, M.; Guarente, L., Mammalian SIRT1 represses forkhead transcription factors. *Cell* **2004,** 116, (4), 551-63.

176. Jing, E.; Gesta, S.; Kahn, C. R., SIRT2 regulates adipocyte differentiation through FoxO1 acetylation/deacetylation. *Cell metabolism* **2007,** 6, (2), 105-14.

177. Dansen, T. B.; Smits, L. M.; van Triest, M. H.; de Keizer, P. L.; van Leenen, D.; Koerkamp, M. G.; Szypowska, A.; Meppelink, A.; Brenkman, A. B.; Yodoi, J.; Holstege, F. C.; Burgering, B. M., Redox-sensitive cysteines bridge p300/CBP-mediated acetylation and FoxO4 activity. *Nature chemical biology* **2009,** 5, (9), 664-72.

178. Perrot, V.; Rechler, M. M., The coactivator p300 directly acetylates the forkhead transcription factor Foxo1 and stimulates Foxo1-induced transcription. *Molecular endocrinology* **2005,** 19, (9), 2283-98.

179. Mahmud, D. L.; M, G. A.; Deb, D. K.; Platanias, L. C.; Uddin, S.; Wickrema, A., Phosphorylation of forkhead transcription factors by erythropoietin and stem cell factor prevents acetylation and their interaction with coactivator p300 in erythroid progenitor cells. *Oncogene* **2002,** 21, (10), 1556-62.

180. Fukuoka, M.; Daitoku, H.; Hatta, M.; Matsuzaki, H.; Umemura, S.; Fukamizu, A., Negative regulation of forkhead transcription factor AFX (Foxo4) by CBP-induced acetylation. *International journal of molecular medicine* **2003,** 12, (4), 503-8.

181. van der Horst, A.; de Vries-Smits, A. M.; Brenkman, A. B.; van Triest, M. H.; van den Broek, N.; Colland, F.; Maurice, M. M.; Burgering, B. M., FOXO4 transcriptional activity is regulated by monoubiquitination and USP7/HAUSP. *Nature cell biology* **2006,** 8, (10), 1064-73.

182. Wang, F.; Chan, C. H.; Chen, K.; Guan, X.; Lin, H. K.; Tong, Q., Deacetylation of FOXO3 by SIRT1 or SIRT2 leads to Skp2-mediated FOXO3 ubiquitination and degradation. *Oncogene* **2012,** 31, (12), 1546-57.

183. Huang, H.; Regan, K. M.; Wang, F.; Wang, D.; Smith, D. I.; van Deursen, J. M.; Tindall, D. J., Skp2 inhibits FOXO1 in tumor suppression through ubiquitin-mediated degradation. *Proceedings of the National Academy of Sciences of the United States of America* **2005,** 102, (5), 1649-54.

184. Kops, G. J.; Dansen, T. B.; Polderman, P. E.; Saarloos, I.; Wirtz, K. W.; Coffer, P. J.; Huang, T. T.; Bos, J. L.; Medema, R. H.; Burgering, B. M., Forkhead transcription factor FOXO3a protects quiescent cells from oxidative stress. *Nature* **2002,** 419, (6904), 316-21.

185. Marinkovic, D.; Zhang, X.; Yalcin, S.; Luciano, J. P.; Brugnara, C.; Huber, T.; Ghaffari, S., Foxo3 is required for the regulation of oxidative stress in erythropoiesis. *The Journal of clinical investigation* **2007,** 117, (8), 2133-44.

186. Nemoto, S.; Finkel, T., Redox regulation of forkhead proteins through a p66shc-dependent signaling pathway. *Science* **2002,** 295, (5564), 2450-2.

187. Chiribau, C. B.; Cheng, L.; Cucoranu, I. C.; Yu, Y. S.; Clempus, R. E.; Sorescu, D., FOXO3A regulates peroxiredoxin III expression in human cardiac fibroblasts. *The Journal of biological chemistry* **2008,** 283, (13), 8211-7.

188. Olmos, Y.; Sanchez-Gomez, F. J.; Wild, B.; Garcia-Quintans, N.; Cabezudo, S.; Lamas, S.; Monsalve, M., SirT1 regulation of antioxidant genes is dependent on the formation of a FoxO3a/PGC-1alpha complex. *Antioxidants & redox signaling* **2013,** 19, (13), 1507-21.

189. Greer, E. L.; Oskoui, P. R.; Banko, M. R.; Maniar, J. M.; Gygi, M. P.; Gygi, S. P.; Brunet, A., The energy sensor AMP-activated protein kinase directly regulates the

mammalian FOXO3 transcription factor. *The Journal of biological chemistry* **2007,** 282, (41), 30107-19.

190. Sidhu, A.; Miller, P. J.; Hollenbach, A. D., FOXO1 stimulates ceruloplasmin promoter activity in human hepatoma cells treated with IL-6. *Biochemical and biophysical research communications* **2011,** 404, (4), 963-7.
191. Hellman, N. E.; Gitlin, J. D., Ceruloplasmin metabolism and function. *Annual review of nutrition* **2002,** 22, 439-58.
192. White, K. N.; Conesa, C.; Sanchez, L.; Amini, M.; Farnaud, S.; Lorvoralak, C.; Evans, R. W., The transfer of iron between ceruloplasmin and transferrins. *Biochimica et biophysica acta* **2012,** 1820, (3), 411-6.
193. Walter, P. L.; Steinbrenner, H.; Barthel, A.; Klotz, L. O., Stimulation of selenoprotein P promoter activity in hepatoma cells by FoxO1a transcription factor. *Biochemical and biophysical research communications* **2008,** 365, (2), 316-21.
194. Speckmann, B.; Walter, P. L.; Alili, L.; Reinehr, R.; Sies, H.; Klotz, L. O.; Steinbrenner, H., Selenoprotein P expression is controlled through interaction of the coactivator PGC-1alpha with FoxO1a and hepatocyte nuclear factor 4alpha transcription factors. *Hepatology* **2008,** 48, (6), 1998-2006.
195. Hoffmann, P. R.; Hoge, S. C.; Li, P. A.; Hoffmann, F. W.; Hashimoto, A. C.; Berry, M. J., The selenoproteome exhibits widely varying, tissue-specific dependence on selenoprotein P for selenium supply. *Nucleic acids research* **2007,** 35, (12), 3963-73.
196. Steinbrenner, H.; Alili, L.; Bilgic, E.; Sies, H.; Brenneisen, P., Involvement of selenoprotein P in protection of human astrocytes from oxidative damage. *Free radical biology & medicine* **2006,** 40, (9), 1513-23.
197. Steinbrenner, H.; Bilgic, E.; Alili, L.; Sies, H.; Brenneisen, P., Selenoprotein P protects endothelial cells from oxidative damage by stimulation of glutathione peroxidase expression and activity. *Free radical research* **2006,** 40, (9), 936-43.
198. Saito, Y.; Hayashi, T.; Tanaka, A.; Watanabe, Y.; Suzuki, M.; Saito, E.; Takahashi, K., Selenoprotein P in human plasma as an extracellular phospholipid hydroperoxide glutathione peroxidase. Isolation and enzymatic characterization of human selenoprotein p. *The Journal of biological chemistry* **1999,** 274, (5), 2866-71.
199. Traulsen, H.; Steinbrenner, H.; Buchczyk, D. P.; Klotz, L. O.; Sies, H., Selenoprotein P protects low-density lipoprotein against oxidation. *Free radical research* **2004,** 38, (2), 123-8.
200. Boyland, E.; Chasseaud, L. F., Enzyme-catalysed conjugations of glutathione with unsaturated compounds. *The Biochemical journal* **1967,** 104, (1), 95-102.

201. Kosower, N. S.; Kosower, E. M.; Wertheim, B.; Correa, W. S., Diamide, a new reagent for the intracellular oxidation of glutathione to the disulfide. *Biochemical and biophysical research communications* **1969,** 37, (4), 593-6.

202. Putker, M.; Vos, H. R.; van Dorenmalen, K.; de Ruiter, H.; Duran, A. G.; Snel, B.; Burgering, B. M.; Vermeulen, M.; Dansen, T. B., Evolutionary acquisition of cysteines determines FOXO paralog-specific redox signaling. *Antioxidants & redox signaling* **2015,** 22, (1), 15-28.

203. Sewastianik, T.; Szydlowski, M.; Jablonska, E.; Bialopiotrowicz, E.; Kiliszek, P.; Gorniak, P.; Polak, A.; Prochorec-Sobieszek, M.; Szumera-Cieckiewicz, A.; Kaminski, T. S.; Markowicz, S.; Nowak, E.; Grygorowicz, M. A.; Warzocha, K.; Juszczynski, P., FOXO1 is a TXN- and p300-dependent sensor and effector of oxidative stress in diffuse large B-cell lymphomas characterized by increased oxidative metabolism. *Oncogene* **2016,** 35, (46), 5989-6000.

204. Urban, N.; Tsitsipatis, D.; Hausig, F.; Kreuzer, K.; Erler, K.; Stein, V.; Ristow, M.; Steinbrenner, H.; Klotz, L. O., Non-linear impact of glutathione depletion on C. elegans life span and stress resistance. *Redox biology* **2017,** 11, 502-515.

205. Fraser, A. G.; Kamath, R. S.; Zipperlen, P.; Martinez-Campos, M.; Sohrmann, M.; Ahringer, J., Functional genomic analysis of C. elegans chromosome I by systematic RNA interference. *Nature* **2000,** 408, (6810), 325-30.

206. Ayala, J. E.; Streeper, R. S.; Desgrosellier, J. S.; Durham, S. K.; Suwanichkul, A.; Svitek, C. A.; Goldman, J. K.; Barr, F. G.; Powell, D. R.; O'Brien, R. M., Conservation of an insulin response unit between mouse and human glucose-6-phosphatase catalytic subunit gene promoters: transcription factor FKHR binds the insulin response sequence. *Diabetes* **1999,** 48, (9), 1885-9.

207. Brunet, A.; Bonni, A.; Zigmond, M. J.; Lin, M. Z.; Juo, P.; Hu, L. S.; Anderson, M. J.; Arden, K. C.; Blenis, J.; Greenberg, M. E., Akt promotes cell survival by phosphorylating and inhibiting a Forkhead transcription factor. *Cell* **1999,** 96, (6), 857-68.

208. Ellman, G. L., A colorimetric method for determining low concentrations of mercaptans. *Archives of biochemistry and biophysics* **1958,** 74, (2), 443-50.

209. Bradford, M. M., A rapid and sensitive method for the quantitation of microgram quantities of protein utilizing the principle of protein-dye binding. *Analytical biochemistry* **1976,** 72, 248-54.

210. Anderson, M. E., Determination of glutathione and glutathione disulfide in biological samples. *Methods in enzymology* **1985,** 113, 548-55.

211. Greiss, S.; Schumacher, B.; Grandien, K.; Rothblatt, J.; Gartner, A., Transcriptional profiling in C. elegans suggests DNA damage dependent apoptosis as an ancient function of the p53 family. *BMC genomics* **2008,** 9, 334.

212. Cebula, M.; Schmidt, E. E.; Arner, E. S., TrxR1 as a potent regulator of the Nrf2-Keap1 response system. *Antioxidants & redox signaling* **2015,** 23, (10), 823-53.

213. Isani, G.; Carpene, E., Metallothioneins, unconventional proteins from unconventional animals: a long journey from nematodes to mammals. *Biomolecules* **2014,** 4, (2), 435-57.

214. Gilge, J. L.; Fisher, M.; Chai, Y. C., The effect of oxidant and the non-oxidant alteration of cellular thiol concentration on the formation of protein mixed-disulfides in HEK 293 cells. *PloS one* **2008,** 3, (12), e4015.

215. Hunt, P. R.; Son, T. G.; Wilson, M. A.; Yu, Q. S.; Wood, W. H.; Zhang, Y.; Becker, K. G.; Greig, N. H.; Mattson, M. P.; Camandola, S.; Wolkow, C. A., Extension of lifespan in C. elegans by naphthoquinones that act through stress hormesis mechanisms. *PloS one* **2011,** 6, (7), e21922.

216. Klaus, V.; Hartmann, T.; Gambini, J.; Graf, P.; Stahl, W.; Hartwig, A.; Klotz, L. O., 1,4-Naphthoquinones as inducers of oxidative damage and stress signaling in HaCaT human keratinocytes. *Archives of biochemistry and biophysics* **2010,** 496, (2), 93-100.

217. Crampton, N.; Kodiha, M.; Shrivastava, S.; Umar, R.; Stochaj, U., Oxidative stress inhibits nuclear protein export by multiple mechanisms that target FG nucleoporins and Crm1. *Molecular biology of the cell* **2009,** 20, (24), 5106-16.

218. Southam, C. M., *Effects of extract of western red-cedar heartwood on certain wood-decaying fungi in culture*. 1943.

219. Lithgow, G. J.; White, T. M.; Hinerfeld, D. A.; Johnson, T. E., Thermotolerance of a long-lived mutant of Caenorhabditis elegans. *Journal of gerontology* **1994,** 49, (6), B270-6.

220. Cypser, J. R.; Tedesco, P.; Johnson, T. E., Hormesis and aging in Caenorhabditis elegans. *Experimental gerontology* **2006,** 41, (10), 935-9.

221. Cascella, R.; Evangelisti, E.; Zampagni, M.; Becatti, M.; D'Adamio, G.; Goti, A.; Liguri, G.; Fiorillo, C.; Cecchi, C., S-linolenoyl glutathione intake extends life-span and stress resistance via Sir-2.1 upregulation in Caenorhabditis elegans. *Free radical biology & medicine* **2014,** 73, 127-35.

222. Heidler, T.; Hartwig, K.; Daniel, H.; Wenzel, U., Caenorhabditis elegans lifespan extension caused by treatment with an orally active ROS-generator is dependent on DAF-16 and SIR-2.1. *Biogerontology* **2010,** 11, (2), 183-95.

223. Bartholome, A.; Kampkotter, A.; Tanner, S.; Sies, H.; Klotz, L. O., Epigallocatechin gallate-induced modulation of FoxO signaling in mammalian cells and C. elegans:

FoxO stimulation is masked via PI3K/Akt activation by hydrogen peroxide formed in cell culture. *Archives of biochemistry and biophysics* **2010,** 501, (1), 58-64.

224. Putker, M.; Madl, T.; Vos, H. R.; de Ruiter, H.; Visscher, M.; van den Berg, M. C.; Kaplan, M.; Korswagen, H. C.; Boelens, R.; Vermeulen, M.; Burgering, B. M.; Dansen, T. B., Redox-dependent control of FOXO/DAF-16 by transportin-1. *Molecular cell* **2013,** 49, (4), 730-42.

225. Delphin, C.; Cahen, P.; Lawrence, J. J.; Baudier, J., Characterization of baculovirus recombinant wild-type p53. Dimerization of p53 is required for high-affinity DNA binding and cysteine oxidation inhibits p53 DNA binding. *European journal of biochemistry* **1994,** 223, (2), 683-92.

226. Rainwater, R.; Parks, D.; Anderson, M. E.; Tegtmeyer, P.; Mann, K., Role of cysteine residues in regulation of p53 function. *Molecular and cellular biology* **1995,** 15, (7), 3892-903.

227. Velu, C. S.; Niture, S. K.; Doneanu, C. E.; Pattabiraman, N.; Srivenugopal, K. S., Human p53 is inhibited by glutathionylation of cysteines present in the proximal DNA-binding domain during oxidative stress. *Biochemistry* **2007,** 46, (26), 7765-80.

228. Das, K. C.; Muniyappa, H., c-Jun-NH2 terminal kinase (JNK)-mediates AP-1 activation by thioredoxin: phosphorylation of cJun, JunB, and Fra-1. *Molecular and cellular biochemistry* **2010,** 337, (1-2), 53-63.

229. Clavel, S.; Siffroi-Fernandez, S.; Coldefy, A. S.; Boulukos, K.; Pisani, D. F.; Derijard, B., Regulation of the intracellular localization of Foxo3a by stress-activated protein kinase signaling pathways in skeletal muscle cells. *Molecular and cellular biology* **2010,** 30, (2), 470-80.

230. Murata, H.; Ihara, Y.; Nakamura, H.; Yodoi, J.; Sumikawa, K.; Kondo, T., Glutaredoxin exerts an antiapoptotic effect by regulating the redox state of Akt. *The Journal of biological chemistry* **2003,** 278, (50), 50226-33.

231. Galic, S.; Hauser, C.; Kahn, B. B.; Haj, F. G.; Neel, B. G.; Tonks, N. K.; Tiganis, T., Coordinated regulation of insulin signaling by the protein tyrosine phosphatases PTP1B and TCPTP. *Molecular and cellular biology* **2005,** 25, (2), 819-29.

232. Barrett, W. C.; DeGnore, J. P.; Keng, Y. F.; Zhang, Z. Y.; Yim, M. B.; Chock, P. B., Roles of superoxide radical anion in signal transduction mediated by reversible regulation of protein-tyrosine phosphatase 1B. *The Journal of biological chemistry* **1999,** 274, (49), 34543-6.

233. Lou, Y. W.; Chen, Y. Y.; Hsu, S. F.; Chen, R. K.; Lee, C. L.; Khoo, K. H.; Tonks, N. K.; Meng, T. C., Redox regulation of the protein tyrosine phosphatase PTP1B in cancer cells. *The FEBS journal* **2008,** 275, (1), 69-88.

List of abbreviations

4-HNE	4-hydroxynonenal
AMPK	AMP-activated kinase
AGE-1	Phosphoinositide-3 kinase age-1
Akt	AKT8 virus oncogene cellular homolog
approx.	approximately
ASK1	Apoptosis signaling kinase-1
ATF4	Activated Transcription Factor
ATPase	Adenosine Triphosphate
BCA	Bicinchoninic Acid
BSA	Bovine Serum Albumin
CBP-1	CREB-binding protein
cDNA	complementary DNA
CDK-1	Cyclin-dependent kinase-1
C. elegans	*Ceanorabditis elegans*
CR-	Conserved regions
ctl-	catalase
Cys	Cysteine
DAF-16	daeur formation
DAE	DAF-16 associated element
DBE	DAF-16 binding element
DEM	Diethyl maleate
DMSO	Dimethyl sulfoxide
DNA	Deoxyribonucleic Acid
D. melanogaster	*Drosophila melanogaster*
DYRK-1a	Tyrosine-regulated kinase-1a
EDTA	Ethylenediaminetetraacetic acid
ECL	Enhanced chemiluminescence
E. coli	*Escherichia coli*
EMSA	electrophoretic mobility shift assay
eNOS	Endothelial Nitric Oxide Synthase
ER	Endoplasmic reticulum
ERK-1/2	Extracellular signal–regulated kinases-1/2
FH/DBD	Forkhead box/DNA-binding domain
FHRE	Forkhead response element
Flk-1	Fetal liver kinase-1
FoxO-	Forkhead box O-

FoxO1-ΔCys5-7	FoxO1 Cys deficient mutant (Cys5-7→Ser)
FoxO1-ΔCys612	FoxO1 Cys deficient mutant (Cys1612→Ser)
ftn-1	Ferritin
G6Pase	Glucose 6-phosphatase
GCL	Glutamate-cysteine ligase
GPCRs	G-protein coupled receptors
GPx-	Glutathione peroxidase
Grx-	Glutaredoxin
GSH	Glutathione
GSK	Glycogen syntase kinase
GSSG	Glutathione disulfide
gst-	Glutathione S-transferase
HCF-1	Host cell factor
HEK293	Human embryonic kidney cells 293
HepG2	Human hepatoma cells
HGF	Hepatocyte growth factor
HNF-3A	Hepatocyte-enriched nuclear factor-3A
HNF-4A	Hepatocyte-enriched nuclear factor-4A
HPRT1	Hypoxanthine Phosphoribosyltransferase 1
HSF-1	Heat-shock transcription factor-1
IGF-1	Insulin-like growth factor-1
JNK-1	c-Jun N-terminal kinase-1
Keap-1	Kelch-like ECH-assosiated protein 1
Luc	Luciferase
MAPK	Mitogen-activated protein kinase
NEM	N-Ethylmaleimide
mtl-	Metallothionein-
mTOR	Mechanistic target of rapamycin
NADPH	Nicotinamide adenine dinucleotide phosphate
NLS	Nuclear localization signal
NF-κB	Nuclear factor-kappa B
PAR-1	Partitioning defective
PBS	Phosphate-buffered saline
PDK-1	Protein kinase-1
PGC-1a	Peroxisome proliferator-activated receptor gamma coactivator 1-alpha
PI3K	Phosphoinositide-3 kinase
PIP2	Phosphatidylinositol diphosphate
PIP3	Phosphatidylinositol triphosphate

PMK-1	Mitogen-activated protein kinase pmk-1
prdx-	Peroxiredoxin
PTEN	Phosphatase and tensin homolog
PTP1B	Protein-tyrosine phosphatase 1B
RNAi	RNA interference
ROS	Reactive oxygen species
Pro	Proline
RTK	Receptor tyrosine kinase
SelP	Selenoprotein P
Ser	Serine
sod-	Superoxide dismutases
SGK-1	Serum/glucocorticoid regulated kinase 1
SKN-1	Skinhead-1
SL1	Sequence leader 1
SL2	Sequence leader 2
SRT-1	Sirtuin-1
TBS	Tris-buffered saline
TGF-β	Transforming Growth Factor-β
TNF	Tumor necrosis factor
TORC1	Rapamycin complex 1
Trx-	Thioredoxin
Trxr-	Thioredoxin reductase
UPR	Unfolded protein response
USP7/ HAUSP	Herpesvirus-associated ubiquitin-specific protease
WT FoxO1	Wild type FoxO1
XBP-1	X-box binding protein 1

List of figures

List of tables

Sworn statement

I declare in lieu of oath that I have researched and written the dissertation by myself (statement of authorship), no passages of the text have been taken from third parties or own exam papers without having been identified as such and that all tools, personal notifications and sources used by the applicants have been indicated in the thesis.

Person who have supported the applicant in selecting and analyzing the material and preparing the manuscript, are declared completely.

The assistance of a professional consultant has not been utilized and no third parties have either directly or indirectly received monetary benefits from the candidate for work related to the contents of the submitted thesis.

The dissertation has not yet submitted as an examination paper for state of other academic examinations.

The dissertation has not submitted to another postsecondary school.

Jena, 1st of November, 2017 _____

Curriculum Vitae

Name:	Dimitrios Tsitsipatis
Nationality:	Greek
Date of Birth:	07.Sept.1989
Address:	Löbderstr. 6 07743 Jena Germany
Mobile:	+306939325058 +4915163364941
E-mail:	dimitrios.tsitsipatis@gmail.com

EDUCATION

2014 - present **Ph.D student**
- Department of Nutrigenomics/Friedrich Schiller University of Jena, Germany

2007 - 2013 **Studies in biology**
- Biology Department/Aristotle University of Thessaloniki, Greece
- Grade 7.55/10, Good

2006 - 2007 **High School**
- High School (Lyceum) of Panorama/Thessaloniki, Greece
- Grade 19/20, Excellent

SCIENTIFIC HISTORY

Feb.14 - present **Ph.D student**
- Department of Nutrigenomics/Friedrich Schiller University of Jena, Germany
  - ♦ Contributions of cysteine residues to the modulation of FoxO1 activity under oxidative Stress
  - ♦ Thiol status affects life span and stress resistance in *C. elegans*

Nov.12 - Nov.13 **Diploma work**
- Institute of Molecular Cell Biology/Friedrich Schiller University of Jena, Germany
  - ♦ Novel approaches to interfere with the proliferation of Acute Myeloid Leukemia cells

Aug.12 - Nov.12 **Erasmus scholarship, extended as internship**

Feb.12 - Aug.12
- Institute of Molecular Cell Biology/Friedrich Schiller University of Jena, Germany
  - ♦ Role of PI3Kγ on macrophage functions

Jul.11 - Aug.11 **Practical training**
- *Theageneio Hospital* for Cancer Treatment, Hematologic Laboratory/Thessaloniki, Greece
  - ♦ Cytometric analysis of Paroxysmal Nocturnal Hemoglobinuria

Jun.08 - Jul.08 **Volunteer**
- *Theageneio Hospital* for Cancer Treatment, Cytogenetic Laboratory/Thessaloniki, Greece

PUBLICATIONS

Tsitsipatis, D.; Jayavelu, A. K.; Muller, J. P.; Bauer, R.; Schmidt-Arras, D.; Mahboobi, S.; Schnoder, T. M.; Heidel, F.; Bohmer, F. D., Synergistic killing of FLT3ITD-positive AML cells by combined inhibition of tyrosine-kinase activity and N-glycosylation. *Oncotarget* 2017, 8, (16), 26613-26624.

Tsitsipatis, D.; Klotz, L. O.; Steinbrenner, H., Multifaceted functions of the forkhead box transcription factors FoxO1 and FoxO3 in skin. *Biochimica et biophysica acta* 2017, 1861, (5 Pt A), 1057-1064.

Urban, N.[*]; **Tsitsipatis, D.**[*]; Hausig, F.; Kreuzer, K.; Erler, K.; Stein, V.; Ristow, M.; Steinbrenner, H.; Klotz, L. O., Non-linear impact of glutathione depletion on C. elegans life span and stress resistance. *Redox biology* 2017, 11, 502-515. ([*] co-first author)

AWARDS

19-25.Sept.16 SFRR-Europe/FEBS Advanced School	**Poster award**
02-04.Sept.15 SFRR-E Meeting	**Young investigator award**

CONFERENCES

Invited speaker

08-11.Jun.16 SFRR-E Meeting

- Contributions of cysteine residues to the modulation of FoxO1 activity under oxidative stress.

Speaker

12-13.Sept.14 Nachwuchswissenschaftler Meeting

- Exposure to thiol depletor DEM alters *C. elegans* life span via DAF-16 and SKN-1 pathways.

Poster

19-25.Sept.16 SFRR-Europe/FEBS Advanced School

- Contributions of cysteine residues to the modulation of FoxO1 activity under oxidative stress **Tsitsipatis D**, Landrock F. M, Gopal K. Klotz LO.

02-04.Sept.15 SFRR-E Meeting

- Modulation of FoxO1a activity through S-glutathionylation? **Tsitsipatis D**, Landrock F. M, Gopal K. Klotz LO.

22-28.Sept.14 SFRR-Europe/IUBMB Advanced School

- Cellular thiol status affects FoxO activity and life span. **Tsitsipatis D**, Urban N, Gille A, Hamann, I, Hou, X, Klotz L.O.

19-22.Nov.08 Greek Hematologic Conference

- Detection of genetic abnormalities in multiple myeloma patients by using flow cytometry and F.I.S.H analysis. Berrou E, Mauroudi S, Nikitidou A, Pasmatzidis Ch, Gastari B, **Tsitsipatis D**, Chatziaggelidou Ch, Lazaridou A, Zervas K.

TECHNIQUES APPLIED

***in vivo* and *in vitro* Culture Techniques**	- Cultivation, starvation, stimulation and transfection of various cell lines - Isolation of primary murine bone marrow cells - Handling and manipulating of *C. elegans* - Cultivation and transformation of bacteria
Molecular Biology	- RNA extraction - cDNA synthesis - q-PCR - RTq – PCR - Plasmid preparation and isolation
Flow Cytometry	- Apoptosis assay (Annexin V/7AAD) - ROS measurement - Phagocytosis - Detection of various cancer cells (Clusters of Differentiation)
Cytogenetic Analysis	- Karyotype - Fluorescence *in situ* Hybridization (FISH)
Microscopy	- Fluorescence microscopy
General Assays	- Viability assay (MTT assay) - Western Blotting (immunoprecipitation/streptavidin pull down) - Thiols and glutathione measurement - Electrophoretic Mobility Shift assay (EMSA assay) - Luciferase Reporter assay

ADDITIONAL SKILLS

Biology	- Handling and manipulating of mice (Certificated Course/ Friedrich Schiller University of Jena, Germany) - Assistant in practical course on "Biochemical and Molecular Biological Methods" (Friedrich Schiller University of Jena, Germany)
Computer Skills	- Microsoft office - End Note - SigmaPlot - Special Software related to Biology: ♦ CalcuSyn (Dose-Effect Analyzer) ♦ Flow Jo (Flow Cytometry Analyzer) ♦ Multi Gauge (Image Analyzer) ♦ Ikaros (Karyotype Analyzer) ♦ SnapGene (Cloning)
Languages	- Greek (native speaker) - English (fluently, Proficiency of Michigan)

REFERENCES

Prof. Klotz, Lars-Oliver
Department of Nutrigenomics/Friedrich Schiller University of Jena, Germany
lars-oliver.klotz@uni-jena.de
+49 3641 - 949751

Prof. Böhmer, Frank-Dietmar
Institute of Molecular Cell Biology/Friedrich Schiller University of Jena, Germany
Boehmer@med.uni-jena.de
+49 3641 - 9395631

Ass. Prof. Müller, Jörg
Institute of Molecular Cell Biology/Friedrich Schiller University of Jena, Germany
Joerg.Mueller2@med.uni-jena.de
+49 3641 - 9395634

Prof. Wetzker, Reinhard
Institute of Molecular Cell Biology/Friedrich Schiller University of Jena, Germany
Reinhard.Wetzker@uni-jena.de
+49 3641 - 9395600

Ass. Prof. Triantafyllidis, Alexandros
Biology Department, Sector of Genetic, Development and Molecular Biology/Aristotle University of Thessaloniki, Greece
atriant@bio.auth.gr
+30 2310 – 998545

Acknowledges

Initially, I would like to express my gratitude to Prof. Dr. Lars-Oliver Klotz not only for giving me the opportunity to fully my dissertation, but also for his support throughout these years. To PD Dr. Holger Steinbrenner for the scientific, and not only, discussions and his great assistance during my PhD time. To Dr. Nadine Urban for passing to me her knowledge and teaching me how to handle *C. elegans*. To Maria Landrock for her great support and assistance throughout all the years.

To the rest members of our lab for providing a pleasant environment working.

To people here in Jena, outside the lab, that they supported me throughout all these years, like I was part of their family.

To my FAMILY for being next to me and support me, even though I know that is really difficult for them to that I am far away..

Thank you